“Analysis of Signal Distortion Techniques in PPDU Frame Based 4G Systems”

Thesis submitted in partial fulfillment of the requirement for the award of

degree of

MASTER OF ENGINEERING

In

ELECTRONICS & COMMUNICATION ENGINEERING

Submitted by

Anoop Kumar

Roll no. 800861003

Under the Guidance of

Mr. Ankush Kansal

Assistant Professor

ECED

Electronics and Communication Engineering Department

Thapar University, Patiala-147004 (PUNJAB)

June 2010

CERTIFICATE

I, Anoop Kumar, hereby certify that the work which is being presented in this thesis entitled **"Analysis of Signal Distortion Techniques in PPDU Frame Based 4G Systems"** by me in partial fulfillment of the requirements for the award of degree of master of Engineering in Electronics & Communication from Thapar University (Deemed University), Patiala, is an authentic record of my own work carried out under the supervision of Mr. Ankush Kansal.

The matter presented in this thesis has not been submitted in any other University/ Institute for the award of Master of Engineering.

Anoop Kumar
Signature of the Student
Date...06/07/10...

This is certified that the above statement made by the candidate is correct to the best of my knowledge.

Ankush Kansal
Assistant Professor,
ECED
Date...6/07/10...

Countersigned by:

Dr. A.K. Chatterjee
Professor & H.O.D., ECED
Thapar University, Patiala
Date.....9.7.10.....

Dr. R.K. Sharma
Dean of Academic Affairs
Thapar University, Patiala
Date.....13.7.10

i

ACKNOWLEGMENT

Any fruitful effort in a new work needs a direction and guiding hands that shows the way. I take this opportunity to express my sincere gratitude to Mr. Ankush Kansal (Assistant Professor, ECED), Thapar University, Patiala for his suggesting new ways for implementing my ideas by his expert guidance throughout my work.

I am further indebted to Dr. A. K. Chatarjee, Professor and Head, Department of Electronics and Communication Engineering, for his moral support at every step. I am also thankful to all the staff members of the Electronics & Communication Engineering Department for their full cooperation and help.

Finally, my thanks to everyone who has in some way or other helped me in completing this project successfully. I should not fail to mention my parents who have always been a source of inspiration. I am grateful to my friends especially to Amisha, Tikka and Yogesh for their valuable support and help.

Anoop Kumar

ABSTRACT

High data rate with high bandwidth efficiency and low power consumption are some of the requirements that the modern wireless communication systems 3G and 4G have to meet for offering new high class services to be distributed to the customers. In wireless communication, signals are mainly damaged by frequency selective fading and multipath delay spreading. This leads to a high probability of errors at the receiver end. Hence single carrier mobile communication systems do not perform well for high speed data rate transmission with maximum throughput at limited bandwidth. To tackle these problems channel coding and adaptive equalization have been used. But due to delay of these techniques and high cost of hardware implementation, it is very difficult to use these techniques in systems which are operating at high bit rates. The solution to all these problems is to use a multi-carrier system; Orthogonal Frequency Division Multiplexing (OFDM) is an example of it.

The attraction of OFDM is mainly due to how the system handles the multipath interference at the receiver. Multipath generates two effects: frequency selective fading and Inter-Symbol Interference (ISI). The "flatness" perceived by a narrow-band channel overcomes the frequency selective fading, and modulating at a very low symbol rate, which makes the symbols much longer than the Channel Impulse Response (CIR), diminishes the ISI. Using powerful error correcting codes together with time and frequency interleaving yields even more robustness against frequency selective fading and the insertion of an extra guard interval between consecutive OFDM symbols can reduce the effects of ISI even more. Thus, an equalizer in the receiver is not necessary.

With so much large advantages of OFDM, there are some limitations and complications in practical systems too. The two main drawbacks of OFDM system are: the large dynamic range of the amplifier also referred as Peak to Average Power Ratio (PAPR) and its sensitivity to frequency errors. PAPR results in inter-modulation among the sub-carriers and undesired out-of-band power radiations. It is impossible to keep the out-of-band power under the limit, if power amplifiers are not operated with large back-offs. So it considerably reduces the efficiency of the High Power Amplifier (HPA) at the

transmitter side. Hence, the reliable reduction of PAPR is important for the practical implementation of OFDM system.

In this thesis the improvement in PAPR of OFDM system is discussed. We have examined many PAPR reduction techniques and compared them and get an optimum result in finding best technique. The success of these techniques in terms of histogram, PAPR-reduction, Bit Error Rate (BER) and average power variation are evaluated. We have done many experiments on clipping techniques and companding techniques and finally it has been found that CC technique has good PAPR reduction performance.

Tables of Contents

LIST OF FIGURES

LIST OF TABLE

List of Acronyms

A:

ADSL:	Asymmetric Digital Subscriber Line
AWGN:	Additive White Gaussian Noise

B:

BER:	Bit Error Rate
BRAN:	Broadband Radio Access Networks

C:

CP:	Cyclic Prefix
CIR:	Carrier-To-Interference Power Ratio
CCDF:	Complementary Cumulative Distributive Function
CDF:	Cumulative Distribution Function
CAF:	Clipping and Filtering
CC:	Classical-Clipping

D:

DC:	Deep-Clipping
DAB:	Digital Audio Broadcasting
DVB-T:	Digital Video Broadcasting -Terrestrial
DMT:	Discrete Multi-Tone
DSP:	Digital Signal Processing
DAC:	Digital to Analog Convertor

F:

FFT:	Fast Fourier Transform

G:

GI:	Guard Interval
3GPP-LTE:	3rd Generation Partnership Project- Long Term Evolution
4G:	Fourth Generation

H:

HIPERLAN-2: High Performance Local Area Network

HC: Heavyside-Clipping

I:

ICI: Inter-Symbol Interference

IFFT: Inverse fast Fourier transform

M:

MCM: Multi-Carrier Modulation

MPDU: Medium Protocol Data Unit

ML: Maximum Likelihood

O:

OFDM: Orthogonal Frequency Division Multiplexing

P:

PLCP: Physical Layer Convergence Procedure

PMD: Physical Medium Dependent

PPDU: PLCP Protocol Data Unit

PRS: Partial Response Signalling

PTS: Partial Transmit Sequences

PSDU: Physical Service Data Unit

PAPR: Peak to Average Power Ratio

Q:

QCQP: Quadratically Constrained Quadratic Program

R:

RF: Radio Frequency

S:

SNR: Lower Signal to Noise Ratio

SAP: Service Access Point

SLM: Selective Mapping

SC: Smooth-Clipping

U:

U-NII: Unlicensed National Information Infrastructure

V:

VLSI: Very Large Scale Integration

W:

WMAN: Wireless Metropolitan Area Networks

Chapter 1

Introduction

1.1 OFDM in Wireless Communication Systems

Wireless technologies have become increasingly more and more involved into people's daily life. Today without wireless technologies, life would have been extremely inconvenient. Wireless communication continues to maintain an exponential growth in wireless internet, cellular telephony and wireless indoor networking areas. The common aspects of the next generation wireless technologies will be the convergence of multimedia services such as speech, audio, video, image, and data [1]. So a high capacity and variable bit rate information transmission with high bandwidth efficiency are just some of the requirements that the modern transceivers have to meet in order for a variety of new high quality services to be delivered to the customers. Wireless communications offers many advantages, such as mobility and flexibility, but in front of communication systems there are many Problems which restrict to achieve desire goal [2]. Some of these are given below:

- Limited radio spectrum
- Inter-symbol interference (ISI) caused by time varying channel
- Frequency selective fading caused by multipath fading
- Interference from radio emissions
- Lower signal to noise ratio (SNR) of received signal due to large link loss

So to support high data rates and deal with these problems in conventional single carrier wireless communication systems, channel coding and equalization can be too complicated and costly to implement. Therefore, a suitable modulation technique supporting high data rates with sufficient strength to radio channel impairments is required. To suppress ICI, efficient use of bandwidth, Multi-Carrier Modulation (MCM) techniques have caught the attention of researchers all over the world. Among those

techniques, Orthogonal Frequency Division Multiplexing (OFDM) is the most well-liked one that uses parallel data streams.

Although the idea of OFDM has been around for several decades, it has not been recognized as a great method for high speed bi-directional wireless data communication until recent years. The initial applications were military HF radio links. Due to the recent improvements in Digital Signal Processing (DSP) and Very Large Scale Integration (VLSI) technologies, the use of fast Fourier transform (FFT) algorithms eliminates arrays of oscillators and coherent demodulation required in parallel data systems and makes the implementation of the technology cost effective [3]. Compared with single carrier modulation systems, OFDM has many advantages:

- Immunity to impulse interference
- High spectral density,
- Robustness to RF interference
- Capability of handling very strong echoes
- Robustness to channel fading [4].

OFDM is currently catching the attention of wireless communication to meet the increasing demands arising from the explosive development of internet, broad services and multimedia. It has been adopted by various WLAN standards such as High Performance Local Area Network (HIPERLAN-2), IEEE 802.11a/g/n in recent years including Wireless Metropolitan Area Networks (WMAN), Digital Video Broadcasting - Terrestrial (DVB-T), 3rd Generation Partnership Project- Long Term Evolution (3GPP-LTE, Asymmetric Digital Subscriber Line (ADSL), Digital Audio Broadcasting (DAB) and Broadband Radio Access Networks (BRAN) [5]. It has also been suggested for power-line communication systems due to its robustness to time dispersive channels and narrowband interferers. Recently the OFDM technique is being considered as a strong runner for the fourth generation (4G) of mobile communication system.

1.2 OFDM System Model

1.2.1 Introduction

OFDM is a special case of Discrete Multi-Tone (DMT) modulation scheme [6], where a single data stream is transmitted over a number of lower rate subcarriers. OFDM offers many well-documented advantages for multi-carrier transmission at high data rate, particularly in mobile applications.

In OFDM model, data stream is divided into low rate data and transmitted simultaneously over a number of subcarriers that are orthogonal to each other. The increase of symbol duration for the lower rate parallel subcarriers reduces the relative amount of spreading in time caused by multipath delay spread. So effects of ISI at the receiver side decreases but total data rate increases

In frequency spectrum, orthogonal subcarriers can overlap, and there is no need of inserting guard bands between the sub-carriers. So another advantage of OFDM is the bandwidth utilization. A traditional frequency division multiplexing is shown in fig. 1.1 (a). The total bandwidth is divided into N (here N=8 is taken) non-overlapping sub-channels. Each sub-channel is modulated with a separate symbol. This arrangement is insufficient in bandwidth utilization [7].

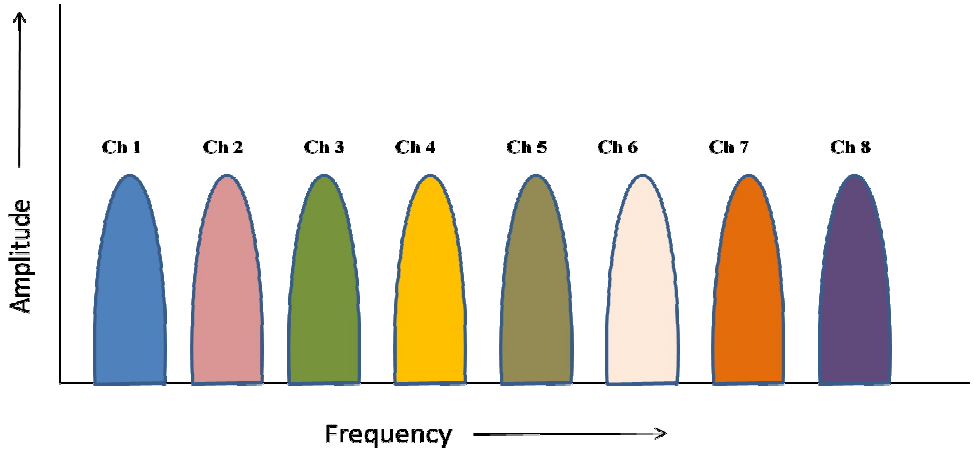

(a)

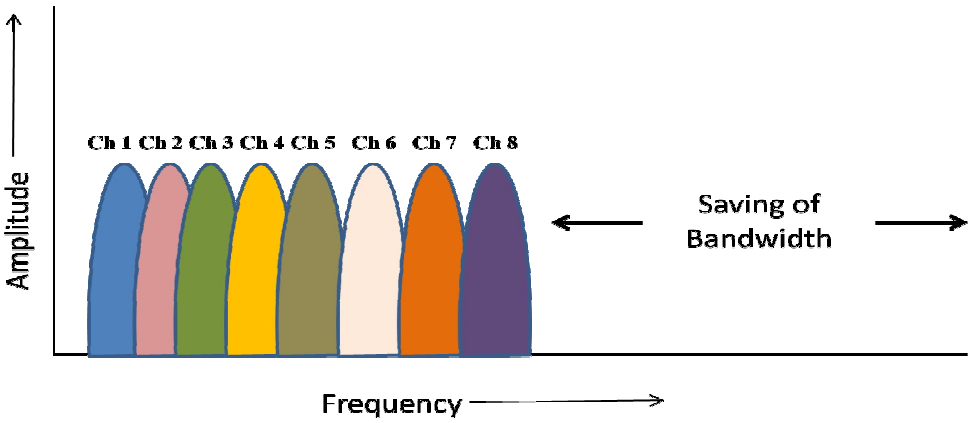

(b)

Figure 1.1(a) Traditional multicarrier system (b) orthogonal multicarrier system

In OFDM systems, as shown in fig. 1.1 (b), the sub-channels overlap. The frequency spacing between subcarriers is chosen such that each subcarrier is located on the other subcarrier's zero crossing points as shown in fig. 1.2. In other words, the subcarriers are organized to be orthogonal with each other. Therefore the overlapping among subcarriers will not cause interference. Thus, the bandwidth efficiency is significantly increased due to orthogonality among all subcarriers and then more sub-channels can be squeezed into the same bandwidth

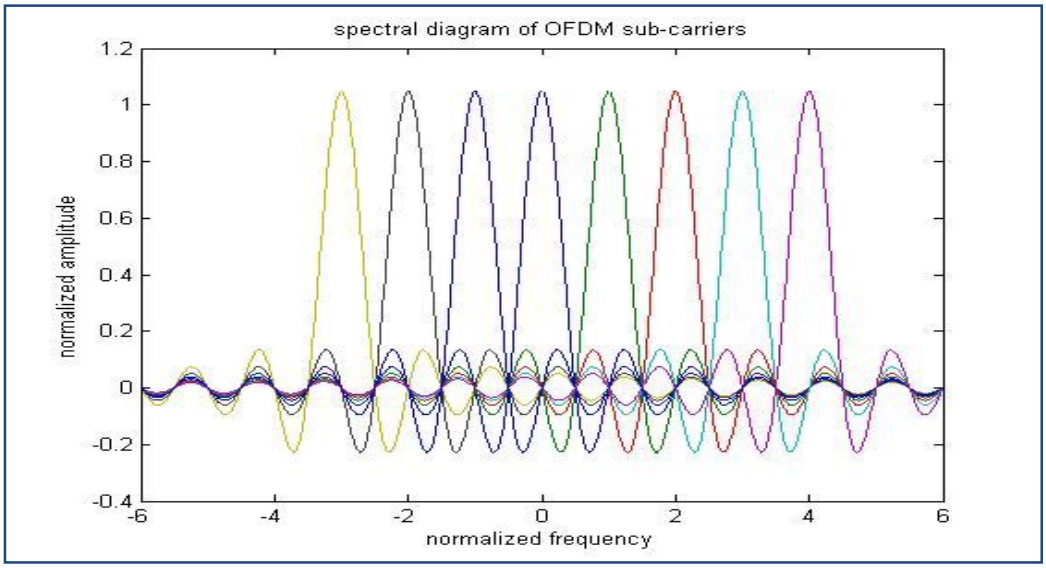

Figure 1.2 Spectral diagram of orthogonal sub-carriers

1.2.2 Signal Model for OFDM

In an OFDM system, data is modulated on narrow-band sub-carriers in frequency domain. Data was transformed into time-domain using IFFT at the transmitter side and transformed back to frequency-domain using FFT at the receiver side. Size of FFT/IFFT corresponds to total number of subcarriers used to transmit the information. In this section we will see the mathematical description of OFDM model.

A. Continuous Baseband OFDM Signal Model

Let $\boldsymbol{X} = \{X_0, X_1, \ldots\ldots X_N\}$, $\boldsymbol{X} \in C^N$ denotes an encoded data sequence to be transmitted as an OFDM symbol over N subcarriers, where X_k represents the complex data transmitted over the kth subcarrier. The complex baseband OFDM symbol is then expressed as

$$x(t) = \frac{1}{\sqrt{N}} \sum_{k=0}^{N-1} X_k \, e^{\frac{j2\pi kt}{T_s}} \, , 0 \le t \le T_s \quad , \tag{1.1}$$

where T_s is the symbol period of the OFDM signal. At the receiver side, the data is recovered by performing FFT on the received signal, i.e.

$$X_k = \frac{1}{\sqrt{N}} \int_{-\infty}^{\infty} x(t) \, e^{\frac{-j2\pi kt}{T_s}} dt \, , 0 \le k \le N-1 \tag{1.2}$$

B. Discrete Baseband OFDM Signal Model

Consider the above OFDM symbol sampled at the specified sampling period $\Delta t = T_s/JN$. Then the discrete-time OFDM signal sampled at time instant t=nΔt is expressed as

$$x_n = x(n\Delta t) = \frac{1}{\sqrt{N}} \sum_{k=0}^{N-1} X_k e^{j2\pi kn/JN} \quad 0 \le n \le N-1$$

Or

$$x_n = x(n\Delta t) = \frac{1}{\sqrt{N}} \sum_{k=0}^{N-1} X_k W^{kn} \quad 0 \le n \le N-1 \tag{1.3}$$

Where J can be considered as an oversampling rate and called as Nyquist rate with J=1. At the receiver side

$$X_k = \frac{1}{\sqrt{N}} \sum_{n=0}^{N-1} x_n \, e^{\frac{-j2\pi kn}{JN}} \, , 0 \le k \le N-1$$

Or

$$X_k = \frac{1}{\sqrt{N}} \sum_{n=0}^{N-1} x_n \, W^{-kn} \, , 0 \le k \le N-1 \tag{1.4}$$

1.2.3 System Description

The OFDM system based on pilot channel estimation is given in fig. 1.3. The OFDM system in 802.11a provides a wireless LAN with data payload communication capabilities of 6, 9, 12, 18, 24, 36, 48, and 54 Mbit/s [8]. The binary information is first scrambled. Scrambling is done for encryption. After scrambled, the data is coded with convolutional coding followed by interleaving. Coding rate (R) depends on the data rate at which data has to be transmitted. Now the mapping is done corresponding to data rate. The coding rate and modulation parameters dependent on data rate used shall be set according to table 1.1.

After interleaving, serial data is converted into parallel form. Then according to IEEE 802.11a standard, pilots are inserted at the prescribed positions for channel estimation in data as shown in fig. 1.4.

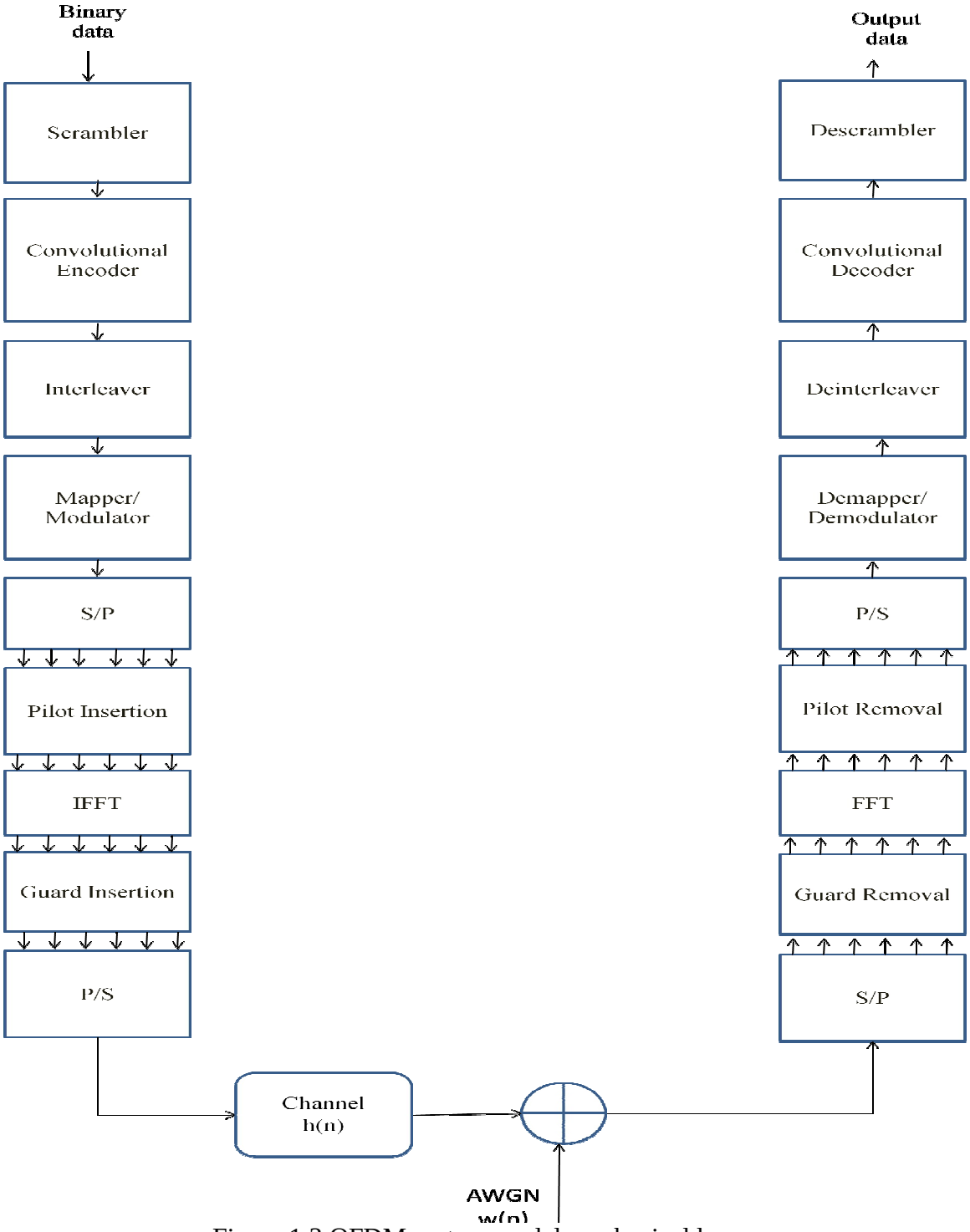

Figure 1.3 OFDM system model on physical layer

Table 1.1- Rate dependent parameters [8]

Data rate (Mbit/s)	Modulation	Coding rate (R)	Coded bits per subcarrier (N_{BPSC})	Coded bits per OFDM symbol (N_{CBPS})	Data bits per OFDM symbol (N_{DBPS})
6	BPSK	1 / 2	1	48	24
9	BPSK	3 / 4	1	48	36
12	QPSK	1 / 2	2	96	48
18	QPSK	3 / 4	2	96	72
24	16-QAM	1 / 2	4	192	96
36	16-QAM	3 / 4	4	192	144
48	64-QAM	2 / 3	6	288	192
54	64-QAM	3 / 4	6	288	216

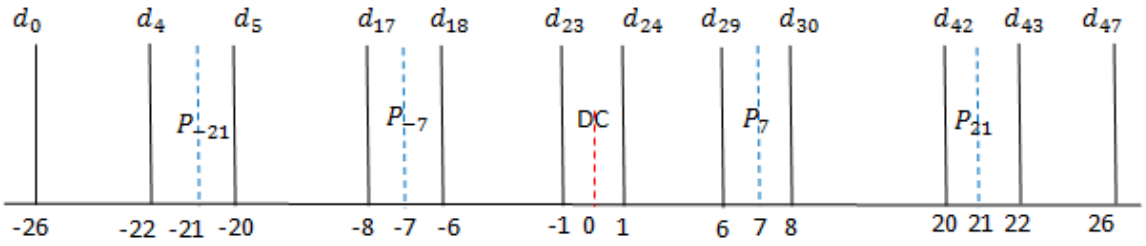

Figure 1.4 subcarrier numbers and positions of data and pilots

After inserting pilots, IDFT block is used to transform the data sequence of length N $\{X_k\}$ into time domain signal $\{x_n\}$ with the equation (1.3). Following IDFT block, guard time is inserted to prevent inter-symbol interference. This guard time is chosen to be larger than the expected delay spread,

This guard time includes the cyclically extended part of OFDM symbol in order to reduce inter-carrier interference (ICI). The resultant OFDM symbol is given as follows:

$$x_g(n) = \begin{cases} x(N+n), & n = -N_g, -N_g+1, \dots, -1 \\ x(n), & n = 0,1,2,\dots,N-1 \end{cases} , \quad (1.5)$$

where N_g is the length of the guard interval. The transmitted signal $x_g(n)$ will pass through the frequency selective time varying fading channel with additive noise. The received signal is given by:

$$y_f(n) = x_g(n) * h(n) + w(n) \quad , \quad (1.6)$$

Where w(n) is Additive White Gaussian Noise (AWGN) and h(n) is the channel impulse response. The channel response h(n) can be represented by [9]:

$$h(n) = \sum_{i=0}^{r-1} h_i e^{j\left(\frac{2\pi}{N}\right) f_{D_i} T_n} \delta(\lambda - \tau_i) \quad 0 \le n \le N-1 \quad , \quad (1.7)$$

where r is the total number of propagation paths, h_i is the complex impulse response of the ith path, f_{D_i} is the ith path Doppler frequency shift, λ is delay spread index, T is the sample period and τ_i is the ith path delay normalized by the sampling time. At the receiver, after passing to discrete domain through A/D and low pass filter, guard time is removed:

$$y_f(n) \quad for - N_g \le n \le N-1 ,$$

$$y(n) = y_f(n + N_g) \quad n = 0,1,\dots,N-1 \quad , \quad (1.8)$$

Then y(n) is sent to DFT block for the following operation (also as in given by equation (1.4)):

$$Y(k) = \frac{1}{\sqrt{N}} \sum_{n=0}^{N-1} y(n) e^{\frac{-j2\pi kn}{N}} , 0 \le k \le N-1 \quad , \quad (1.9)$$

Assuming there is no ISI, [10] shows the relation of the resulting Y(k) to H(k)=DFT{h(n)} ,I(k) that is ICI because of Doppler frequency and W(k)=DFT{w(n)} , with the following equation :

$$Y(k) = X(k)H(k) + I(k) + W(k) \quad k = 0,1,\dots,N-1 \tag{1.10}$$

Following DFT block, the pilot signals are extracted and the estimated channel $H_e(k)$ for the data sub-channels is obtained in channel estimation block. Then the transmitted data is estimated by:

$$X_e(k) = \frac{Y(k)}{H_e(k)} \quad k = 0,1,\dots,N-1 \tag{1.11}$$

Then the binary information data is obtained back after processing the reverse steps such as demodulating, deinterleaving, convolutional decoding and descrambling. This was all about the brief summary of whole OFDM system. Now here we will see each and every block of OFDM transmitter and receiver of our OFDM model based on IEEE 802.11a standard.

1.3 Physical layer of OFDM

IEEE Wireless LAN Working Group proposed and released a new standard 802.1la for wireless LAN system in 1999. This standard supports a high data rate up to 54 Mbit/s in the 5GHz unlicensed national information infrastructure (U-NII) band [8]. Various data rates are given in table 1.1. The system uses 52 subcarriers that are modulated BPSK, QPSK, 16-QAM or 64-QAM. Forward error correction coding (convolution coding) is used with a coding rate of 1/2, 2/3 or 3/4. In this section, we will see how the data is transmitted through the physical layer.

The OFDM physical layer described in IEEE 802.11 a 5GHz OFDM WLAN system consists of two protocol functions or sub-layers depicted in fig 1.5.

1. Physical Layer Convergence Procedure (PLCP) sub-layer
2. Physical Medium Dependent (PMD) sub-layer

1. PLCP sub-layer:

PLCP communicates to MAC via primitives through physical layer Service Access Point (SAP). It prepares PLCP protocol data unit (PPDU) by appending required fields (such as

PLCP preamble and PLCP header) to medium protocol data unit (MPDU) received from MAC layer. In physical layer MPDU is also called as physical service data unit (PSDU). PPDU provides for asynchronous transfer of MPDU between stations.

2. PMD Sublayer

PMD provides actual transmission and reception of physical layer entities through wireless medium. It interfaces directly to medium and provides modulation and demodulation of transmission frames.

Since aim of this thesis is to analyze the performance of OFDM on physical layer, so we will not concern about MAC layer and. So we will continue with the PLCP sublayer and PMD layer. In this section, how the PSDU is converted to PPDU during data transmission is described.

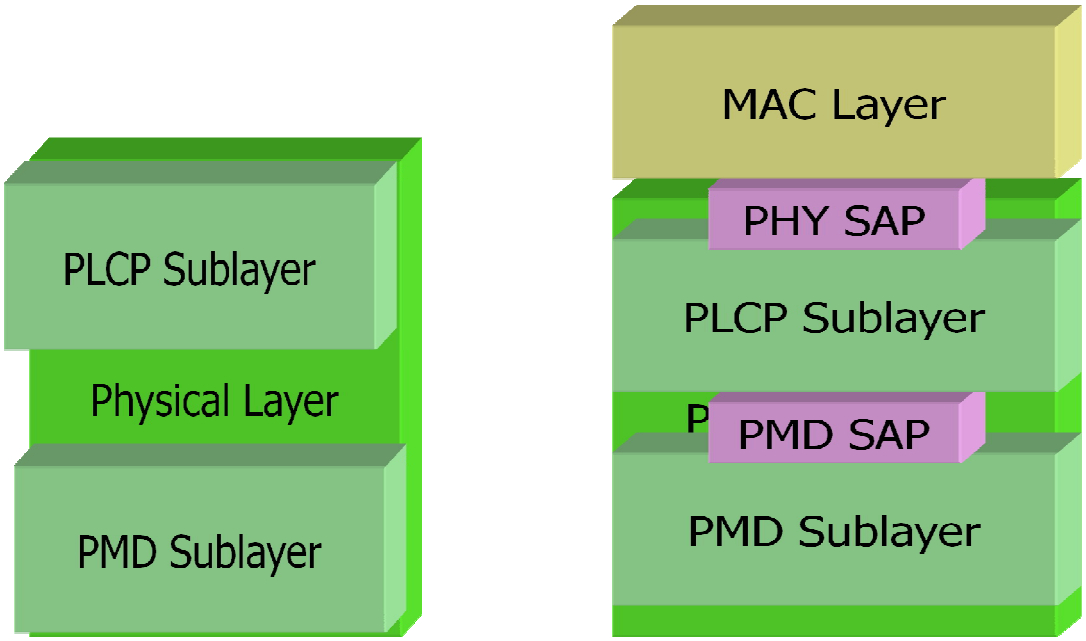

(a) (b)

Figure 1.5 (a) Physical layer with sub-layers (b) MAC and physical layer of 802.11a

1.3.1 PLCP Sublayer

This sublayer describes a convergence procedure in which PSDUs are converted to PPDUs. During data transmission PLCP preamble and PLCP header are appended to PSDU to create PPDU. At the receiver side, PLCP preamble and header are processed to aid in demodulation and reception of PSDU. A special training structure defined in preamble field is used for synchronization. PLCP header contains the information about the amount of data and data rate at which data has to be transmitted [8].

1.3.1.1 PPDU Frame Format

PPDU frame format, described in fig. 1.6 , includes the OFDM PLCP preamble, OFDM PLCP header, PSDU, tail bits, and pad bits. The PLCP preamble consists of 10 "Short" symbols and 2 "Long" symbols. The 10 "Short" symbols are used for signal detection, AGC, diversity selection, coarse frequency offset estimation and timing synchronization at the receiver side. The 2 "Long" symbols are used for channel and fine frequency offset estimation.

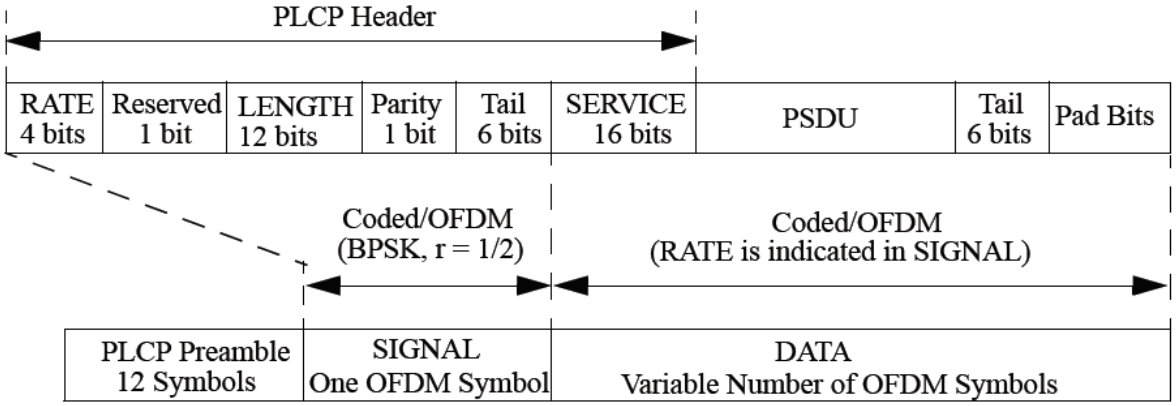

Figure 1.6 802.11a PPDU Frame Formats [8]

The PLCP header contains the following fields: LENGTH, RATE, a reserved bit, an even parity bit, and the SERVICE field. The SIGNAL field is composed of the information bits containing the LENGTH, RATE, reserved bit, and parity bit (with 6 zero" tail bits appended); and the SIGNAL is transmitted with BPSK modulation and a coding rate of R

= 1/2. The DATA field contains the SERVICE field of the PLCP header and the PSDU (with 6 "zero" tail bits and pad bits appended); and the DATA may constitute multiple OFDM symbols that are transmitted at the data rate described in the RATE field. The tail bits in the SIGNAL symbol enable decoding of the RATE and LENGTH fields immediately after the reception of the tail bits. The RATE and LENGTH are required for decoding the DATA part of the packet.

A. PLCP preamble

The PLCP preamble field, shown in fig. 1.7, consists of totally 12 symbols, including 10 "short training sequence" and 2 "Long training sequence", are designed for synchronization between the transmitter and the receiver. A short training symbol consists of 12 subcarriers, modulated by elements of sequence S, given by (1.12).

$S_{-26,26}$= √(13/6) × {0, 0, 1+j, 0, 0, 0, -1-j, 0, 0, 0, 1+j, 0, 0, 0, -1-j, 0, 0, 0, -1-j, 0, 0, 0, 1+j, 0, 0, 0, 0, 0, 0, 0, -1-j, 0, 0, 0, -1-j, 0, 0, 0, 1+j, 0, 0, 0, 1+j, 0, 0, 0, 1+j, 0, 0, 0, 1+j, 0,0} (1.12)

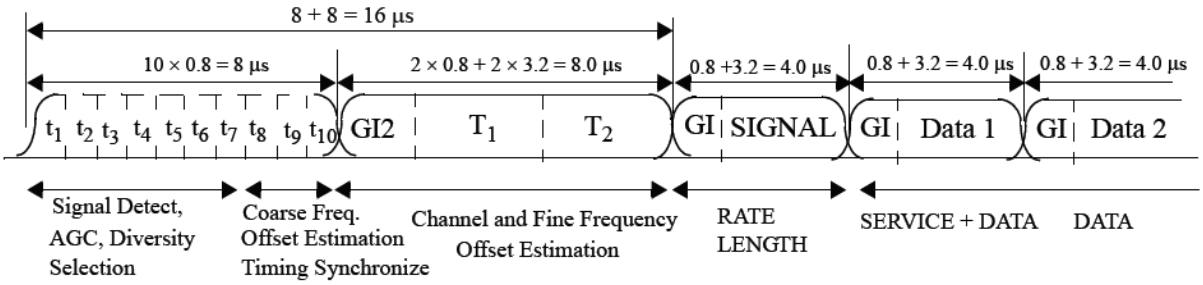

Figure 1.7: 802. 11a OFDM Training Structure [8]

The multiplication by a factor of √ (13/6) is in order to normalize the average power of the resulting OFDM symbol, which utilizes 12 out of 52 subcarriers. A long OFDM training symbol consists of 53 subcarriers (including a zero value at dc), which are modulated by the elements of the sequence L, given by (1.13)

$L_{-26,26}$ = {1, 1, -1, -1, 1, 1, -1, 1, -1, 1, 1, 1, 1, 1, 1, -1, -1, 1, 1, -1, 1, -1, 1, 1, 1, 1, 0, 1, -1, -1, 1, 1, -1, 1, -1, 1, -1, -1, -1, -1, -1, 1, 1, -1, -1, 1, -1, 1, -1, 1, 1, 1, 1} (1.13)

Each "Short training sequence" represents an OFDM "Short" symbol of 0.8μs long, and each "Long training sequence" represents an OFDM "Long" symbol of 3.2 μs long. The ten repetitions of the "Short training sequence" are used for signal detection, AGC convergence, diversity selection, timing acquisition, and coarse frequency acquisition [11]. So total time of short training sequence is

$$T_{short} = 0.8\mu s \times 10 = 8\ \mu s. \quad (1.14)$$

The two repetitions of a "Long training sequence", preceded by a guard interval (GI), are used for channel estimation and fine frequency acquisition in the receiver. So total time of long sequence is

$$T_{long} = 3.2\mu s \times 2 = 6.4\ \mu s. \quad (1.15)$$

The guard interval is used for shifting the time to create the "circular prefix" used in OFDM, to avoid ISI from the previous frame. The "Short training sequence" has no guard interval. The "Long training sequence" has the longest guard interval of 1.6μs. The guard intervals in the "Signal" and "Data" fields are only 0.8μs.

$$T_{training} = T_{short} + T_{long} + T_{guard} = 8 + 6.4 + 1.6 = 16\ \mu s. \quad (1.16)$$

B. Signal Field

Signal field of PPDU have 24 bits, as shown in fig. 1.8. The four bits from 0 to 3 contains the information of RATE field, it tells about the rate at which rest of packet is to be transmitted, type of modulation and coding rate [12]. The bits R1.R4 shall be set, dependent on RATE, according to the values in table 1.2. Bit 4 shall be reserved for future use. Bit 4 shall be reserved for future use. Bits 5-16 shall encode the LENGTH field that indicates number of octets in PSDU that the MAC is currently requesting the Physical layer to transmit.

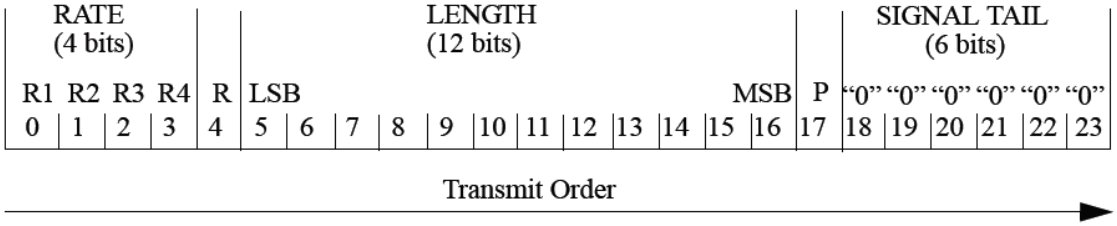

Figure 1.8 Signal field of PPDU [8]

It has 12 bit unsigned integer, so a maximum of 4096 octets can be transmitted in one PPDU frame at a time.

The LSB of LENGTH field shall be transmitted first in time. Bit 17 shall be a positive Parity (even parity) bit (P) for bits 0-16. The bits 18-23 constitute the SIGNAL TAIL field, and all 6 bits shall be set to 0.

Table 1.2 Contents of rate field

Rate (Mbit/s)	**R1-R4**
6	1101
9	1111
12	0101
18	0111
24	1001
36	1011
48	0001
54	0011

The contents of the SIGNAL field are not scrambled. The encoding of the SIGNAL single OFDM symbol is performed with BPSK modulation of the subcarriers and using convolutional coding at R = 1/2. The encoding procedure, which includes convolutional encoding, interleaving, modulation mapping processes, pilot insertion, and OFDM modulation are done for transmission of SIGNAL field at a 6 Mbit/s rate.

C. Data Field

The DATA field contains the SERVICE field, the PSDU, the TAIL bits, and the PAD bits, if needed. All bits in the DATA field are scrambled.

I. SERVICE field

The IEEE 802.11 SERVICE field has 16 bits, which shall be denoted as bits 0-15 as shown in fig. 1.9. The bit 0 shall be transmitted first in time. The bits from 0-6 of the SERVICE field, which are transmitted first, are set to zeros and are used to synchronize the descrambler in the receiver. The remaining 9 bits (7-15) of the SERVICE field shall be reserved for future use. All reserved bits shall be set to 0.

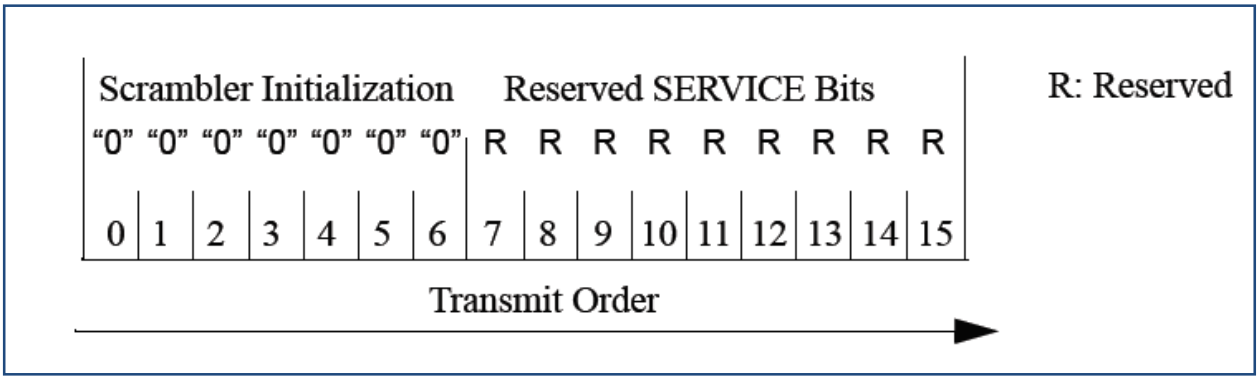

Figure 1.9 SERVICE field bit assignment

II. PPDU TAIL field

The PPDU TAIL field shall be six bits of zero, which are required to return the convolutional encoder to the zero state. This procedure improves the error probability of the convolutional decoder, which relies on future bits when decoding and which may be

not be available past the end of the message. The PLCP tail bit field shall be produced by replacing six scrambled zero bits following the message end with six non-scrambled zero bits.

III. Pad bits (PAD)

The number of bits in the DATA field shall be a multiple of N_{CBPS}, the number of coded bits in an OFDM symbol (48, 96, 192, or 288 bits). To achieve that, the length of the message is extended so that it becomes a multiple of N_{DBPS}, the number of data bits per OFDM symbol. At least 6 bits are appended to the message, in order to accommodate the TAIL bits. The number of OFDM symbols, N_{SYM}; the number of bits in the DATA field, DATA; and the number of pad bits, N_{PAD}, are computed from the length of the PSDU (LENGTH) as follows:

$$N_{SYM} = \text{Ceiling}\left((16 + 8 \times \text{LENGTH} + 6)/ N_{DBPS}\right) \quad (1.17)$$

$$N_{DATA} = N_{SYM} \times N_{DBPS} \quad (1.18)$$

$$N_{PAD} = N_{DATA} - (16 + 8 \times \text{LENGTH} + 6) \quad (1.19)$$

The function ceiling (.) is a function that returns the smallest integer value greater than or equal to its argument value. The appended bits (pad bits) are set to zeros and are subsequently scrambled with the rest of the bits in the DATA field. This is all about that what a PPDU frame includes. Now in next section description of encoding devices with the help of which PSDUs are converted to PPDUs, is done.

1.3.2 PLCP Data Scrambler and Descrambler

The DATA field, composed of SERVICE, PSDU, tail, and pad parts, is scrambled with a length-127 frame-synchronous scrambler [13]. Scrambling is done from the least significant bit (LSB) of data. The frame synchronous scrambler uses the generator polynomial *S(x)* as follows, and is shown in fig. 1.10:

$$S(x) = x^7 + x^4 + 1 \quad (1.20)$$

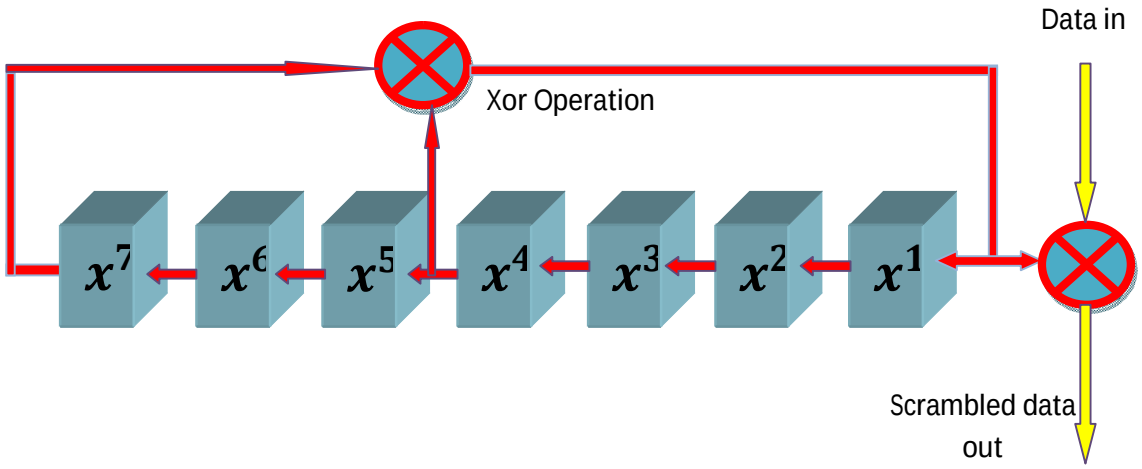

Figure 1.10 Synchronous data scrambler

When transmitting, the initial state of the scrambler is set to a 7 digit pseudo-random non-zero state. If state is set to al zeros then there will be no change in states. If initial state is set with "1011101" then 127 bit sequence generated repeatedly will be [01101100 00011001 10101001 11001111 01101000 01010101 11110100 10100011 01110001 11111100 00111011 11001011 00100100 00001000 10011000 1011101]. The same scrambler is used to scramble transmit data and to descramble receive data. Since 7 seven LSBs of the SERVICE field are zeros i.e. [0000000], so after scrambling it yields [1011101] same to initial state of scrambler. That's so why 7 LSB's of service fields are used to enable estimation of the initial state of the scrambler in the receiver.

1.3.3 Error Control Convolutional encoder

Error-control coding techniques are used to detect and/or correct errors that occur in the message transmission in a wireless communication system. The transmitting side of the error-control coding adds redundant bits to the original information data. The receiving side of the error-control coding uses these redundant bits of symbols to detect and/or correct the errors that occurred during transmission. The coding process at transmitter side is known as encoding, and at the receiving side coding process is known as decoding [14].

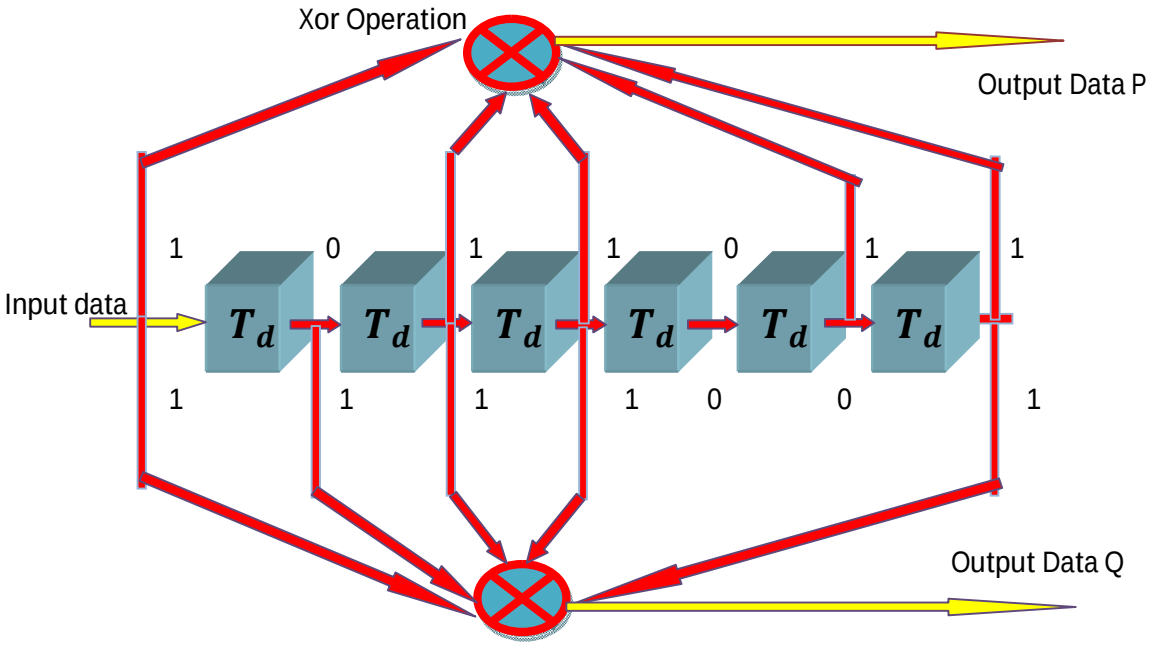

Figure 1.11 Convolutional encoder

There are many types of coding techniques such as block codes, convolutional codes and line codes. In 802.11a systems convolutional codes are used. In convolutional codes if M is number of input data and N is number of output data. Then the ratio M/N is known as coding rate(R). The *Viterbi method* is used for decoding the convolutional codes at the receiver side. The Viterbi algorithm is a *maximum likelihood* (ML) decoding procedure

The signal field is coded with a convolutional encoder of coding rate R=1/2 and DATA field is coded with coding rate of R = 1/2, 2/3, or 3/4, corresponding to the desired data. The convolutional encoder with the industry-standard generator polynomials, $g_0 = 133_8$ and $g_1 = 171_8$, of rate R = 1/2, with the constraint length of 7 is shown in fig. 1.11. The bit denoted as "P" is the output from the encoder before the bit denoted as "Q". Higher rates are derived from it by employing puncturing. Puncturing is a procedure for omitting some of the encoded bits in the transmitter (thus reducing the number of transmitted bits and increasing the coding rate) and inserting a dummy "zero" metric into the convolutional decoder on the receive side in place of the omitted bits. The puncturing patterns are illustrated in fig. 1.12. Decoding by the Viterbi algorithm is recommended.

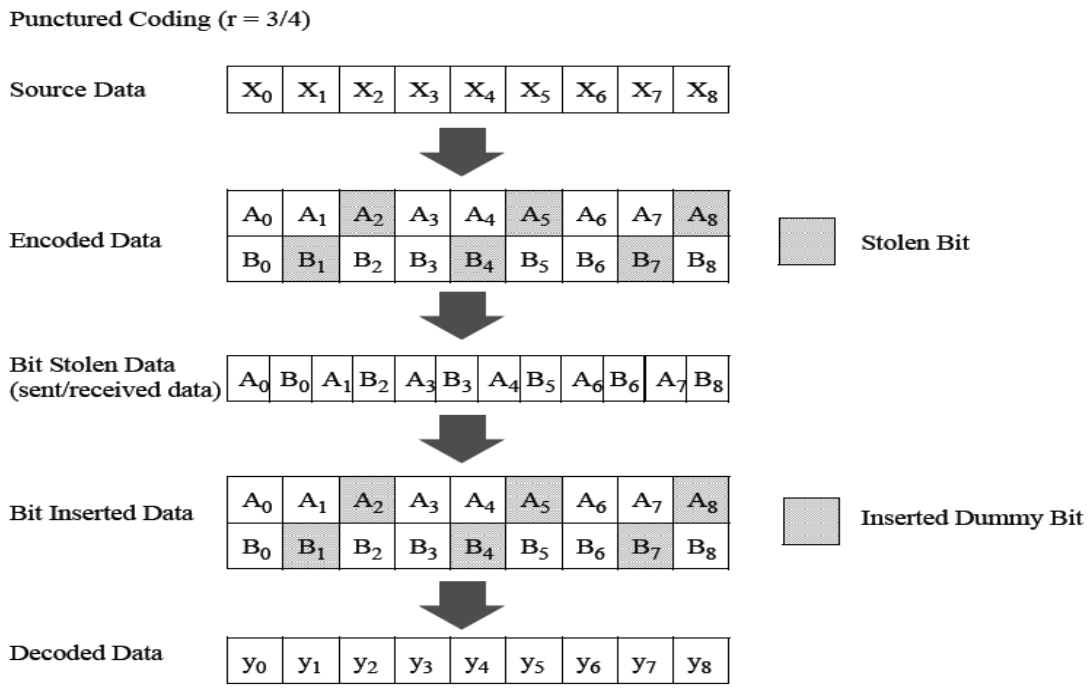

(a)

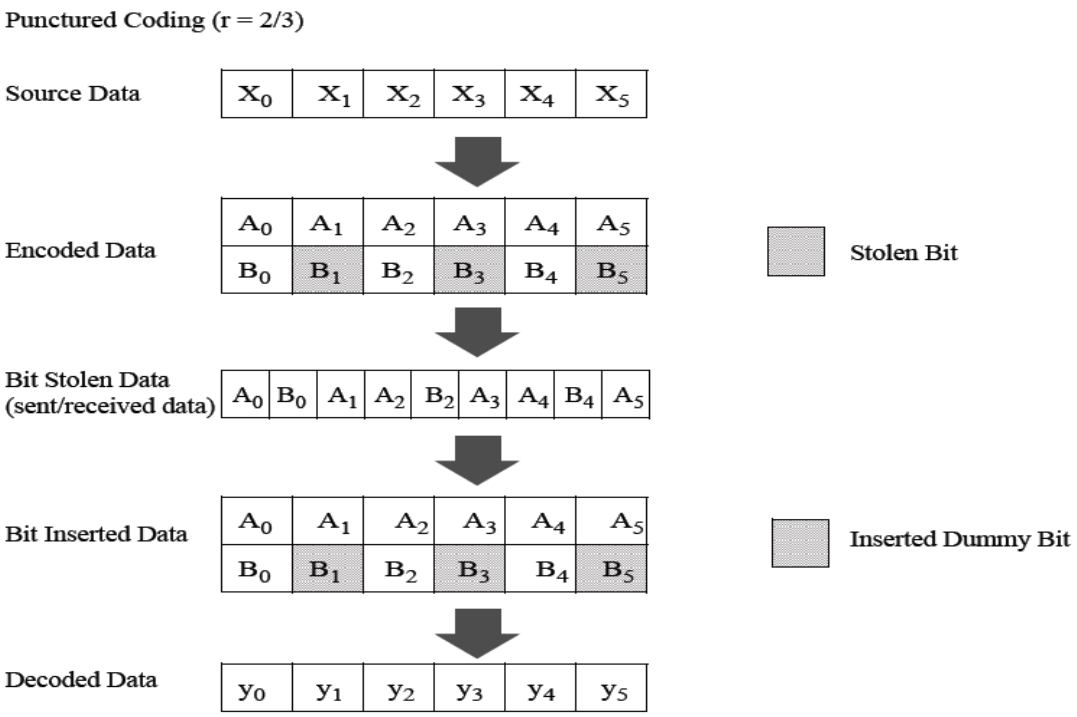

(b)

Figure 1.12 puncturing pattern for (a) code rate of 3/4 and (b) code rate of 2/3

1.3.4 Data interleaving and deinterleaving

Interleaver: After coding process data is interleaved by a block interleaver with a block size corresponding to the number of coded bits in a single OFDM symbol, N_{CBPS}. The interleaver is defined by a two-step transformation [15]. The first transformation guarantees that adjacent coded bits are mapped onto nonadjacent subcarriers. The second guarantees that adjacent coded bits are mapped alternately onto less and more significant bits of the constellation. The first transformation is defined by the rule

$$i = (N_{CBPS}/16)\,(k \bmod 16) + \text{floor}\,(k/16) \qquad k = 0, 1, N_{CBPS} - 1 \tag{1.21}$$

The second transformation is defined by the rule

$$j = \text{s} \times \text{floor}\,(i/\text{s}) + (i + N_{CBPS} - \text{floor}\,(16 \times i/N_{CBPS})) \bmod \text{s} \qquad i = 0, 1\ldots, N_{CBPS} - 1 \tag{1.22}$$

Where

k= index of the coded bit before the first transformation,

i= index after the first and before the second transformation,

j= index after the second transformation, just prior to modulation mapping.

The value of s is determined by the number of coded bits per subcarrier,N_{BPSC}, according to

$$\text{s} = \max\,(N_{BPSC}/2, 1) \tag{1.23}$$

Deinterleaver: This performs the inverse function of interleaving, is also defined by two transformations. Here the index of the original received bit before the first transformation is denoted by *j*; *i* shall be the index after the first and before the second transformation; and *k* shall be the index after the second transformation, just prior to delivering the coded bits to the convolutional (Viterbi) decoder. The first transformation is defined by the rule

$$i = s \times \text{floor}\,(j/\text{s}) + (j + \text{floor}\,(16 \times j/N_{CBPS})) \bmod s \quad j = 0, 1\ldots\ N_{CBPS} - 1 \tag{1.24}$$

where *s* is defined in Equation (1.23).

This transformation is the inverse of the transformation described in Equation (1.21). The second transformation is defined by the rule

$$k = 16 \times i - (N_{CBPS} - 1) \times \text{floor}\,(16 \times i/N_{CBPS})\ i = 0, 1 \ldots N_{CBPS} - 1 \qquad (1.25)$$

This transformation is the inverse of the transformation described in Equation (1.22).

1.3.5 Subcarrier Mapping and Modulation

The OFDM subcarriers are modulated by using BPSK, QPSK, 16-QAM, or 64-QAM, depending on the RATE at which data is to transmit. After coding and interleaving process, serial input data is divided into groups of N_{BPSC} (1, 2, 4, or 6) bits and converted into complex numbers (I+j.Q) representing BPSK, QPSK, 16-QAM, or 64-QAM constellation points respectively.

BPSK Modulation

For BPSK modulation serial data is divided into group of 1 bit (b_0). bit b_0 determines the real value (I) of complex number. Imaginary value (Q) is always 0. It is illustrated in table 1.3.

Table 1.3 BPSK encoding values

Input data (b0)	Real value (I)	Imaginary value(Q)
0	-1	0
1	1	0

QPSK Modulation

For QPSK modulation serial data is divided into group of 2 bit ($b_0 b1$). b_0 is the earliest bit. b0 determines the real value (I) and b1 decides imaginary value (Q) of complex number [8]. It is shown in table 1.4.

Table 1.4 QPSK encoding values

Input bit (b_0)	Real value (I)
0	-1
1	1

Input bit (b_1)	Imaginary value (I)
0	-1
1	1

16-QAM Modulation

For QPSK modulation serial data is divided into group of 4 bit ($b_0b_1b_2b_3$). b_0b_1 determines the real value (I) and b_2b_3 decides imaginary value (Q) of complex number as shown in table 1.5 .

Table 1.5 16-QAM encoding values

Input bits (b_0b_1)	Real value (I)
00	-3
01	-1
11	1
10	3

Input bits (b_0b_1)	Imaginary value (Q)
00	-3
01	-1
11	1
10	3

64-QAM Modulation

For 64-QAM modulation serial data is divided into group of 6 bit ($b_0b_1b_2b_3b_4b_5$). $b_0b_1b_2$ determines the real value (I) and $b_3b_4b_5$ decides imaginary value (Q) of complex number. It is shown in table 1.6.

The conversion is done according to Gray-coded constellation mappings. The output values, *d*, are formed by multiplying the resulting (*I*+*j*.*Q*) value by a normalization factor K_{MOD}, as described in Equation (1.26).

$$d = (I + j.Q) \times K_{MOD} \tag{1.26}$$

Table 1.6 64-QAM encoding values

Input bits ($b_0 b_1 b_2$)	**Real value(I)**
000	-7
001	-5
011	-3
010	-1
110	1
111	3
101	5
100	7

Input bits ($b_3 b_4 b_5$)	**Imaginary value(Q)**
000	-7
001	-5
011	-3
010	-1
110	1
111	3
101	5
100	7

The normalization factor, KMOD, depends on the base modulation mode, as prescribed in table 1.7. Note that the modulation type can be different from the start to the end of the transmission, as the signal changes from SIGNAL to DATA, as shown in fig. 1.6. The purpose of the normalization factor is to achieve the same average power for all mappings [16].

Table 1.7 Modulation dependent normalization factor (K_{MOD})

Modulation	K_{MOD}
BPSK	1
QPSK	$1/\sqrt{2}$
16-QAM	$1/\sqrt{10}$
64-QAM	$1/\sqrt{42}$

1.3.6 Serial to parallel convertor

After modulation of interleaved data, serial data is converted into parallel form of group 48 for 48 subcarriers out of 52 subcarriers.

1.3.7 Pilot Subcarriers

Pilots are added for channel estimation. There are main two methods to transmit pilots as shown in fig.1.13:

1. **Comb type:** Some part of the sub-carriers is always reserved as pilot for each symbol.
2. **Block type:** All sub-carriers is used as pilot but for a specific period [17].

In 802.11a, Comb type pilots are used and out of 52 subcarriers are reserved for pilots. In each OFDM symbol, four of the subcarriers are dedicated to pilot signals in order to make the coherent detection against frequency offsets and phase noise

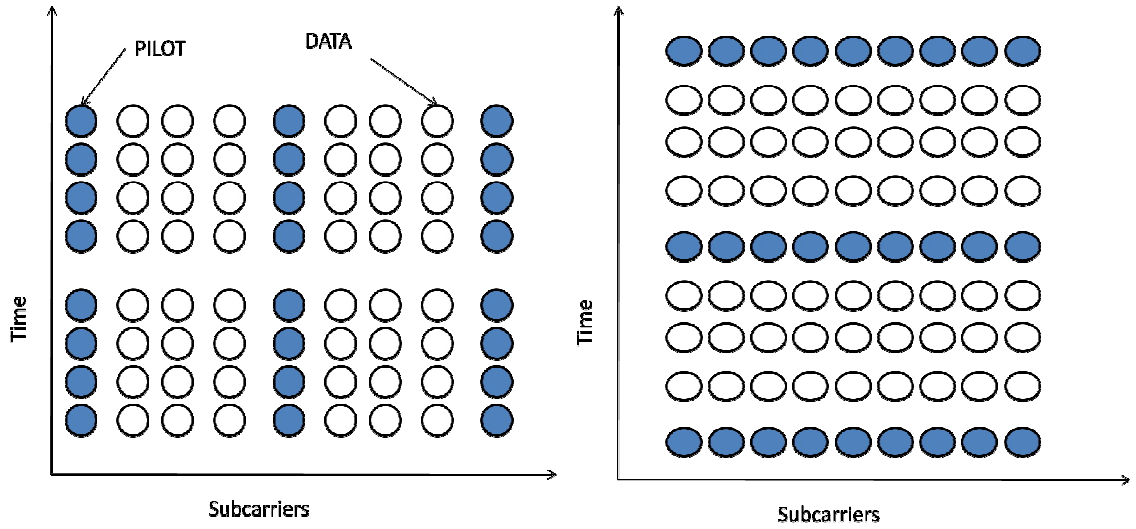

(a) (b)

Figure 1.13 Pilot insertion of (a) Comb type (b) Block type

Values of 4 pilots are [1 1 1 -1]. These pilot signals are put in subcarriers -21, -7, 7, and 21 as shown in fig. 1.4. The polarity of pilots is controlled by a pseudo-binary sequence to prevent the generation of spectral lines. This sequence is generated by the scrambler, same as is used in scrambling operation. Initial state of scrambler is chosen to all ones, and replacing all 1's with -1 and all 0's with 1. This sequence is given as

$p_{0,126}$ = [1,1,1,1, -1,-1,-1,1, -1,-1,-1,-1, 1,1,-1,1, -1,-1,1,1, -1,1,1,-1, 1,1,1,1, 1,1,-1,1, 1,1,-1,1, 1,-1,-1,1, 1,1,-1,1, -1,-1,-1,1, -1,1,-1,-1, 1,-1,-1,1, 1,1,1,1, -1,-1,1,1, -1,-1,1,-1, 1,-1,1,1, -1,-1,-1,1, 1,-1,-1,-1, -1,1,-1,-1, 1,-1,1,1, 1,1,-1,1, -1,1,-1,1, -1,-1,-1,-1, -1,1,-1,1, 1,-1,1,-1, 1,1,1,-1, -1,1,-1,-1, -1,1,1,1, -1,-1,-1,-1, -1,-1,-1] (1.27)

Each sequence element is used for one OFDM symbol. The first element, $p_0$multiplies the pilot subcarriers of SIGNAL symbol, while $p_1$to p_{126}be used for DATA symbols.

1.3.8 OFDM modulation

Modulation and demodulation in OFDM system can be achieved by IFFT and FFT, respectively. A data symbol in the "frequency domain" is transformed to "time-domain"

by performing the N (in 802.11a N=64) point IFFT operation, before being sent across to the wireless channel for transmission after radio frequency modulation.

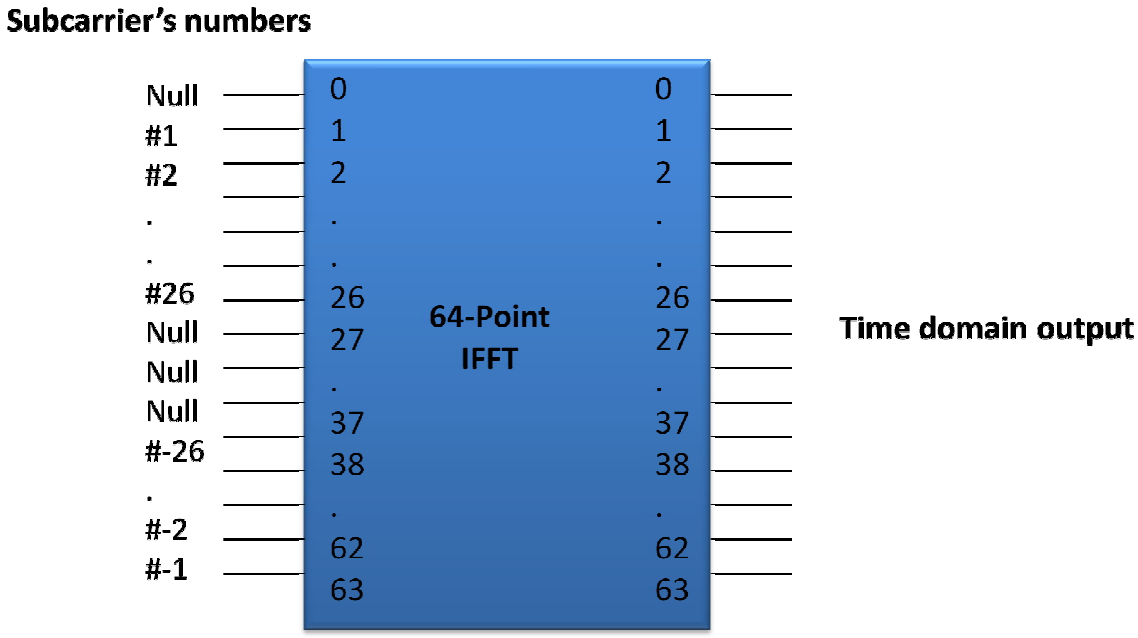

Figure 1.14 inputs and outputs of IFFT with subcarriers numbers

After adding pilot subcarriers, we have a total of 52 data in an OFDM symbol. These 52 data are allocated to their corresponding subcarriers as shown in fig.1.3. Additional null points are added to these data to make a total of 64, and then Inverse Fast Fourier transform (IFFT) of size 64 is taken to modulate data on different orthogonal subcarriers. Mathematical relation of data with IFFT is shown in equation (1.3), and location of different subcarriers with IFFT block numbers is shown in fig.1.14

1.3.9 Guard Insertion or Cyclic Prefix

In OFDM system, the use of Cyclic Prefix (CP) can promise orthogonality of signals even when they travel through multipath channels. To avoid ISI, the condition: $T_g > T_{max}$ should be satisfied, where T_g is the length of CP and T_{max} is the maximum delay spread in the environment [18]. To insert guard interval a last part of each OFDM symbol is appended to the front of symbol as shown in fig. 1.15.

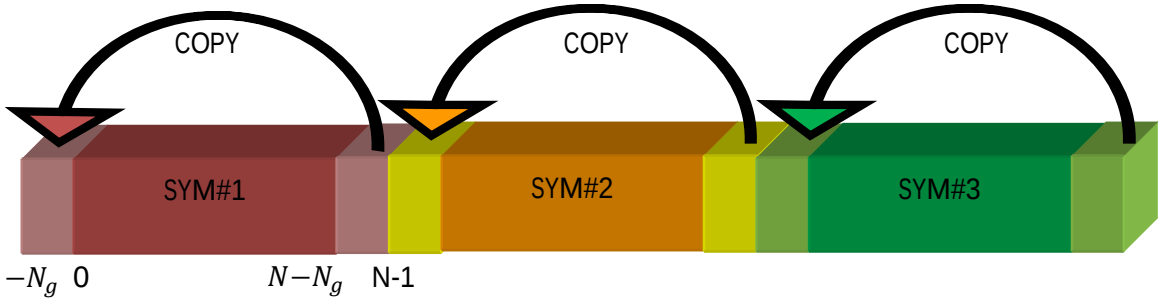

Figure 1.15: Guard insertion or cyclic prefix in OFDM

Assuming that the number of the extended OFDM symbol is N_g, then the period of a practical OFDM symbol is $T+T_g$, where T is single OFDM symbol time, T_g is the length of guard interval, which is inserted to suppress ISI caused by multipath distortion. An OFDM symbol including CP is expressed in equation (5). In 802.11a OFDM system a guard interval (T_g) of T/4 is taken. Since there are 64 bits per OFDM symbol including data bits, pilot bits and null bits. So 64/4=16 bits from last part of symbol is copied to front end of symbol so a total of 80 bits per OFDM symbol are sent.

1.4 Drawbacks of OFDM

- Problem of synchronization
    1. Symbol synchronization
    2. Frequency synchronization

- Need FFT units at transmitters and receiver
- Complexity of computation
- Sensitive to carrier frequency offset and phase noise. The frequency offset and phase noise will destroy the orthogonality among subcarriers and hence introduces ICI.
- The problem of high peak to average power ratio (PAPR) which reduces the efficiency of RF (radio frequency) amplifier.
- OFDM needs an adaptive or coded scheme to overcome spectral nulls in the channel.
- Efficiency gains reduced by requirement for guard interval.[19]

1.5 PAPR PROBLEM

In OFDM, after IFFT operation input data symbols are modulated on orthogonal subcarriers which are superimposed. So output is superposition of multiple subcarriers. In this situation some instantaneous output power may increase greatly and become far higher than the average power of the system [20]. This is defined as Peak to Average Power Ratio (PAPR). In the worst case, when the N signals are added with the same phase, they will produce a peak power that is N times the average power.

1.5.1 Effects of PAPR

High PAPR is one of the most serious problems in OFDM system. To transmit signals with high PAPR, it requires power amplifiers with very high linear dynamic range. These kinds of amplifiers are very expensive. When the signal input to the amplifier is increased, the output also increases. But this type of corresponding increment occurs up to a limit, beyond that limit amplifier becomes saturated and cannot produce any more output; this is called clipping, and results in distortion. This non-linear distortion changes the superposition of the signal spectrum resulting in performance degradation and spectral splatter [21]. If there are no actions to reduce the high PAPR, OFDM system could face serious limitation for practical applications. To avoid this distortion, for high PAPR, the RF power amplifiers needs to be operated under large back-offs due to the limited linear region. Thus high PAPR reduces the efficiency of RF power amplifiers. However, these types of amplifiers are generally very costly and therefore are of no practical use. On the other side, certain algorithms having good performance were introduced to reduce the high PAPR. Hence, in this thesis, some currently promising PAPR reduction methods are studied and compared. The performance of these reduction schemes are done by using simulation software, Matlab.

1.5.2 Mathematical Description of PAPR

Theoretically, high peaks in OFDM system can be represented as Peak-to-Average Power Ratio, or referred to as PAPR, in some literatures, also written as PAR. It is defined as the

ratio of peak power to average power. It is usually expressed in dB. It is usually defined as [22]:

$$PAPR\ or\ PAR = \frac{P_{peak}}{P_{average}} = 10\ log_{10}\left(\frac{\max\left([|x_n|^2]\right)}{E[|\ x_n|^2]}\right)\ in\ dB \qquad (1.28)$$

Where P_{peak} represents peak output power, $P_{average}$ means average output power. $[\cdot]$ denotes the expected value, x_n represents the transmitted OFDM signals which are obtained by taking IFFT operation on modulated input symbols X_k, as shown in equation (1.3).

By observing the simulation result in fig. 1.16, we can make a conclusion that the appearance of peak amplitude is very rare, thus it does not make sense to use $\max([|x_n|^2])$ to represent peak value in real application. Therefore, PAPR performance of OFDM signals is commonly measured by certain characterization constants which are related to probability

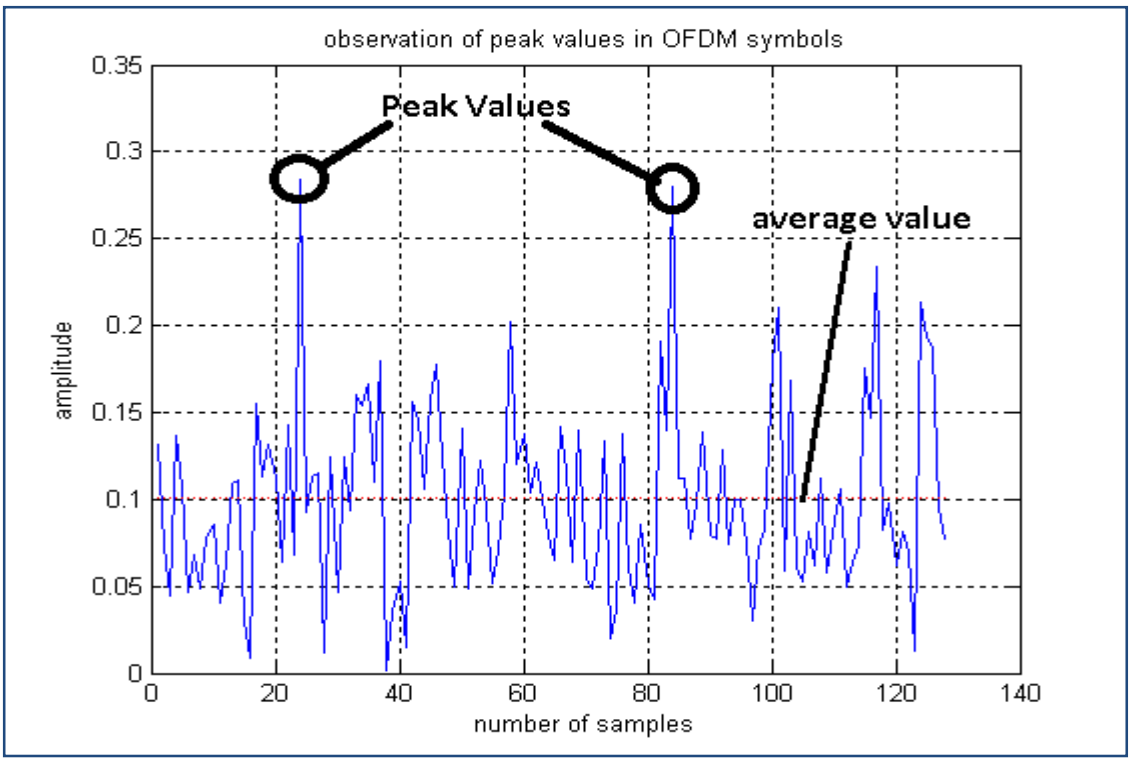

Figure 1.16 High peak values in OFDM symbols

1.6 Various PAPR Reduction Techniques

There are many different algorithms that have been proposed to solve the high PAPR problem of OFDM system. These reduction solutions can be roughly divided into three categories [23]**:**

1.6.1 Signal distortion techniques

This kind of techniques includes clipping, peak windowing, peak cancellation and companding [24]. Out of these, Clipping and Filtering is the most used and easiest approach. It can clip the signal at the transmitter to a clip level so as to remove the appearance of high peaks above that level. Clipping can be implemented to the discrete samples earlier to Digital to Analog Convertor (DAC) and RF amplifier. This process causes nonlinear distortion. So orthogonality will be destroyed to some extent which results in band noise and out of band noise. In-band noise cannot be removed by filtering, it increases the bit error rate (BER). Out-of- band noise reduces the bandwidth efficiency but filtering can be employed to minimize the out-of-band power. Although filtering removes out of band radiations, it may cause peak re-growth. To overcome this drawback, the whole process is repeated several times until a desired situation is achieved. Furthermore, some other novel proposals which combine this method with coding and/or signal scrambling have already been studied by other researcher.

1.6.2. Signal Scrambling Techniques

In this algorithm, OFDM symbol is scrambled with different scrambling sequences and select one which has the smallest PAPR value for transmission. It can reduce the probability of high PAPR to a great extent. This type of approach includes:

- Selective Mapping (SLM)
- Partial Transmit Sequences (PTS).

SLM method [25] applies scrambling rotation to all sub-carriers independently while PTS method [26] only takes scrambling to part of the sub-carriers. Performance of these techniques does not depend on the number of sub-carriers and type of modulation. While scrambling techniques are very efficient in reducing PAPR, they still have some

problems. The scrambling techniques have to calculate PAPR at the transmitter and the information of the selected scrambling sequence needs to be known at the receiver for descrambling. They suffer from high computational complexity and a slight loss of transmission rate. This results in low bandwidth utilization and high hardware complexity for implementation.

16.3 Coding Techniques

The main idea of coding techniques is to pick some code words with low PAPR . Some code words will also have some error correcting capability. The classical schemes include linear block code [27], Golay codes [28] and Reed-Muller code [29]. Among them, Golay complementary sequences derived from Reed-Muller codes are good codeword candidates and also provide a good error correcting performance at the same time. As far as linear block code method is concerned, it is only suitable to the scenario which has a small number of sub-carriers, which results in limited applications. Although coding is a good approach to the PAPR problem, it is hard to find enough code words with small PAPR, especially for OFDM system with large N.

Chapter 2

Literature Review

In this chapter, the technical background of this thesis is reviewed. Many schemes have been proposed to solve the PAPR problem. However, none of these schemes have produced significant reduction of PAPR without affecting other performance such as bit error rate or headache of sending additional information.

S.H. Muller et al. [30] proposed a very flexible method to reduce PAPR with almost zero redundancy. This new method works with any number of subcarriers. In this proposal a partial transmit sequence (PTS) is added to minimize PAPR distortion less. In Partial Transmit Sequence (PTS) approach, transmitted symbols are multiplied with the weighting factors or rotation factors that are selected by transmitter to modify the subcarrier amplitude. So PAPR was reduced with different weighting factors for different symbols. But in PTS there was a drawback of transmitting the weighting factors explicitly, since they are required for decoding at the receiver side. This needs also a number of iterations to find the optimum combination of factors for OFDM symbols.

Adaptive PTS was proposed by A.D.S. Jayalath et al. [31]. This algorithm offered to reduce number of iterations by fixing a desired threshold level of PAPR and trial for different weighting factors until the PAPR reduced below that threshold level. In this 256 subcarriers are used with QPSK modulation technique. Results showed that PAPR can be reduced by 4.0 dB and 4.1 dB with adaptive and without adaptive PTS respectively. But there was a problem of sending side information which results in a decrease in the bandwidth efficiency.

Theodoros et al. [32] proposed a low-complexity PTS-based technique. In this new technique, there is no burden of transmitting side information for weighting factors. In this, at the receiver side the proposed decoder uses the predetermined values of pilot tones and investigates all the allowed combinations of weighting factors, so as to identify the factor combination employed by the transmitter.

A technique to reduce PAPR with combined interleaving and peak windowing method is given by H. Sakran et al. [33]. By using proposed scheme, a PAPR reduction of 3.5 dB is achieved over the original system and also SNR decreases by more than 3dB for BER of 10^{-3} over the original system.

R.W. Bauml et al. [34] proposed a Selected Mapping (SLM) technique to reduce PAPR for arbitrary number of sub-carriers. In SLM, a small amount of redundancy, required to reduce PAPR, is spread over all sub carriers.

The sequence modification (SM) method has been suggested by Yan Xin et al. [35]. Due to addition of PTS technique, the number of sub-blocks in the system increases so the complexity also increases. Conventional PTS system involves generation of all partial transmit sequences through IFFT operations and optimization of the weighted PTS. By use of SM, complexity of system and number of IFFT operations significantly reduces.

A new technique for OFDM BPSK systems to reduce PAPR, based on the auto-correlation property of data symbol sequence, is proposed by Pavol Svac et al. [36]. In this technique amount of PAPR reduction does not changes with the number of sub-carriers. For implementing this technique, some complementary parity encoder needs to be employed. This gives a low complexity solution. Moreover, the redundancy of the code enables simple error control. But it requires more bandwidth.

Tone-reservation (TR) technique is proposed by J. Tellado-Mourelo [37], this technique exploits a small number of unused subcarriers (reserved tones) to generate a peak-canceling signal. TR does not degrade the BER performance but requires an efficient generation of the peak-canceling signal. An optimal solution for peak-canceling signal is obtained by solving a Quadratically Constrained Quadratic Program (QCQP), which is a type of convex optimization problem. A drawback of this optimal solution is its slow convergence which leads to a high complexity of computation. And another thing is that in 802.11a OFDM system there are total of 52 sub-carriers and all of these are occupied by data and pilots. So no question arises for not using this technique in 802.11a OFDM system.

J. Davis et al. [38] proposed coding techniques (Golay complementary sequences, and Reed-Muller codes) with the capabilities of both PAPR reduction, as well as error correction. However, these codes significantly reduce the overall throughput of the system, especially if there are a relatively large number of subcarriers.

Desire Guel et al. [39] analyzed and compared various clipping techniques to reduce the PAPR. In this paper, Classical-Clipping (CC), Heavyside-Clipping (HC), Deep-Clipping (DC) and Smooth-Clipping (SC) are implemented for reducing the PAPR of an OFDM system. The effectiveness of these techniques in terms of PAPR-reduction, average power variation and total system degradation are evaluated. From the analysis and simulation results, it is very difficult to say which of these four is the best. But, because of its flexibility in PAPR reduction, in total system degradation and in average power variation, DC technique appears to be the best of the four.

The effects of clipping techniques on Partial Response Signaling (PRS)-OFDM are discussed by Sharifah K. Syed-Yusof [40].In this work, integer PRS polynomial that maximizes the Carrier-to-Interference power Ratio (CIR) are used. However, the PRS-OFDM system suffers PAPR increment due to the partial response polynomial functions. In this paper, the performance of suboptimum PRS-OFDM at different polynomial length, *K* when clipping is used as a method to reduce the PAPR are investigated.

Two clipping techniques: the separate clipping of the real and imaginary parts of the complex envelope (denoted “type 1” clipping) and the envelope clipping (denoted “type 2” clipping) are discussed by Rui Dinis et al. [41]. The impact of oversampling and filtering issues is taken into account, together with the type of clipping and the choice of the clipping level, when calculating power spectral densities and BER performances. Their results show that an appropriate envelope clipping, together with a small oversampling factor and a mild filtering, leads to the best performances and is strongly recommendable for OFDM applications.

Two new algorithms are discussed by Farzaneh Kohandani et al. [42] to reduce the PAPR. The first algorithm is carried out by selecting the input sequences properly using a

look up table and the second by scaling the input envelope or subcarriers before they are transformed to the time domain by IFFT.

Due to the simplest way for PAPR reduction, the clipping techniques [43-46] have been proposed. In this thesis, we focus on clipping-based PAPR reduction techniques and also commanding techniques since all techniques come under the category of signal distortion techniques. In all these techniques there is no need of sending side information to the receiver side. So a saving in bandwidth efficiency is there.

Chapter 3

Gaps in Studies, Objectives and Methodology

3.1 Gaps in Studies

Various PAPR reduction techniques are discussed such as SLM, PTS and Tone Injection etc in [31-38]. But a problem in all these techniques was that OFDM transmitter has to send side information for the receiver side.

S.H. Muller et al. [30] proposed a very flexible method to reduce PAPR with almost zero redundancy with PTS. But there was a drawback of transmitting the weighting factors explicitly, since they are required for decoding at the receiver side. This needs also a number of iterations to find the optimum combination of factors for OFDM symbols.

J. Davis et al. discussed about the Golay complementary sequences, and Reed-Muller codes with the capabilities of both PAPR reduction, as well as error correction [38]. However, these codes significantly reduce the overall throughput of the system, especially if there are a relatively large number of subcarriers. But in our 802.11a system there are no large numbers of subcarriers, so these codes will not work in our system.

Four clipping techniques have also been discussed by Desire GUEL et al. [39]. In this paper, DC has been found to have better performance over all clipping techniques. So in this thesis we will also see the performance of these clipping techniques and will find out the best clipping technique out of these four techniques.

In this paper ΔPAPR is evaluated for various clipping techniques. In this ΔPAPR is defined as the difference of PAPR value with clipping technique from the PAPR value without the clipping technique. Since clipping technique will reduce PAPR, so this difference should come negative but it is shown positive and all graphs related to this shows positive values. Here in this thesis discussion of ΔPAPR is also done to show the problem that has evaluated from this paper.

3.2 Objectives

The primary objectives of this thesis can be summarized as follows:

- To study and simulate the OFDM transmitter and receiver on PPDU frame format base structure.
- To show that the PAPR of system does not depend on the bit rate or modulation scheme of the OFDM system and to prove that Deep Clipping Technique has no optimum value of Deep Clipping Factor (α) for which it gives a good PAPR reduction performance
- To discuss and study the various clipping and companding techniques to reduce PAPR.
- To study and analyze the various PAPR reduction techniques on the basis of histogram, Complementary Cumulative Distributive Function (CCDF), BER, average power variation and ΔPAPR.

3.3 Methodology

In this thesis to evaluate the performance of various PAPR reduction techniques, many parameters are presented and discussed. Then an experiment is done to show the relation of PAPR with the various modulation schemes or data rate systems. Then a various PAPR reduction techniques are discussed with their mathematical formulation and by their characteristics plots. Experimental results are then obtained using various Clipping Techniques with well known characteristics in order to show the efficiency and accuracy of them.

In addition different data rate systems are used for different experiments to show the broad applicability of the optimum PAPR reduction technique.

The experimental results of various clipping and companding techniques, when applied to the system of same data rate and same raw data, are also reported to show the comparisons with one another.

Chapter 4

Simulations and Results using Matlab

4.1 Performance Parameters

The system simulations are performed using an IEEE 802.11a WLAN standard. And the performances of different techniques are performed with the following performance parameters.

4.1.1 Histogram Performances

In this, we make a histogram of number of symbols along with their corresponding PAPR values [47]. This gives two statics about PAPR. First it shows the upper limit of PAPR value that the symbols may have. And second distribution of number of symbols corresponding to their PAPR values

4.1.2 Complementary Cumulative Distribution Function (CCDF)

To measure the efficiency of any PAPR reduction technique Cumulative Distribution Function (CDF) is one of the most frequently used parameters. Normally, the Complementary CDF (CCDF) is used instead of CDF [48], which helps to find the probability that the PAPR of a certain data block exceeds the given threshold PAPR i.e. $PAPR_0$. Statistics are given in terms of the CCDF. The CCDF shows the probability of an OFDM frame exceeding a given PAPR.

We can evaluate the high peak of the signal using a distribution of instantaneous power that is normalized by the mean power. In this paper, we evaluate the distribution based on a Complementary Cumulative Distribution Function (CCDF), denoted as

$$CCDF(PAPR_0) = \Pr\{PAPR \geq PAPR_0\}, \tag{4.1}$$

Which shows a probability or fractions of PAPRs that exceeds a threshold level of $PAPR_0$.

4.1.3 Delta PAPR (ΔPAPR)

We denote ΔPAPR the performance in terms of PAPR reduction defined as [49]

$$\Delta PAPR = PAPR_{No\ Clip} - PAPR_{Clip} \ , \qquad [dB] \tag{4.2}$$

Where $PAPR_{Clip}$ is the required PAPR to obtain a specific value of the CCDF when clipping is used, while $PAPR_{No\ Clip}$is the required PAPR to obtain the same value of the CCDF when clipping is not used, i.e., when none PAPR reduction is done.

4.1.4 BER performance

Performance of PAPR reduction is also done with bit error rate analysis [50]. All PAPR reduction techniques reduce PAPR to a considerable limit but on the other side there is an increment in data loss also. So an analysis on BER should also be done to find an optimum result.

4.1.5 Average Power Variation (ΔE)

Another aspect of performance evaluated in this paper is the average power variation denoted ΔE and expressed as [49]:

$$\Delta E = P_{Clip} - P_{No\ Clip} \ , \quad [dB] \tag{4.3}$$

Where P_{Clip} is the average power of the signal when clipping is used, while $P_{No\ Clip}$ is the average power of the signal when none PAPR reduction is done [49].

4.2 Influence of Different Bit Rates on PAPR

In 802.11a OFDM system different bit rate systems include different modulation techniques and coding rate. So an analysis of different data rate systems on PAPR performance is shown in fig. 4.1. It displays a set of CCDF curves which are transmitted by different data rates with the number of sub-carriers N=64. Results show that there is only small difference between different data rates or modulation schemes or coding schemes on PAPR performance. Thus, different data rates have minimum influence on PAPR performance.

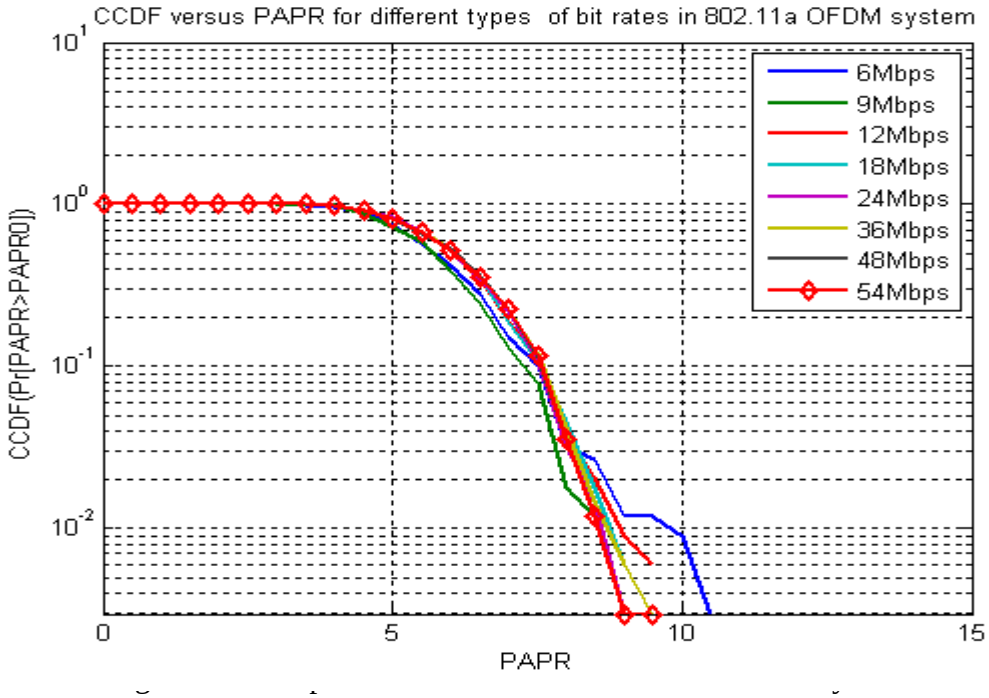

4.3 Signal Distortion Techniques

4.3.1. Clipping Techniques

As stated in chapter 1, clipping is the simplest PAPR reduction technique. OFDM system with clipping and filtering is shown in fig 4.2. In this system, the behavior of clipper is represented by a clipping function $f_c(.)$ which changes according to the type of clipping technique used to reduce PAPR.

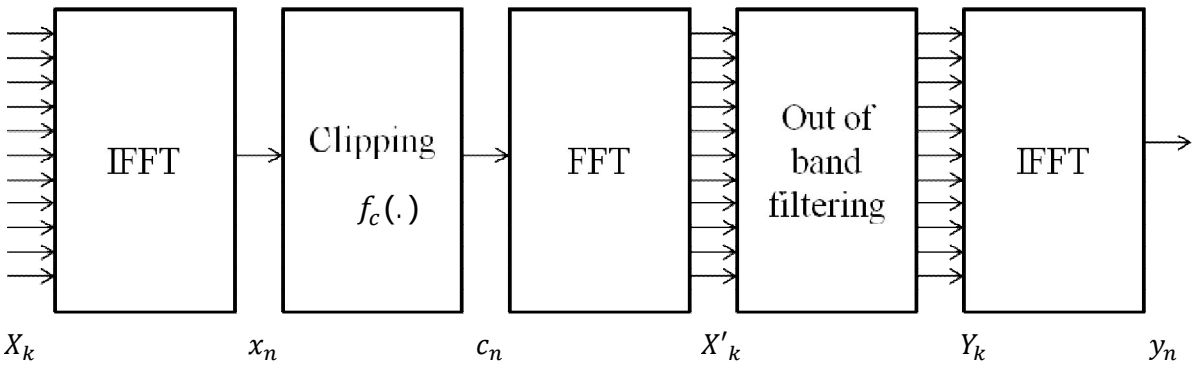

Figure 4.2: OFDM system with Clipping and Filtering

Rewriting the discrete-time OFDM signal x_n to polar coordinates gives $x_n = r_n e^{j\varphi_n}$, where r_n represents the amplitude of x_n and φ_n represents the phase of x_n. The clipped signal c_n is expressed as

$$c_n = f_c(r_n)\, e^{j\varphi_n} \tag{4.4}$$

where the clipping function $f_c(r_n)$ is according to the type of clipping used.

After clipping operation, OFDM symbol x_n is transformed to c_n. The filter used in fig. 4.2 for out-of-band filtering is based on FFT/IFFT pair. This filter consists of a FFT followed by an IFFT operation [39]. The forward FFT transforms c_n back to the frequency-domain to obtain X'_k. In between we processed this frequency data with low pass filter to get Y_k . The components of $\boldsymbol{X'}$ in the in-band are passed unchanged while the components of $\boldsymbol{X'}$ in out-of-band are fixed to zero, The IFFT operation transforms Y_k back to the time-domain. This results in the filtered clipped signal y_n at the output of the filter-based FFT/IFFT pair [51]

Clipping Ratio (A): Any technique which clips the signal at a level is denoted as A. if the average value of a signal is denoted as P_x. We define the Clipping Ratio (CR) as [52]

$$CR = 20\, log_{10}(A/\sqrt{P_x}) \text{ [dB]} \tag{4.5}$$

In this section, we focus on four clipping-based PAPR reduction techniques:

1. Classical-Clipping (CC) or Hard Clipping,
2. Heavyside-Clipping (HC),
3. Deep-Clipping (DC) and
4. Smooth-Clipping (SC).

Their effectiveness in terms of PAPR-reduction, average power variation and BER are studied and compared with each other in context of OFDM-based WLAN system.

4.3.1.1 Classical Clipping (CC) technique.

The Classical Clipping (CC) proposed by J. Armstrong [43], is one of the most admired clipping techniques for PAPR reduction. It is sometimes also called hard clipping or soft clipping. The clipping function for CC technique is defined below and shown in fig. 4.3.

$$f_c(r_n) = \begin{cases} r_n & \text{if } r_n \leq A \\ A & \text{if } r_n > A \end{cases} \quad (4.6)$$

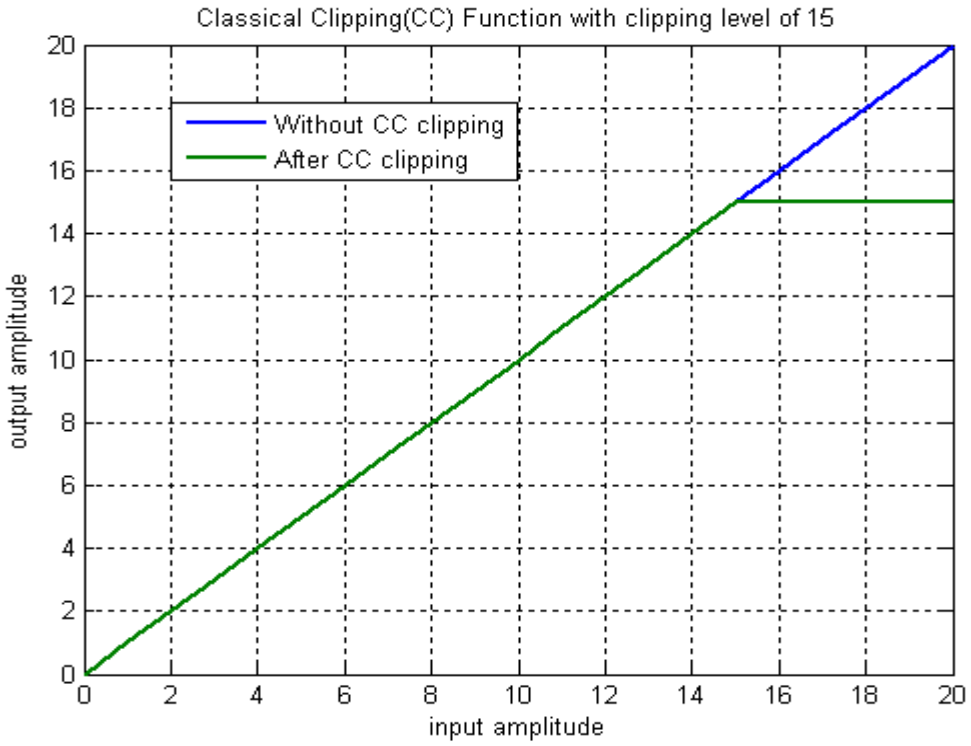

Figure 4.3: Classical Clipping Technique

In this technique, the signal having amplitude greater than a predefined threshold level A is limited to that level i.e. A and signal having amplitude lower than A are passed through undisturbed.

Histogram performance:-

Fig 4.4 and fig 4.5represents the histogram of number of OFDM symbols corresponding to their PAPR values. Fig 4.4 shows the histogram of original OFDM system without any

clipping at 36 Mbit/s data rate and a data of 8000 bits is done for simulation. Here maximum value of PAPR is going up to 9.5 dB. In fig 4.5 histogram of OFDM system with classical clipping technique at the clipping ratio of 2.5 dB is shown, where the maximum value of PAPR is observed to be 5 dB. So a total of 4.5 dB gain is received after the CC clipping.

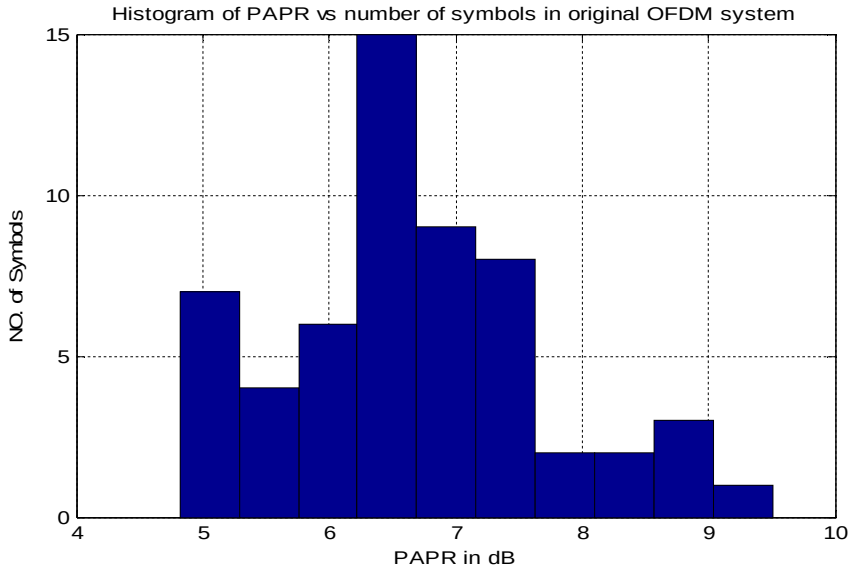

Figure 4.4: Histogram of PAPR in original OFDM system

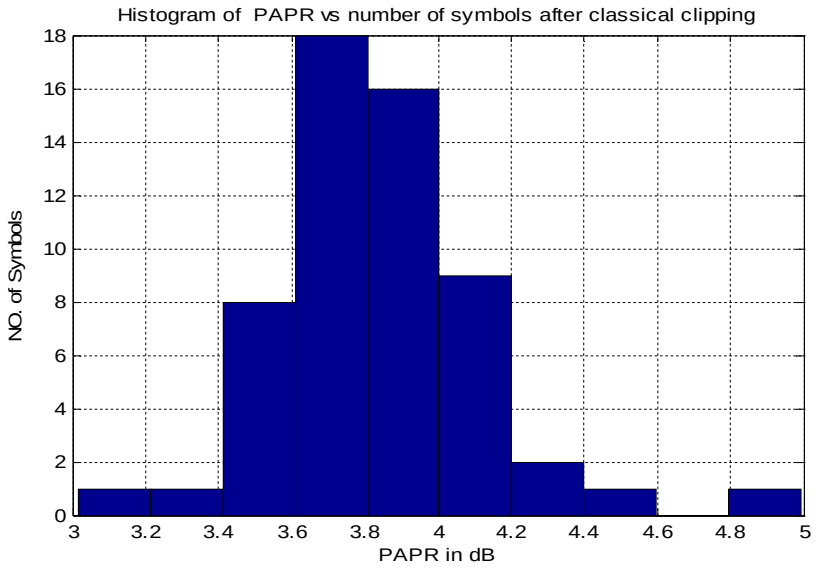

Figure 4.5: Histogram of PAPR for OFDM with CC technique

CCDF Plot:-

A CCDF plot of CC technique is shown in fig. 4.6. In this CCDF plot of CC technique is compared with the original OFDM system. More the PAPR reduces more the plot of CCDF moves towards the origin. In this fig. we observe that in CC technique, probability of symbols having PAPR greater than 5 dB is near to zero.

Delta PAPR (ΔPAPR):

The variation of ΔPAPR with clipping ratio is shown in fig. 4.7 from this simulation we observe that we gain maximum gain of 5.5 dB at clipping ratio of 0dB i.e. when we clip the signals at average value of whole signal we get maximum gain. As we increase the clipping ratio or increase the clipping level above the average level, the PAPR reduction gain decreases. After 7.5 dB there is no gain in PAPR reduction so clipping is done between 0 to 7.5db range to affect the PAPR.

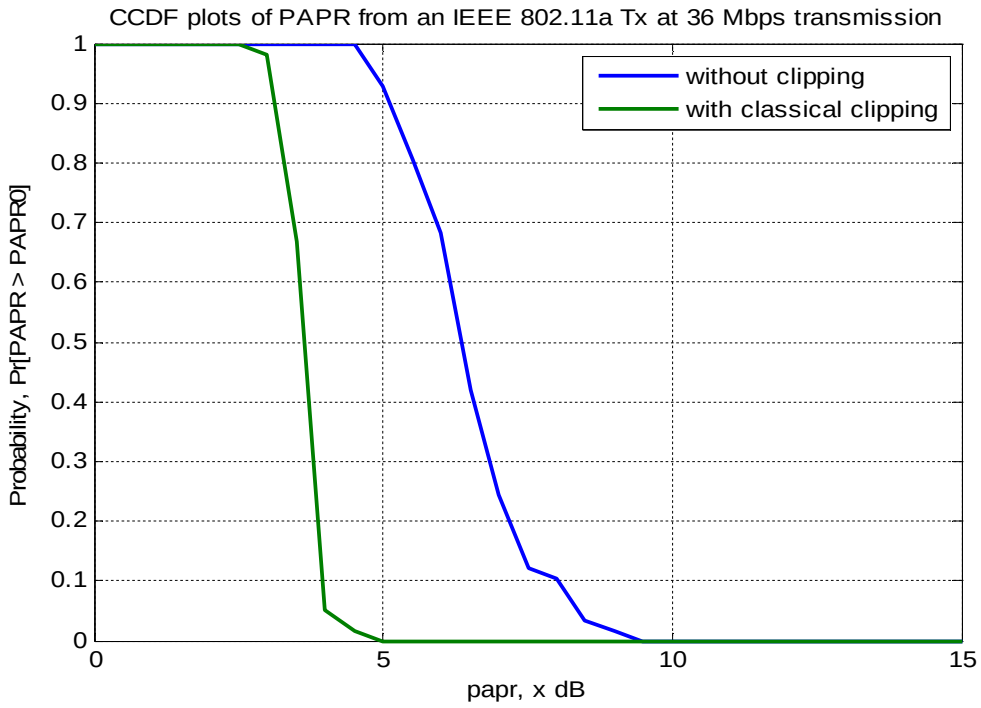

Figure 4.6: PAPR reduction performance of CC technique

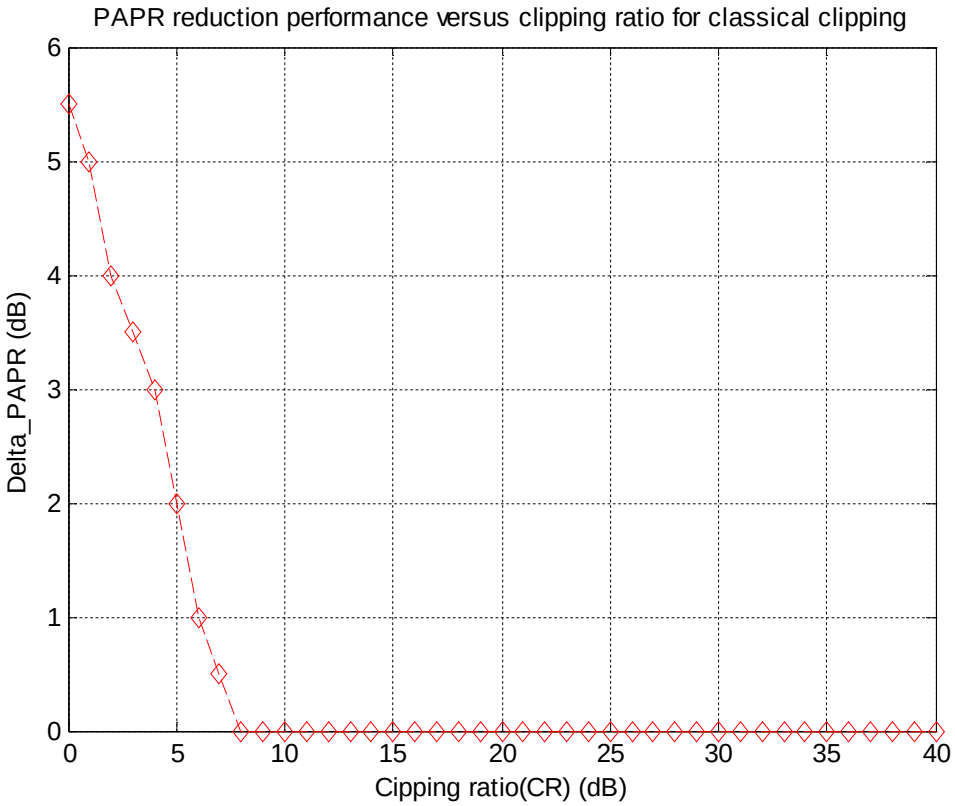

Figure 4.7: ΔPAPR performance for CC technique

BER Performance and Average Power Variation:-

BER performance and average power variation of CC technique will be done with the all clipping techniques in the last to show the comparison between them at the same clipping ratio.

4.3.1.2 Heavyside Clipping (HC) Technique

HC is used as a baseband nonlinear transformation technique to improve the overall communication system performance [46]. It is used in this paper for OFDM PAPR reduction. The Heavyside function is expressed below and depicted in fig. 4.8.

$$f_c(r_n) = A \quad \forall\, r_n \tag{4.7}$$

The HC technique is a case of school; it is widely used in theory but very rarely in practice. We will see further in simulation results that it is the worst of the four techniques studied in this paper.

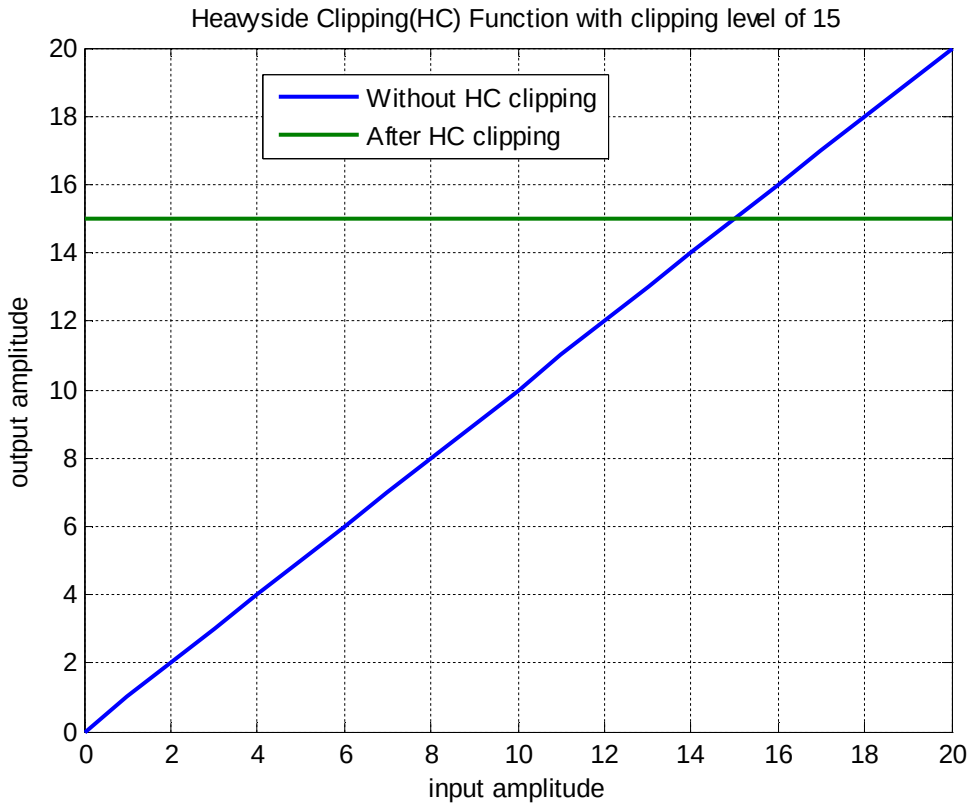

Figure 4.8: Heavyside Clipping Technique

Histogram performance:-

Histogram performance of HC is shown in fig. 4.9 and 4.10. Since Heavyside is an ideal case of clipping, so in this technique PAPR reduces from 8.25 dB to 3×10^{-15} i.e. nearly 0 dB at the clipping ratio (CR) of 2.5 dB.

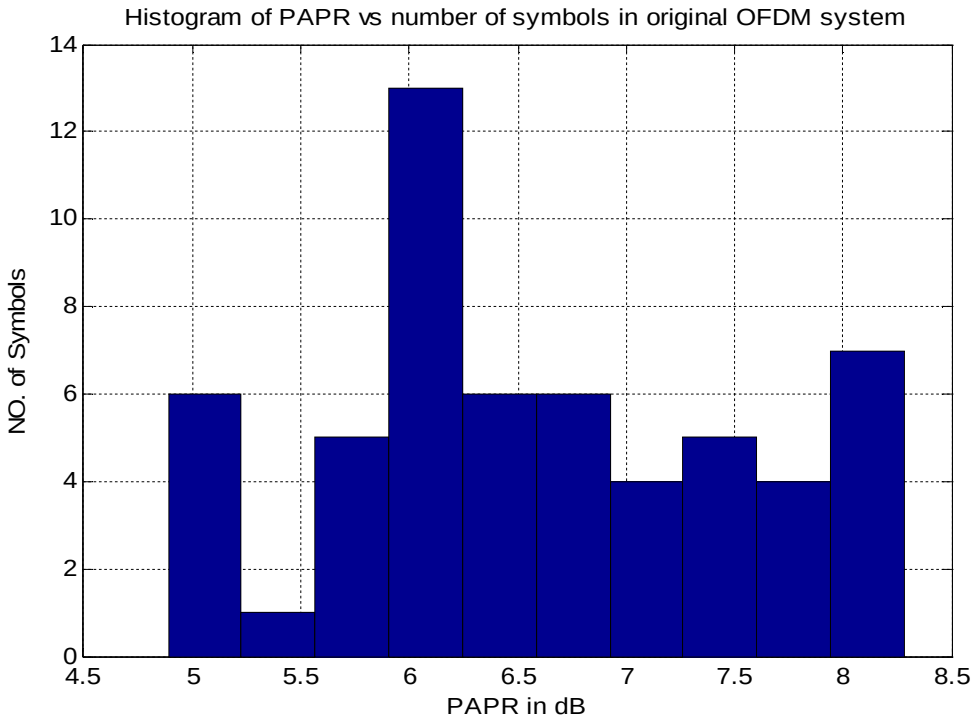

Figure 4.9: Histogram of PAPR with original OFDM system

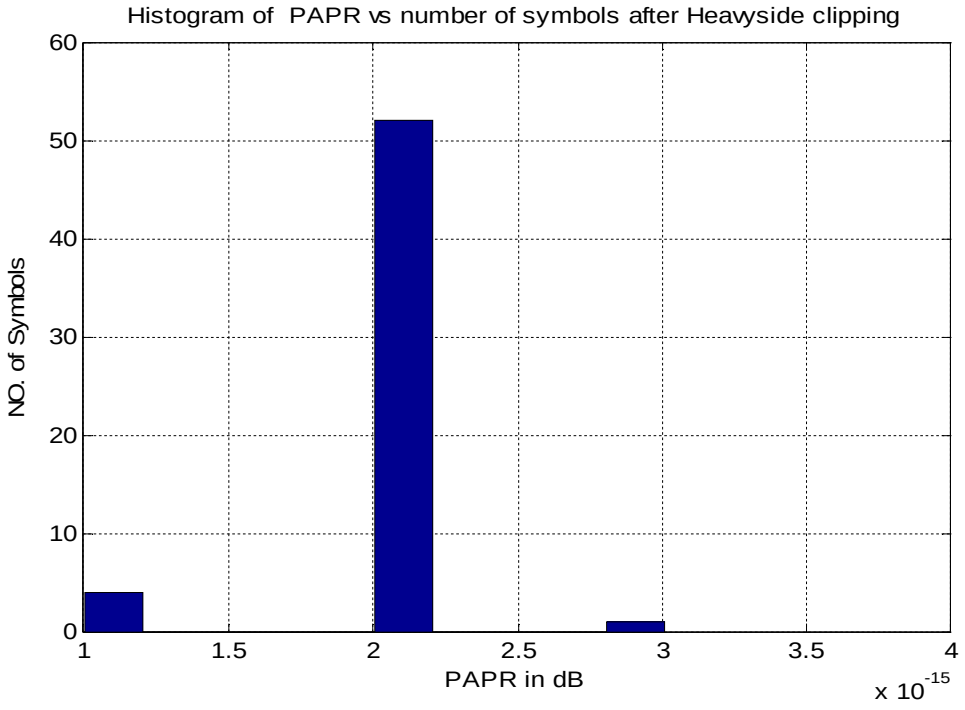

Figure 4.10: Histogram of PAPR for OFDM with Heavyside clipping technique

CCDF plot:-

CCDF or probability curve of HC technique is shown in fig. 4.11. In this the CCDF plot is not appearing in the fig. it is because due to a perfect clipping technique its PAPR value goes to zero. So this is appeared in the bottom zero line of graph with the green line.

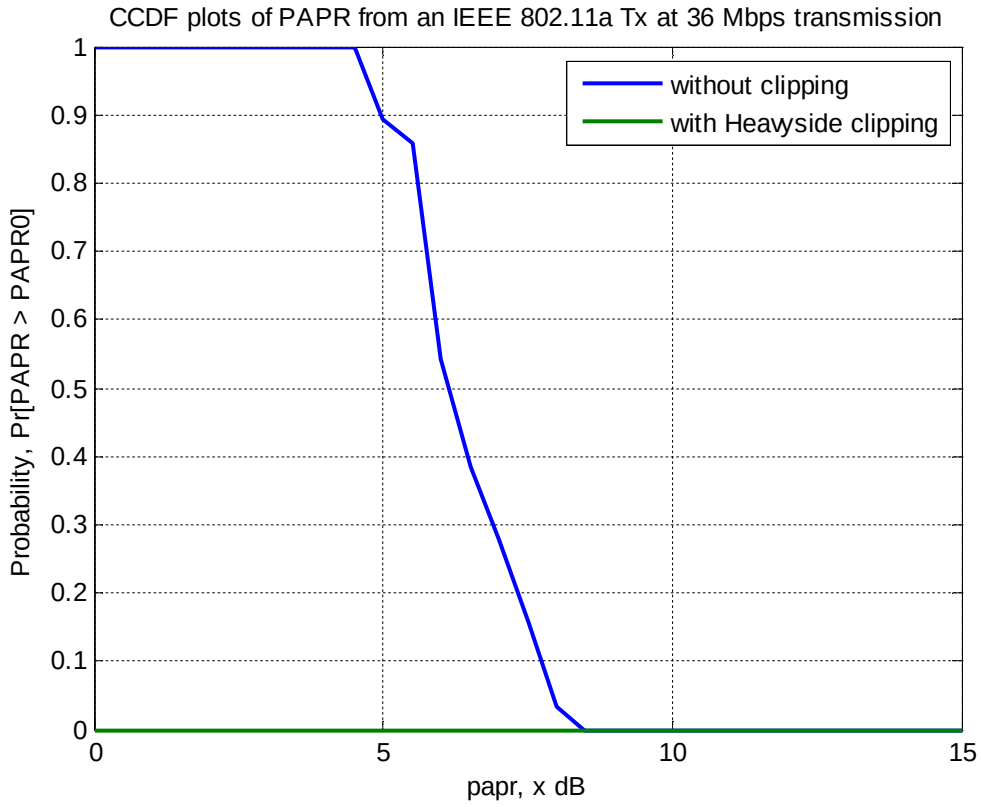

Figure 4.11: PAPR reduction performance of Heavyside clipping technique

Delta PAPR (ΔPAPR):

The ΔPAPR versus CR is shown in fig. 4.12 from this we observe that for all values of clipping ratio, gain in PAPR reduction remains constant and it gives a maximum PAPR gain of 9.5 dB out of all clipping and companding techniques.

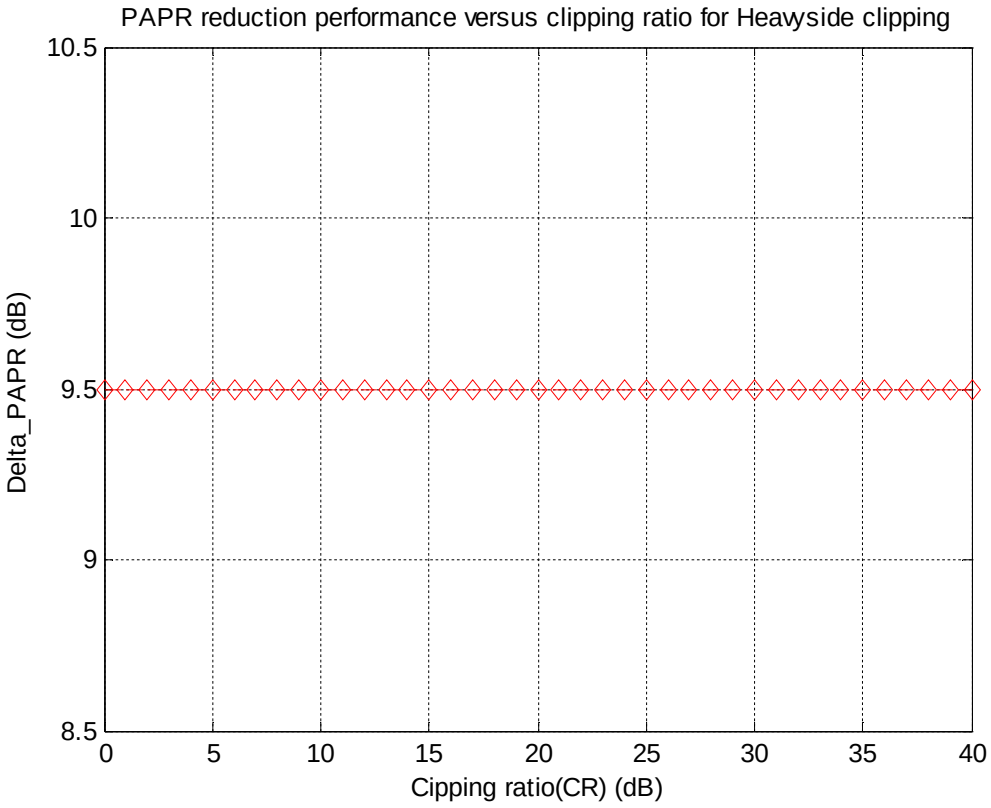

Figure 4.12: ΔPAPR performance for Heavyside clipping technique

4.3.1.3 Deep Clipping (DC) Technique

One problem of Clipping and Filtering (CAF) is peak re-growth due to the filtering for the clipped signal. Deep clipping method is used suppress the peak re-growth and to reduce the Peak-to-Average power Ratio (PAR) of OFDM signals without iteration of CAF blocks [46]. So, in DC technique, the clipping function is modified in order to "deeply" clip the high amplitude peaks. A parameter called clipping depth factor has been introduced in order to control the depth of the clipping. The function based clipping used for DC technique is defined below and shown in fig 4.13.

$$f_c(r_n) = \begin{cases} r_n & if\ \ r_n \le A \\ A - \alpha(r_n - A) & if\ A < r_n \le \dfrac{1+\alpha}{\alpha} A \\ 0 & if\ r_n > \dfrac{1+\alpha}{\alpha} A \end{cases} \tag{4.8}$$

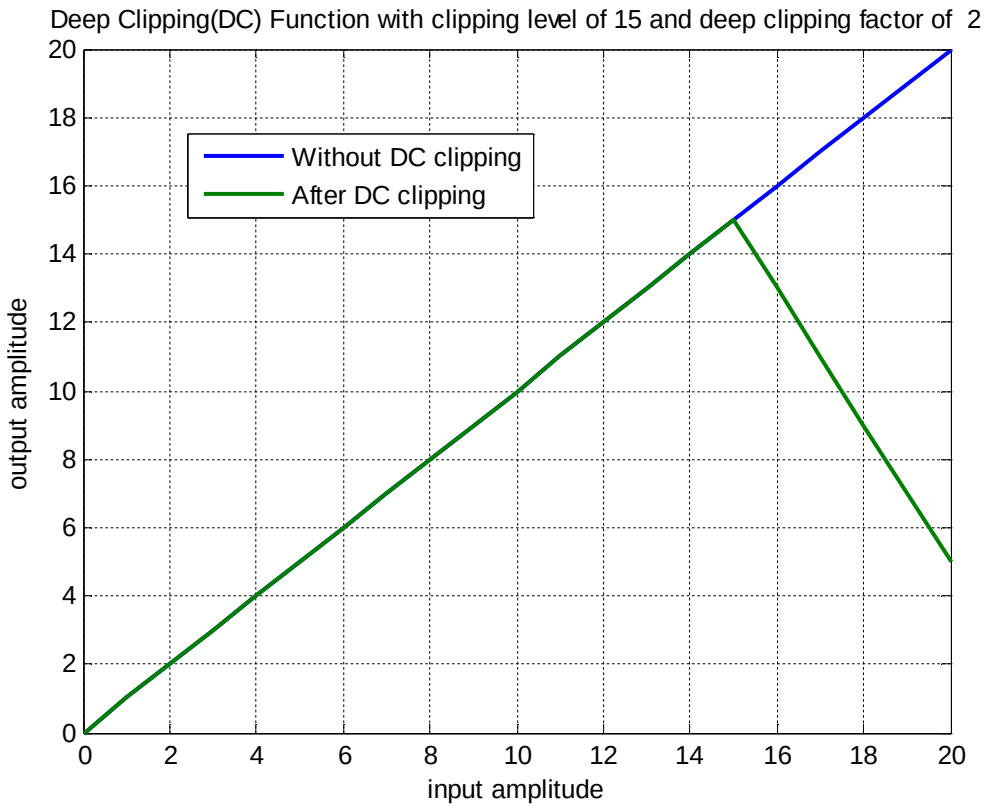

Figure 4.13: Deep Clipping Technique

Where α is called the clipping depth factor. As the input amplitude values go beyond the threshold level, clipped values do not remains at the threshold level as in case of CC but decreases below that level, and rate of decrement to zero depends on the value of deep cleaning factor (α). The effect of α on clipped output signal is shown in fig. 4.14, by taking different values. From the fig. 3.5 we observe that as we increase the values of α, the rate of decrement also increases. If we set α to zero, then DC will be same as of CC. so it can be said that CC is special case of DC

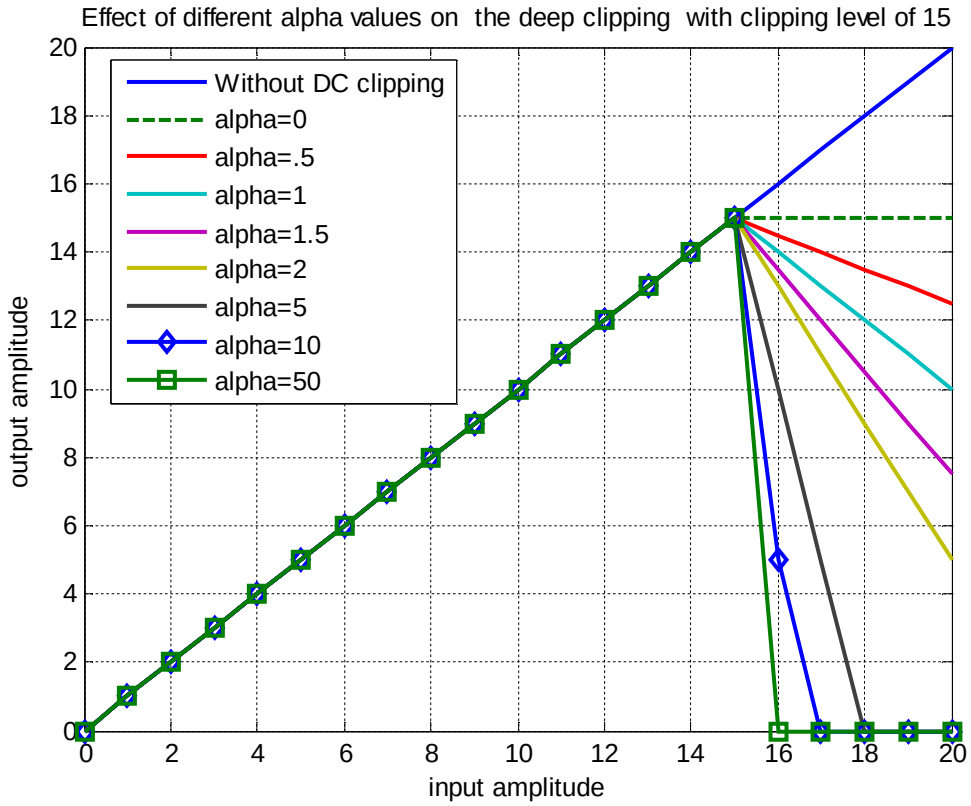

Figure 4.14: Effect of different α values in Deep clipping

Histogram performance:-

Histogram of original OFDM and OFDM with DC technique is shown in fig 4.15 and fig. 4.16 respectively. Here a gain of 5 dB is achieved in PAPR raduction at 2.5 dB of CR and value of clipping depth factor is taken to be 0.3. Unlike CC, signals having level greater than clipping level do not have a constant value of clipping level but this decreases corresponding to clipping depth factor (α). So there are a large number of signals having low value of PAPR is generated, as shown in fig 4.16.

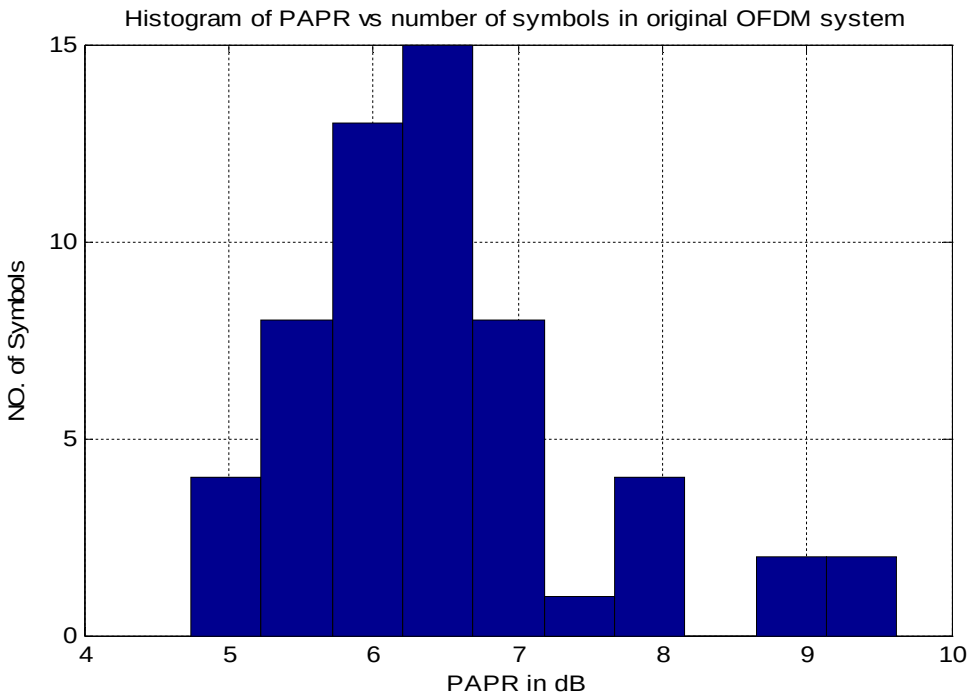

Figure 4.15: Histogram of PAPR with original OFDM system

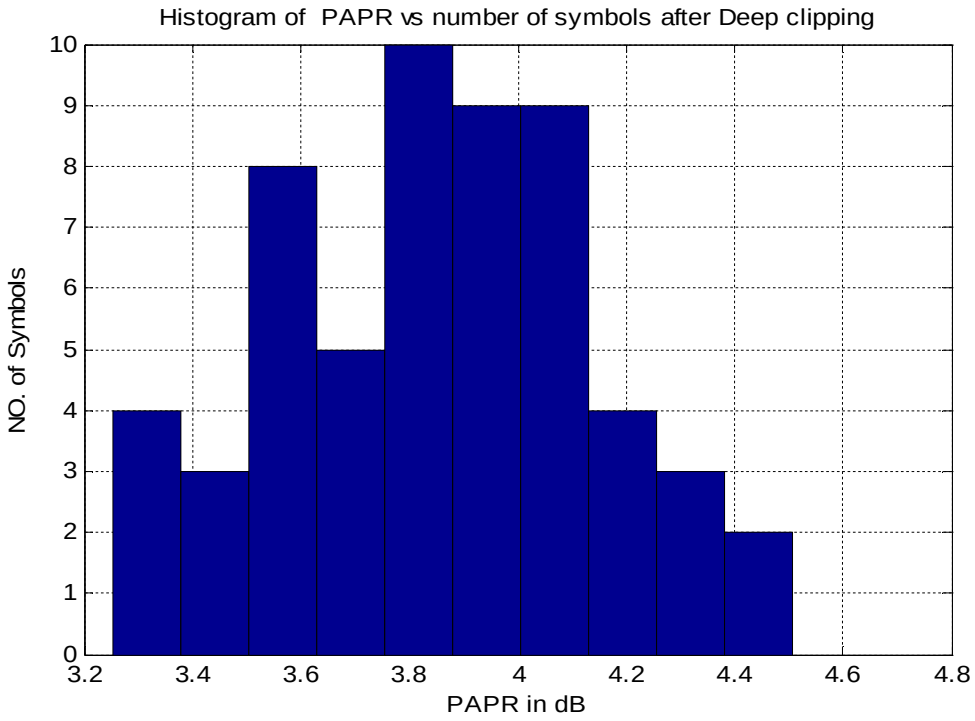

Figure 4.16: Histogram of PAPR for OFDM with DC technique

CCDF Plot:

A CCDF plot of DC technique is shown in fig. 4.17 in this CCDF plot of DC technique is compared with the original OFDM system. In this fig. we observe that in DC technique, probability of symbols having PAPR greater than 4.5 dB is near to zero. This is better than CC technique at the basis of probability of PAPR. In CC this value is 5 dB so a 0.5 dB gain is achieved by DC technique.

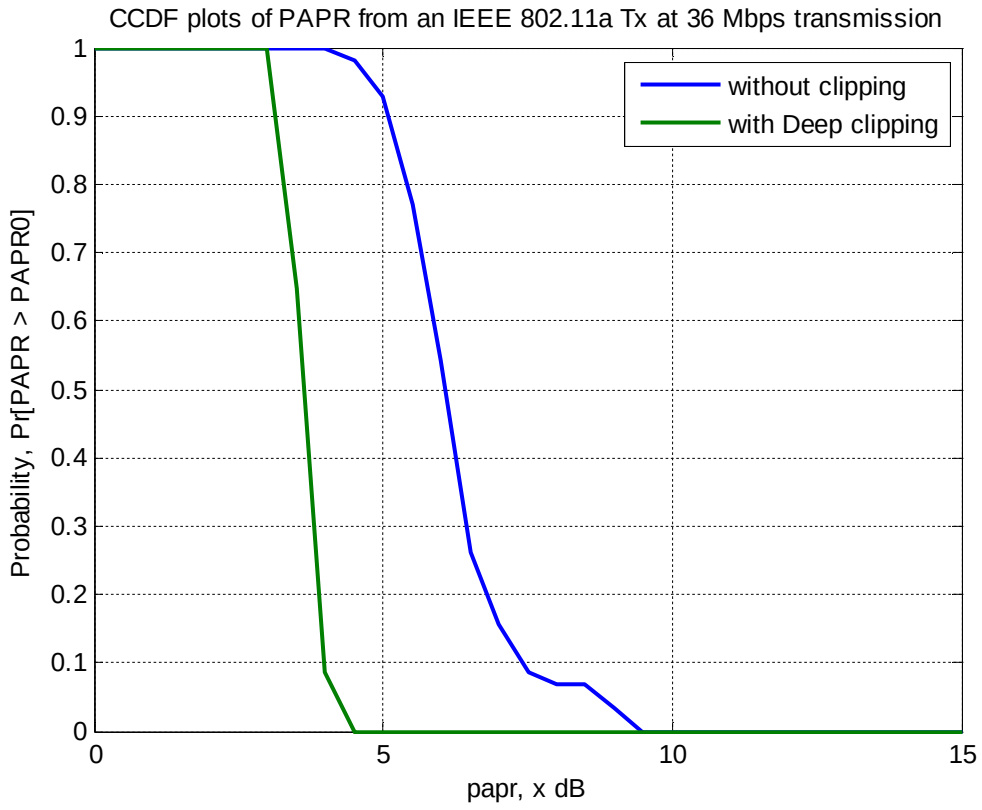

Figure 4.17: PAPR reduction performance of DC technique

Delta PAPR (ΔPAPR):

The variation of ΔPAPR with clipping ratio is shown in fig. 4.18 from this simulation we observe that we gain maximum gain of 5 dB at clipping ratio of 0 to 2.5 dB. After 9.5 dB

there is no gain in PAPR reduction so clipping is done between 0 to 9.5db range to affect the PAPR.

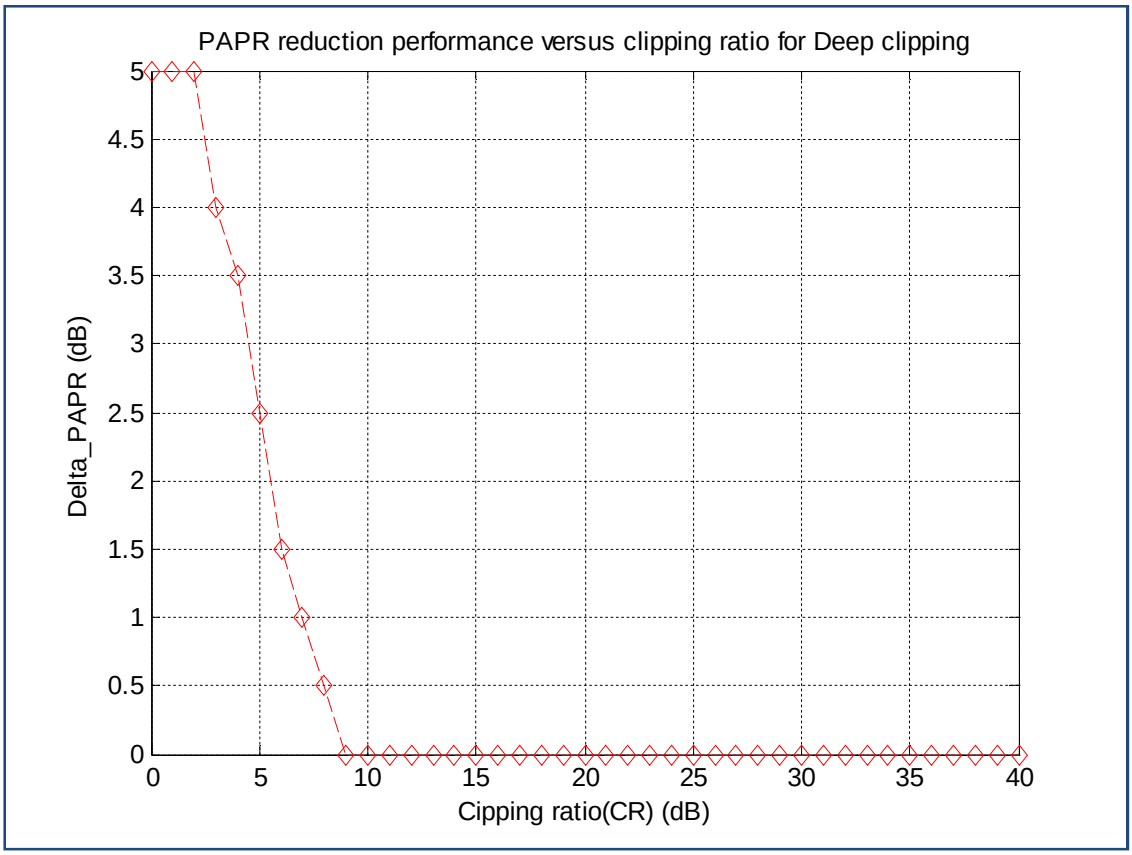

Figure 4.18: ΔPAPR performance for DC technique

Deep Clipping Performance

In this subsection, we analyze the effect of α on ΔPAPR in order to find the optimal α for WLAN systems. Fig. 4.19 shows the variation of clipping depth factor effect on the PAPR reduction performance and table shows the corresponding ΔPAPR for different CR values. It is observed that there is an optimum value of α of the value of zero at which it gives maximum PAPR reduction gain. In our simulation we varied the α for the CR value of 0.0, 0.5, 1.0, 1.5 and 2.5 dB. And get the response of PAPR reduction gain. We observe that as we increase the value of α, gain decreases correspondingly. For CR of 0dB we get maximum gain of 6.1dB but at clipping depth factor of 0. For all CR values, there is maximum gain at zero value of clipping depth factor. So at α=0, we get the

optimum result. But if we see the DC technique equation sincerely then we comes at this conclusion that at α=0 DC converts to CC technique. So we think that there is no usage of introduction of DC technique in OFDM system.

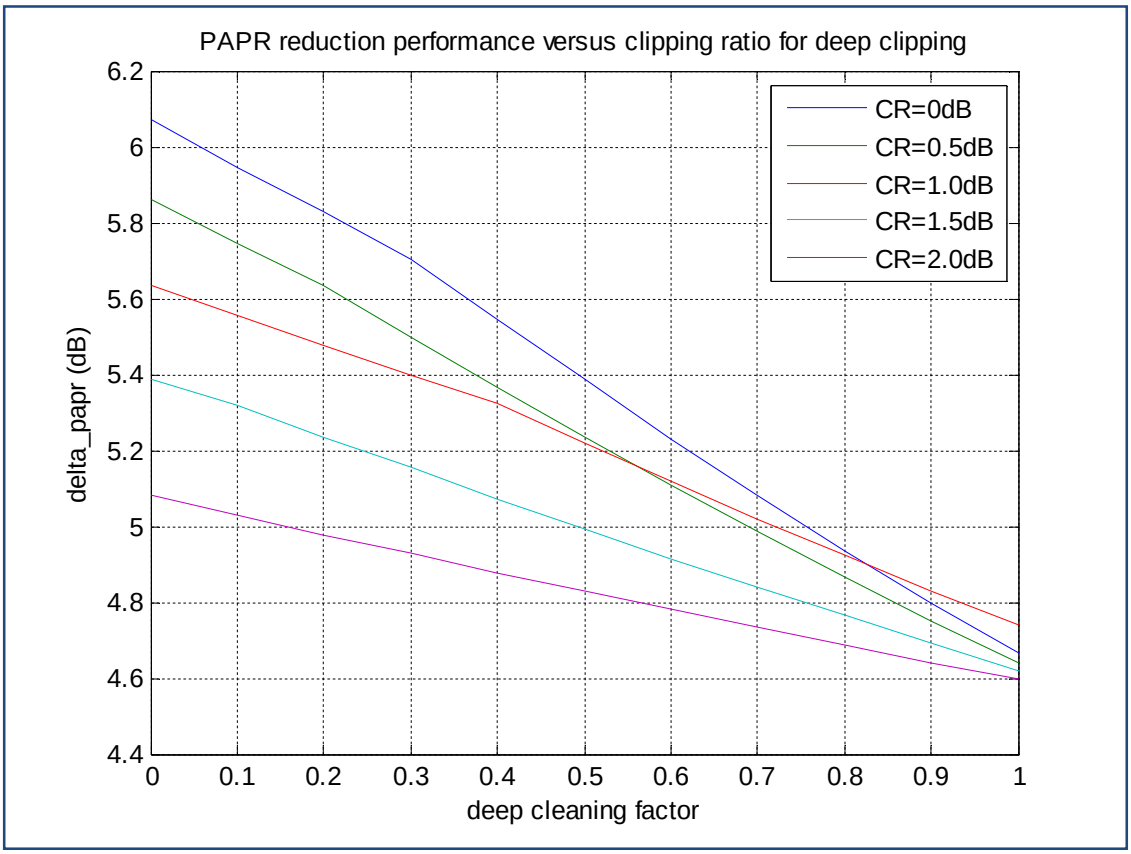

Figure 4.19: ΔPAPR performance for different values of α

4.3.1.4 Smooth Clipping (SC) technique

A Smooth Clipping technique used to reduce the OFDM PAPR is described by P. Boonsrimuang et al. [46]. In this paper, the function based-clipping for SC technique is defined below and depicted in fig. 4.20.

$$f_c(r_n) = \begin{cases} r_n - \dfrac{{r_n}^3}{b} & r_n \le 3A/2 \\ A & r_n > 3A/2 \end{cases}, \qquad (4.9)$$

where $b = \frac{27}{4}A^2$.

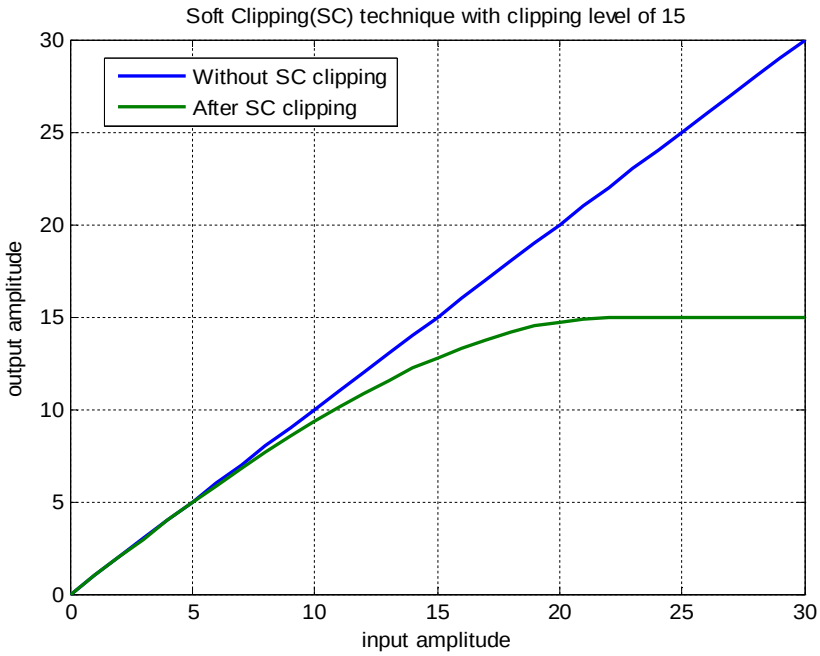

Figure 4.20: Soft Clipping Technique

Histogram performance:-

Histogram of original OFDM and OFDM with SC technique is shown in fig. 4.21 and fig. 4.22 respectively. Here a gain of 4.75 dB is achieved in PAPR raduction at 2.5 dB of CR.

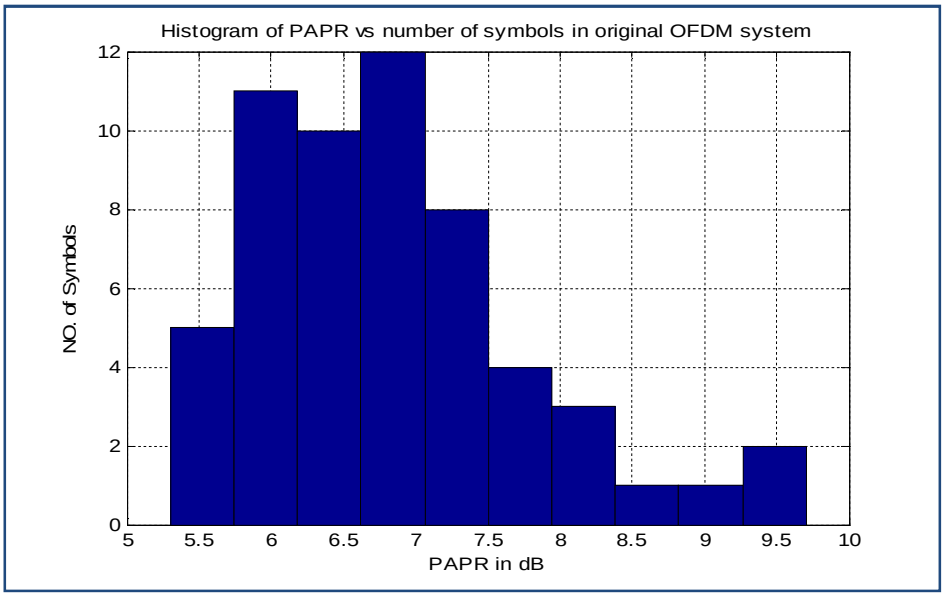

Figure 4.21: Histogram of PAPR with original OFDM technique

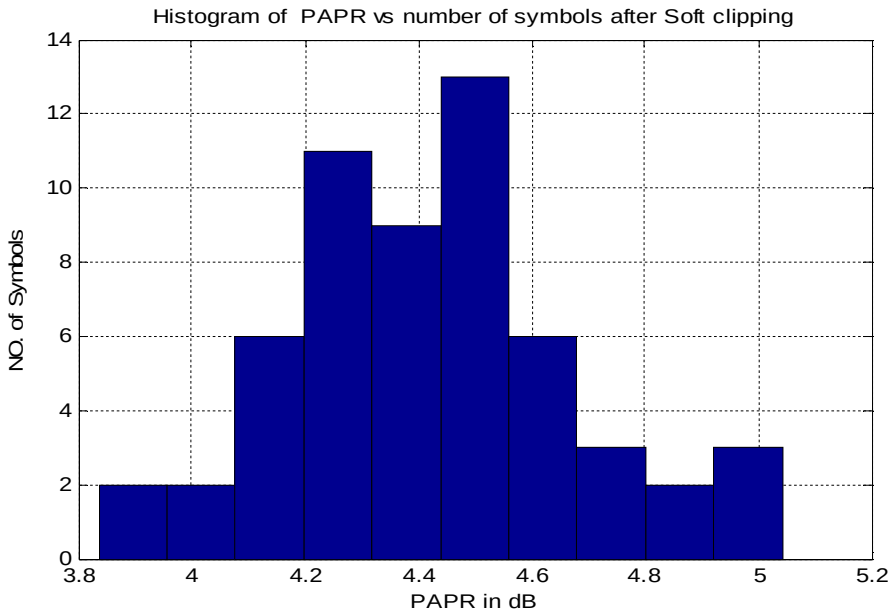

Figure 4.22: Histogram of PAPR for OFDM with SC technique

CCDF Plot:-

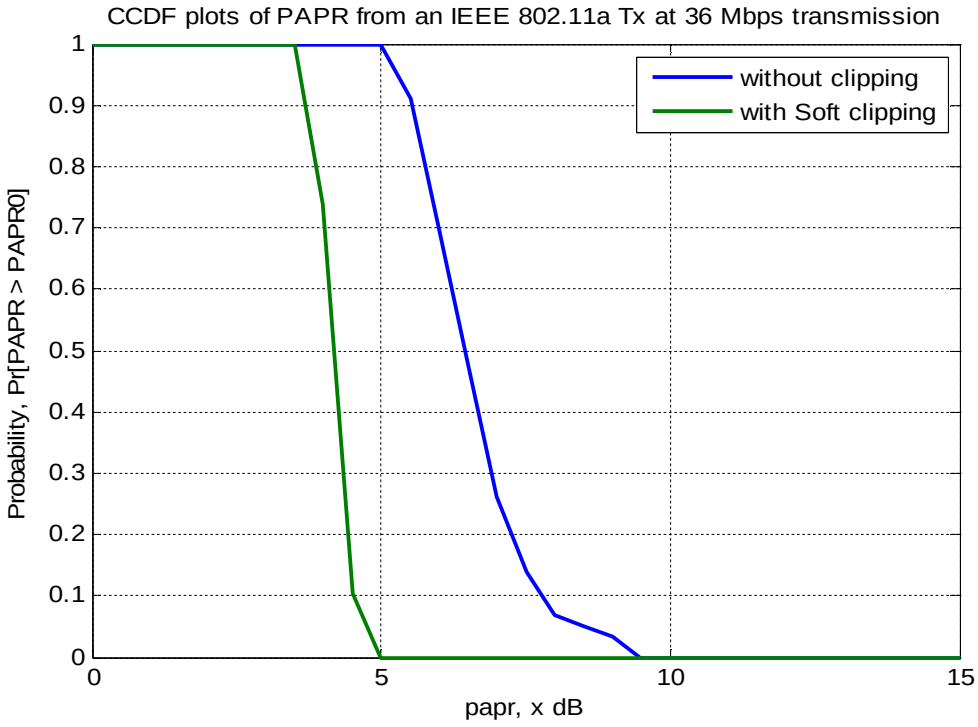

Figure 4.23: PAPR reduction performance of SC technique

A CCDF plot of SC technique is shown in fig. 4.23 in this CCDF plot of DC technique is compared with the original OFDM system. In this fig we observe that in SC technique, probability of symbols having PAPR greater than 5.0 dB is near to zero. In CCDF performance it is nearly same to CC technique.

Delta PAPR (ΔPAPR):

The variation of ΔPAPR with clipping ratio is shown in fig. 4.24 from this simulation we observe that we gain maximum gain of 6 dB at clipping ratio of 0 dB. After 12.5 dB there is no gain in PAPR reduction so clipping may be done between 0 to 12.5db range to affect the PAPR. From this simulation we also observe that 3 to 6 dB gain in PAPR reduction can be obtained for CR values from 0 to 5 dB.

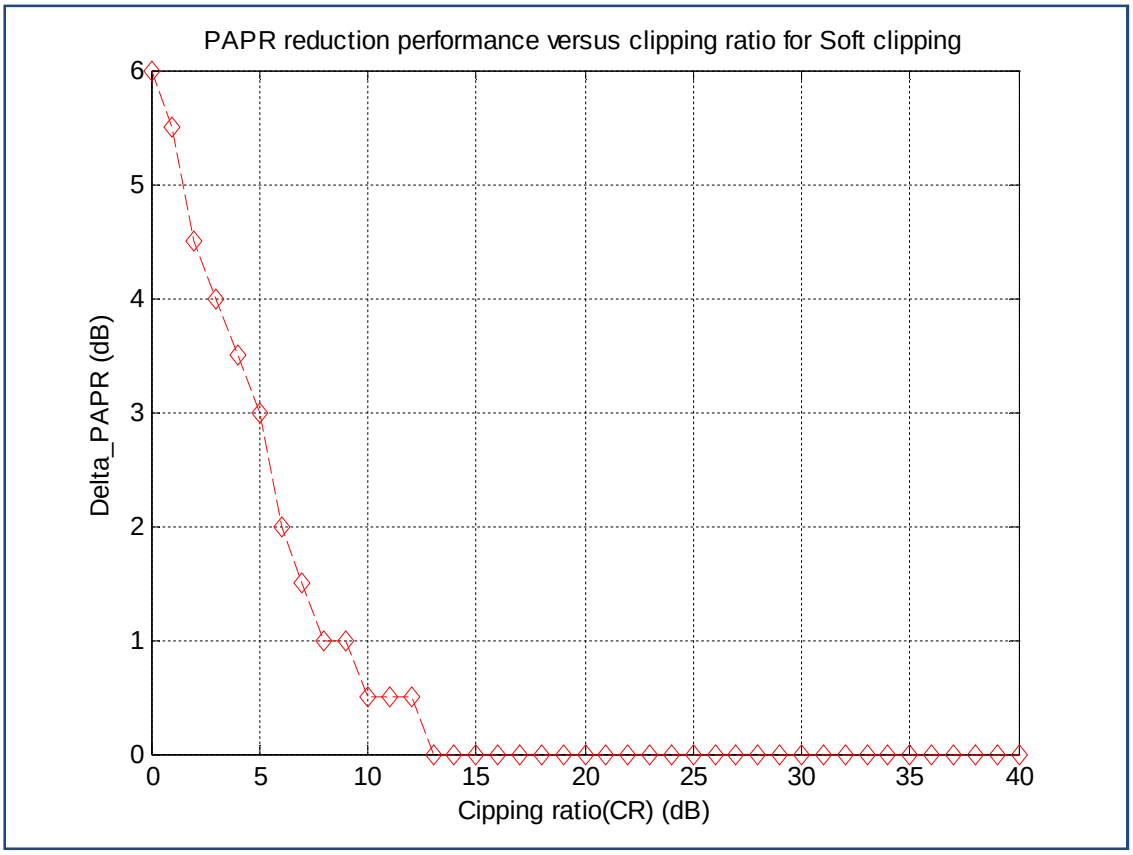

Figure 4.24: ΔPAPR performance for SC technique

4.3.2 Companding Techniques

In OFDM system, peak signals occur very infrequently like the speech signal. So the concept of companding process in speech processing can be implemented to OFDM. The same companding technique may be used to improve OFDM transmission performance.

The compander consists of compressor and expander. The compressor is a simple logarithm computation. The reverse computation of a compressor is called an expander. At the transmitter side, after IFFT operation compression is used, while at the receiver side expander is used before FFT operation. Using the companding technique, small signals are enlarged, while the large signals remain unchanged. So average power of input signals is increased and correspondingly PAPR is reduced, since PAPR is the ratio of peak power to average power. This scheme appreciably increases the average power, but it also enlarges the noise. Therefore companding technique has high BER which is caused by the significant noise enhancement at the receiver. There are two types of companders that are used here, are:

1. μ-law companding technique
2. A-law companding technique

4.3.2.1 μ -law companding technique

The μ-law compander employs the logarithmic function at the transmitting side. In general a μ law compression characteristic [53]:

$$y_n = \frac{V \log_e(1+\mu\, r_n/V)}{\log_e(1+\mu)} \qquad \mu > 0 \tag{4.10}$$

Where μ is the μ-law parameter of the compander and it controls the amount of compression, where r_n is amplitude of input signal x_n. V is the maximum amplitude of the signal x_n . The maximum value of output y_n is the same maximum of input x_n is equal to V.

The μ-law expander is the inverse of the compressor:

$$r_n = \frac{V}{\mu}\left(e^{y_n \frac{\log_e(1+\mu)}{V}} - 1\right) \tag{4.11}$$

The compression characteristic is shown in fig. 4.25 for different μ.

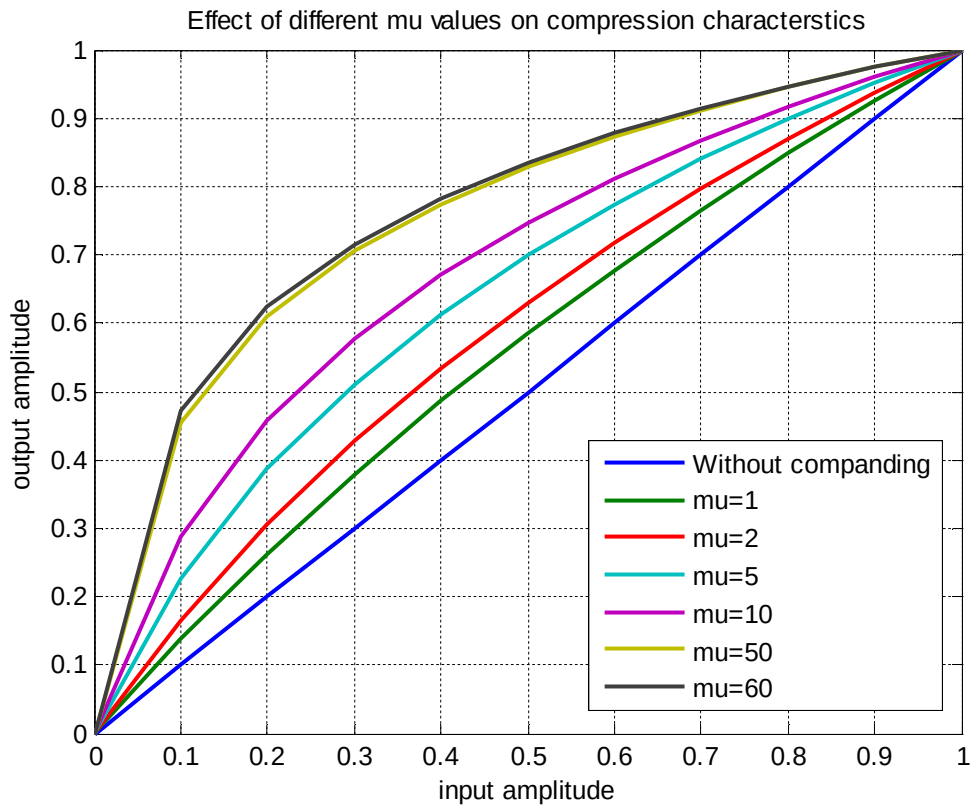

Figure 4.25: μ-law companding technique with different values of μ

Histogram performance:-

Histogram of original OFDM and OFDM with μ-law companding technique is shown in fig. 4.26 and fig. 4.27 respectively. In original OFDM maximum value of PAPR goes to 10 dB. But by using μ-law companding technique with values of $\mu = 50$, maximum PAPR reaches up to 2.7 dB. So a PAPR reduction of 7.3 dB is achieved. This gain is larger than all clipping techniques.

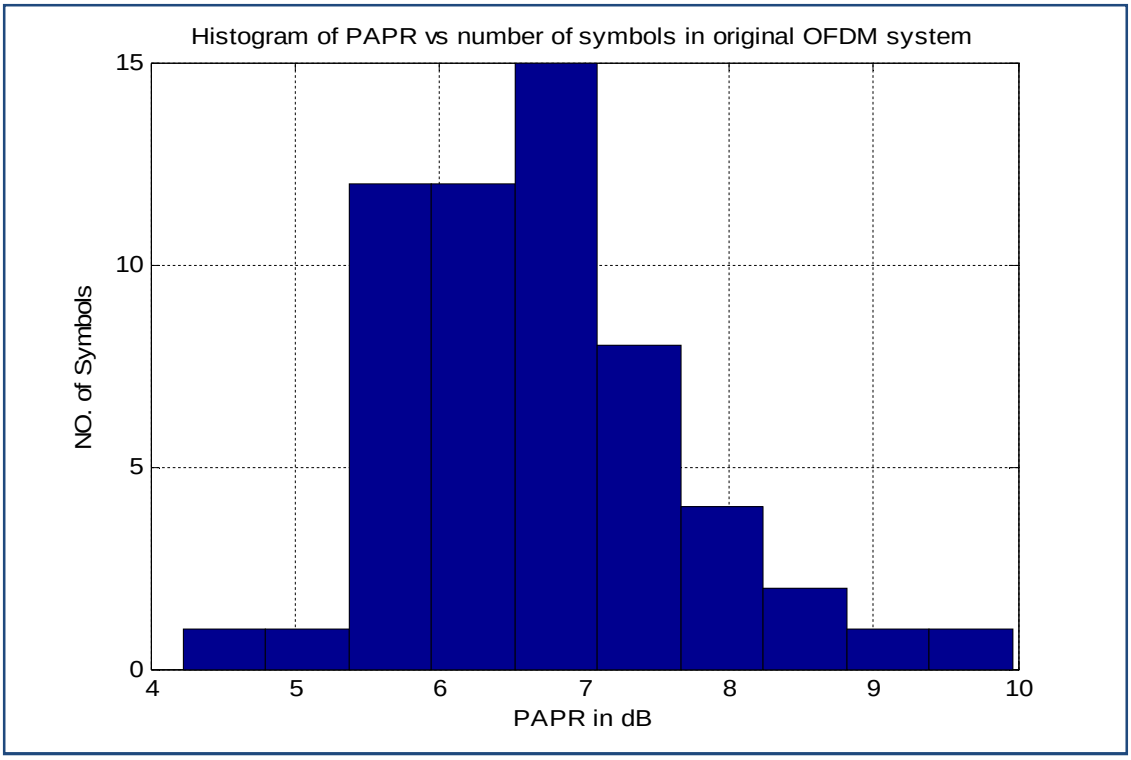

Figure 4.26: Histogram of PAPR with original OFDM system

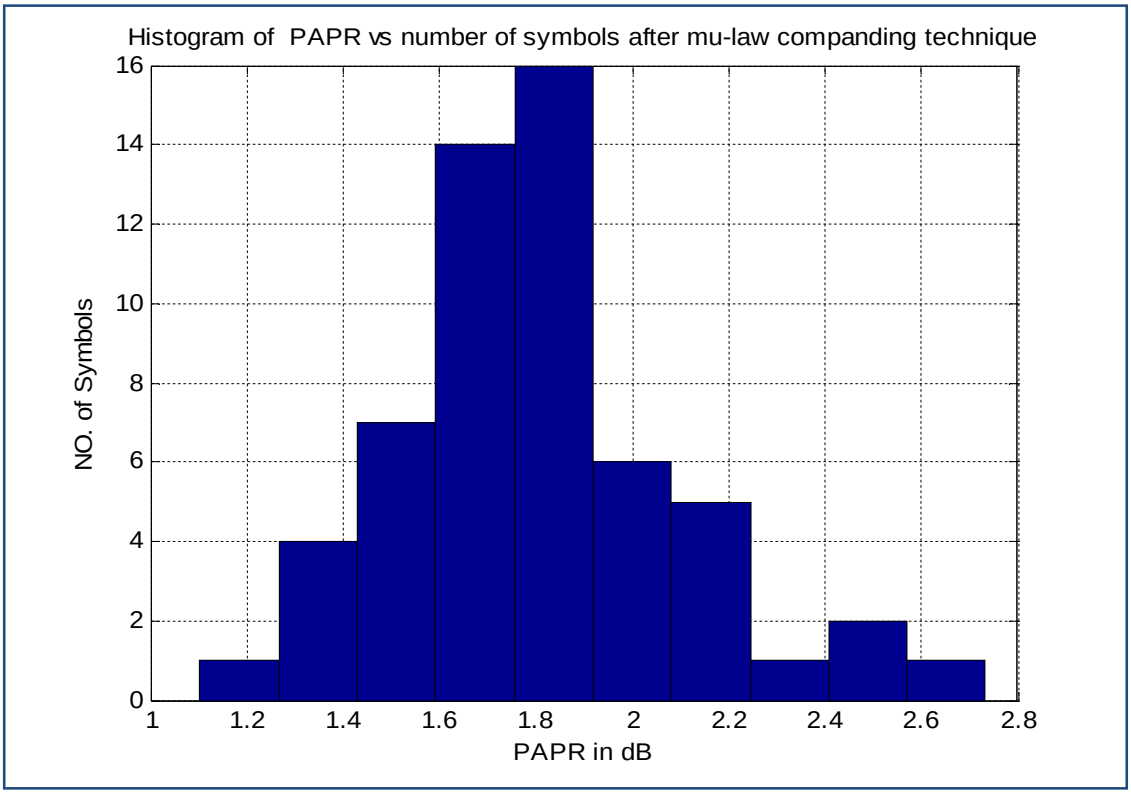

Figure 4.27: Histogram of PAPR for OFDM with mu-law companding technique

CCDF Plot:-

CCDF plot of μ-law companding technique with values of $\mu = 50$ is shown in the fig. 4.28 with the original OFDM system. From the graph it is clear that probability of PAPR exceeding 2.5 dB is very small. So this looks much better technique compared to all previous techniques.

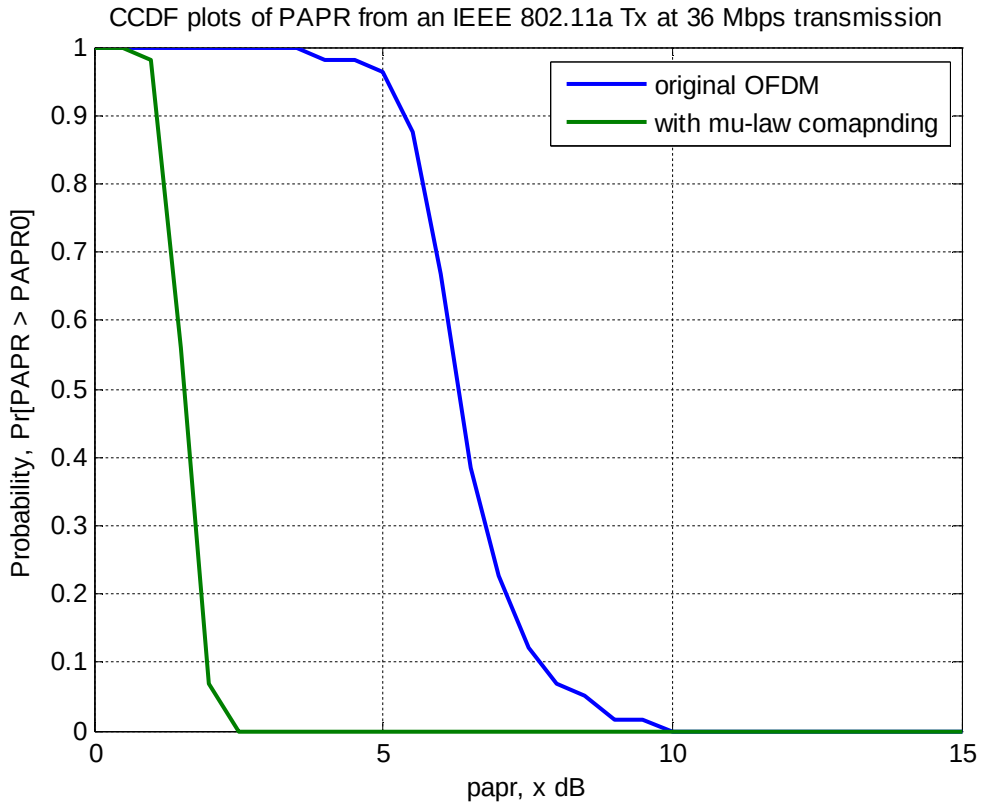

Figure 4.28: CCDF plot of μ-law companding technique

Variation of ΔPAPR with the μ:-

A simulation of Δ PAPR with the μ as shown in fig. 4.29 is done to observe at which value of μ, there is large value of PAPR reduction gain of OFDM system with the μ-law companding technique. From the graph it is observed that values of μ from 60 to onwards give 6 dB gain in reduction of PAPR. So companding technique should be used with value of μ greater than 60.

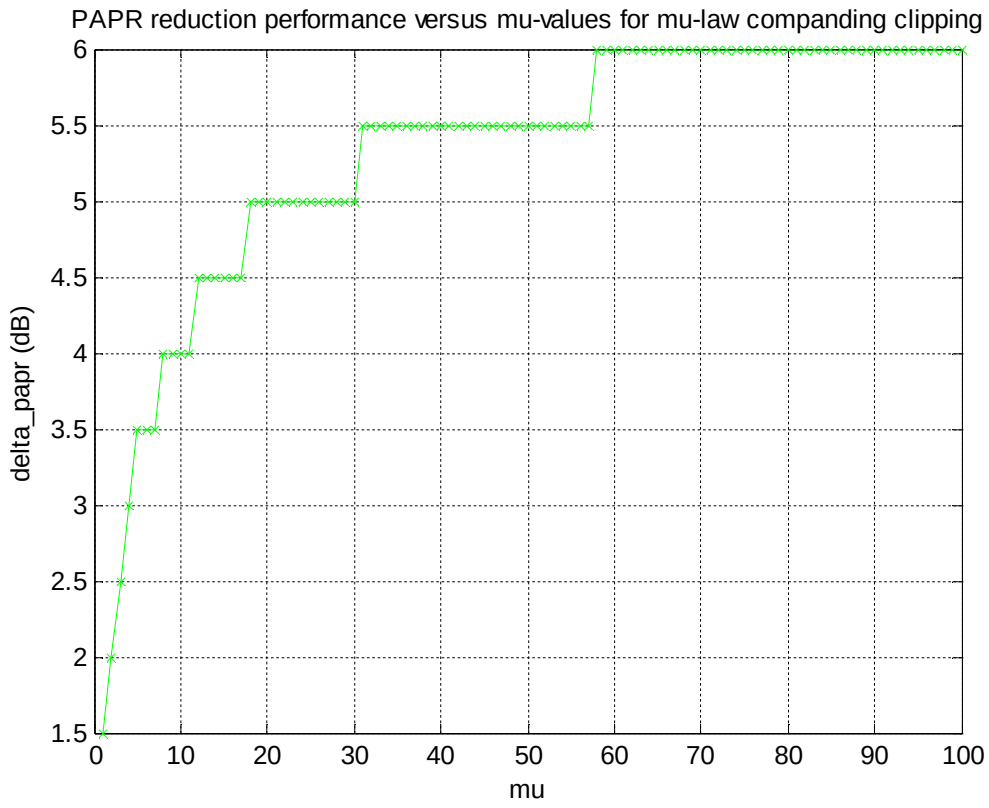

Figure 4.29: Δ PAPR performance for mu-law companding clipping

4.3.2.2. A-law companding

The characteristic of this compander is given by [54]:

$$y_n = \begin{cases} \dfrac{A\, r_n}{1 + log_e(A)} & 0 \le r_n \le \dfrac{V}{A} \\ V\dfrac{1 + log_e\left(\dfrac{A\, r_n}{V}\right)}{1 + log_e(A)} & \dfrac{V}{A} \le r_n \le V \end{cases} \tag{4.12}$$

A: parameter controls the amount of compression and $A \geq 1$. Here $r_n$is normalized with its maximum amplitude so that $0 \leq r_n \leq 1$. For A=1 there is no compression. The compression characteristic is shown in fig. 4.30 for different values of A.

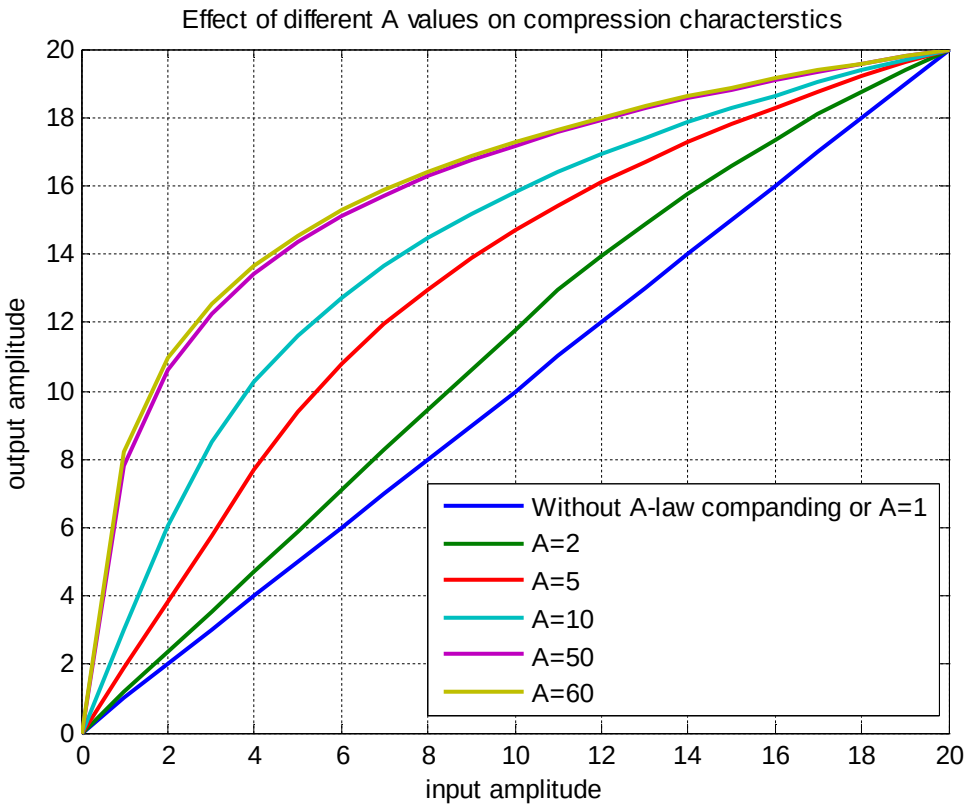

Figure 4.30: A law companding technique with different value of A

And A-law expander is the inverse of the compressor:

$$r_n = \begin{cases} \dfrac{(1 + log_e(A))\, y_n}{A} & 0 \le y_n \le \dfrac{V}{1 + log_e(A)} \\ \dfrac{V}{A}\, e^{y_n(1+log_e(A))/V - 1} & \dfrac{V}{1 + log_e(A)} \le y_n \le V \end{cases} \tag{4.13}$$

Histogram performance:-

Histogram of original OFDM and OFDM with A-law companding technique is shown in fig. 4.31 and fig. 4.32 respectively. In original OFDM maximum value of PAPR goes to 9.5 dB. But by using A-law companding technique with values of $A = 50$, maximum PAPR reaches up to 2.8 dB. So a PAPR reduction of 6.7 dB is achieved. This gain is comparable to CC technique.

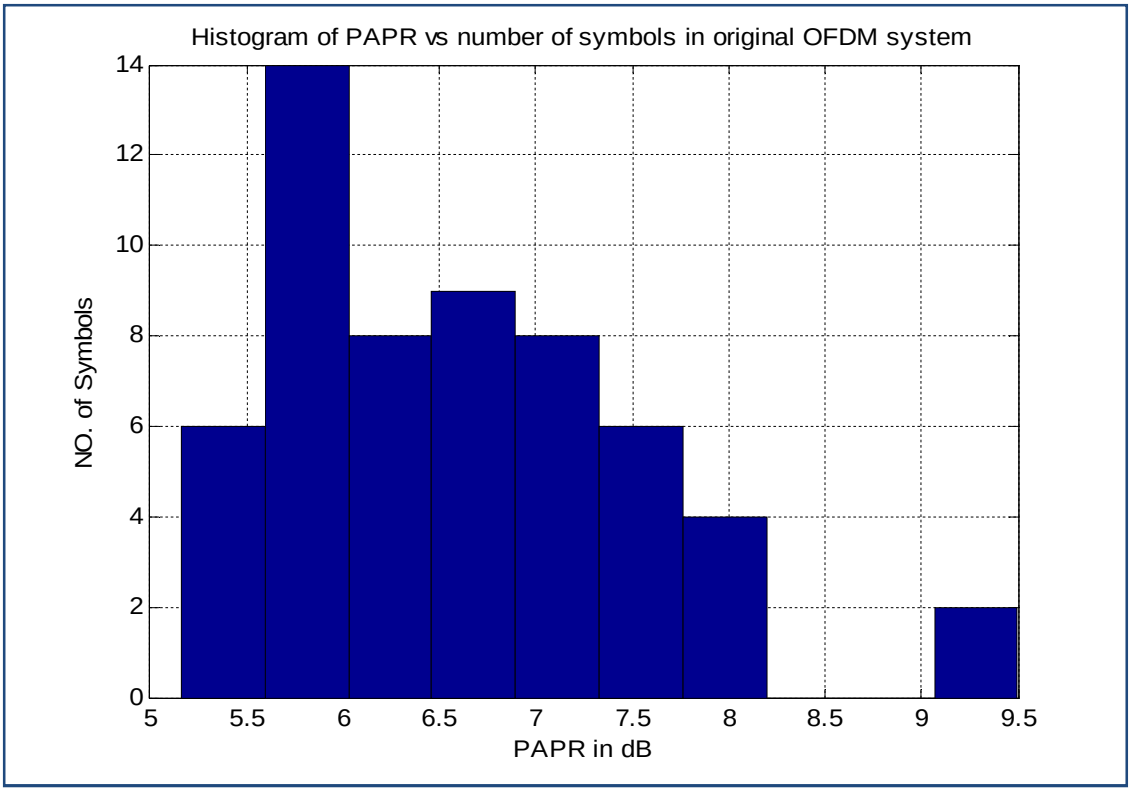

Figure 4.31: Histogram of PAPR with original OFDM system

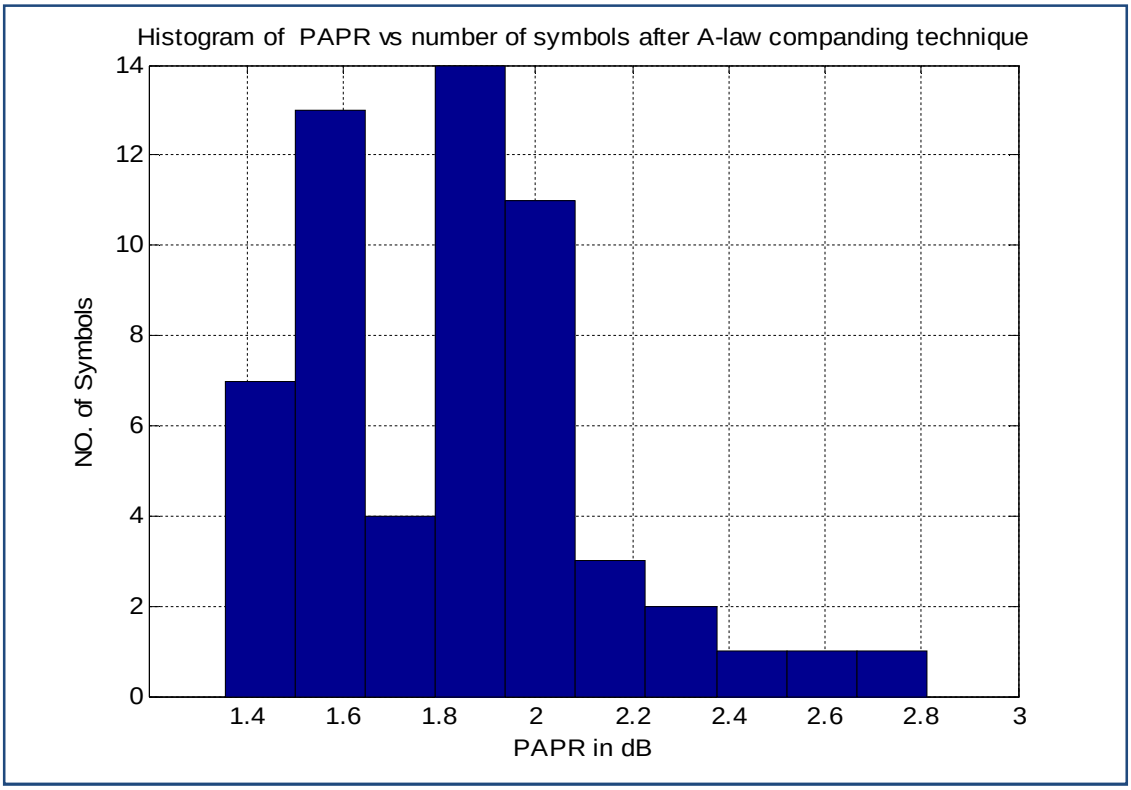

Figure 4.32: Histogram of PAPR for OFDM with A-law companding technique

CCDF Plot:-

CCDF plot of A-law companding technique with values of $A = 50$ is shown below with the original OFDM system at bit rate of 36 Mbit/s. From the graph it is clear that probability of PAPR exceeding 2.6 dB is very small. This is comparable to μ-law companding technique

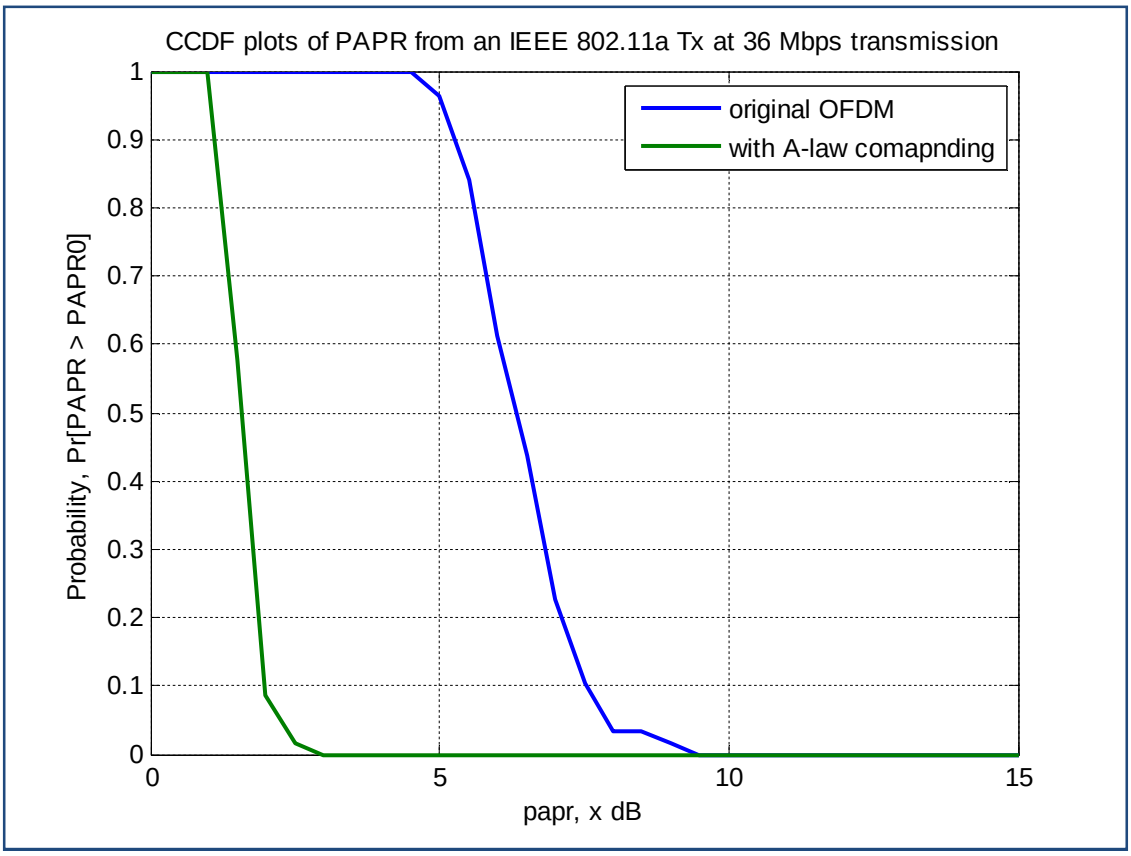

Figure 4.33: CCDF plots of A law companding technique

Delta PAPR versus A values:

A simulation of Δ PAPR with the A as shown in fig. 4.34 is done to observe at which value of A, there is large value of PAPR reduction gain of OFDM system with the A-law companding technique. From the graph it is observed that values of μ from 90 to onwards give 6 dB gain in reduction of PAPR. So companding technique should be used with value of A greater than 90.

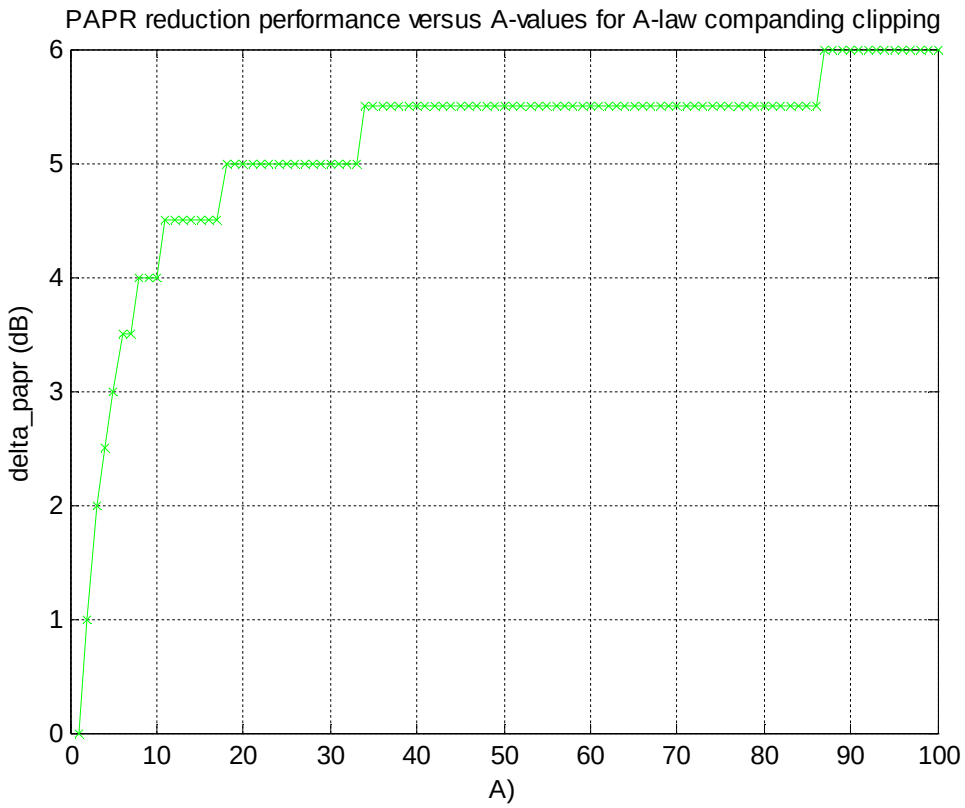

Figure 4.34: ΔPAPR performance for A law companding with different values of A

4.4 Comparisons of Various Clipping Techniques

4.4.1 Delta PAPR (ΔPAPR):-

The four clipping techniques are compared by evaluating the ΔPAPR performance of each technique varying the CR value. This comparison is shown in fig. 4.35 and corresponding values are represented in table 4.1. From table it is observed that HC tech has a constant and high PAPR reduction gain of 9 dB. For remaining 3 techniques, as we increase the value of CR, gain in PAPR reduction decreases. It is observed that up to a considerable range of CR from 0 to 5 dB, CC technique has larger or equal value of ΔPAPR compared to others techniques. So in this parameter performance CC technique looks good.

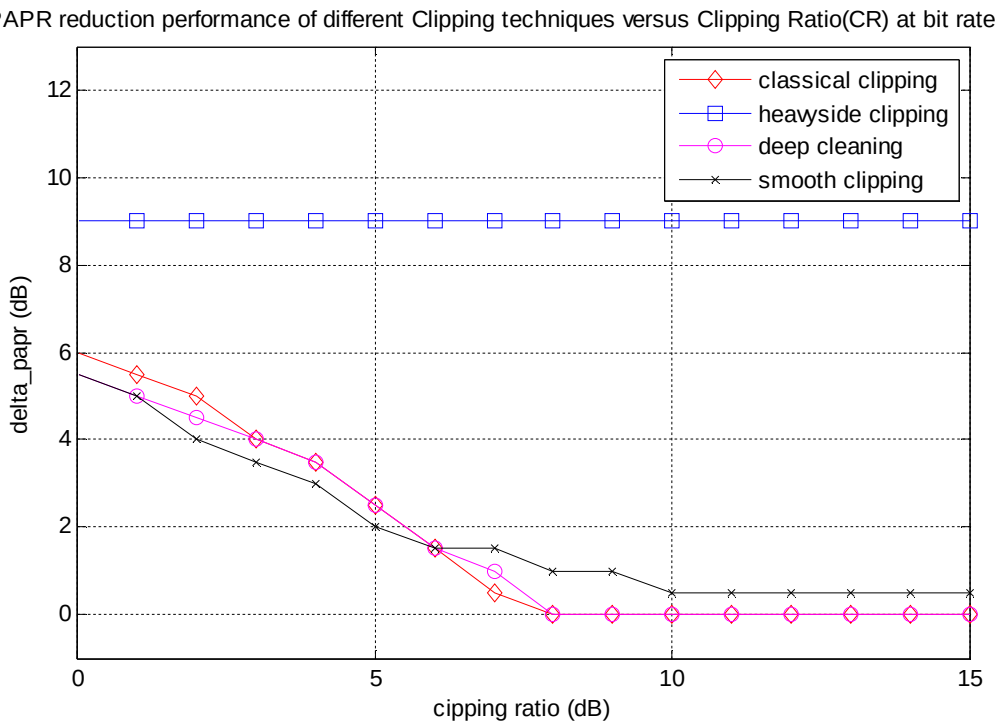

Figure 4.35: Delta PAPR performance for all clipping techniques

Table 4.1: Values of delta PAPR for all clipping techniques

Clipping ratio (CR)	PAPR without clipping	PAPR for CC	PAPR for HC	PAPR for DC	PAPR for SC	Delta PAPR for CC	Delta PAPR for HC	Delta PAPR for DC	Delta PAPR for SC
0	9	3	0	3.5	3.5	6	9	5.5	5.5
1	9	3.5	0	4	4	5.5	9	5	5
2	9	4	0	4.5	5	5	9	4.5	4
3	9	5	0	5	5.5	4	9	4	3.5
4	9	5.5	0	5.5	6	3.5	9	3.5	3
5	9	6.5	0	6.5	7	2.5	9	2.5	2
6	9	7.5	0	7.5	7.5	1.5	9	1.5	1.5
7	9	8.5	0	8	7.5	0.5	9	1	1.5
8	9	9	0	9	8	0	9	0	1
9	9	9	0	9	8	0	9	0	1
10	9	9	0	9	8.5	0	9	0	0.5
11	9	9	0	9	8.5	0	9	0	0.5

4.4.2 CCDF plots

CCDF plots of all four clipping techniques with original OFDM system is shown in fig. 4.36. This performance is done at the CR value of 3dB.from this we observe that CC technique has much better response than others techniques. Here clipping depth factor of 0.4 is used in DC technique. Plot of HC does not appear in the graph. It is because due to ideal case it quickly falls to 0 from 1. Its values can be seen in table 4.2.

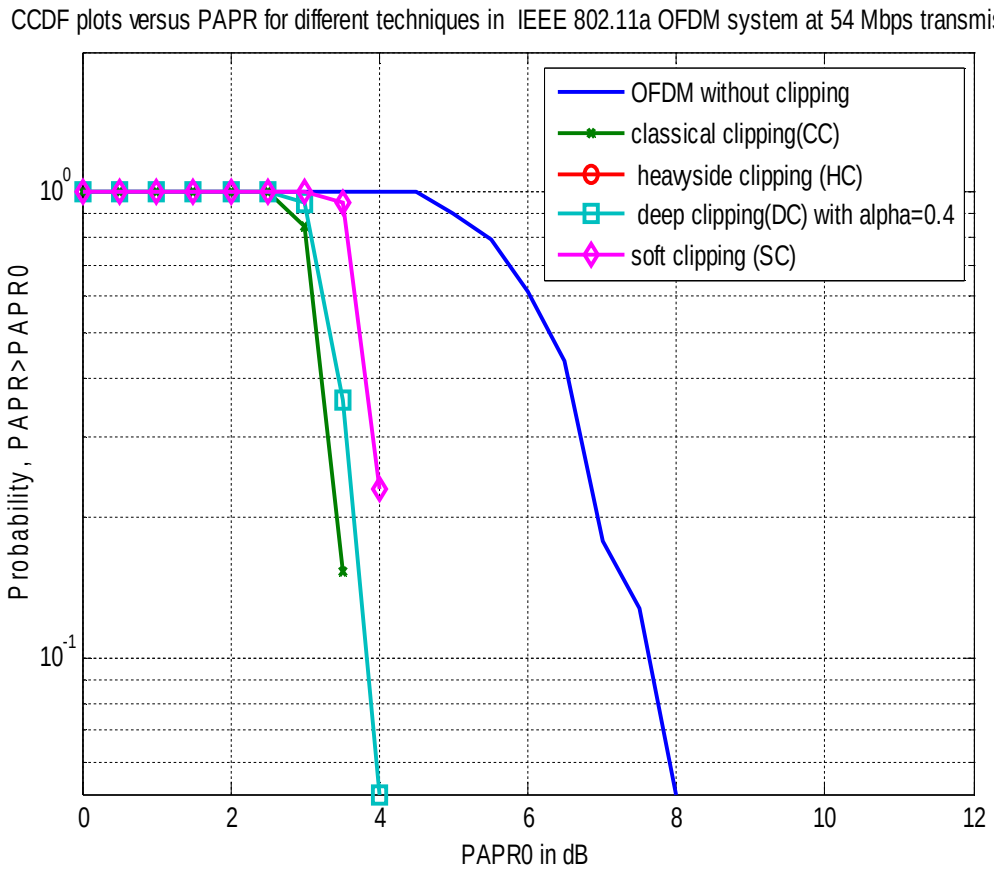

Figure 4.36 CCDF plots of all clipping techniques

Table 4.2: CCDF values for all clipping techniques at CR=3 dB

$PAPR_0$	CCDF ($PAPR_0$) for original OFDM system	CCDF ($PAPR_0$) for CC technique	CCDF ($PAPR_0$) for HC technique	CCDF ($PAPR_0$) for DC technique	CCDF ($PAPR_0$) for SC technique
0	1	1	0	1	1
0.5	1	1	0	1	1
1	1	1	0	1	1
1.5	1	1	0	1	1
2	1	1	0	1	1
2.5	1	1	0	1	1
3	1	0.846154	0	0.948718	1
3.5	1	0.153846	0	0.358974	0.948718
4	1	0	0	0.051282	0.230769
4.5	1	0	0	0	0
5	0.897436	0	0	0	0
5.5	0.794872	0	0	0	0
6	0.615385	0	0	0	0
6.5	0.435897	0	0	0	0
7	0.179487	0	0	0	0
7.5	0.128205	0	0	0	0
8	0.051282	0	0	0	0
8.5	0	0	0	0	0
9	0	0	0	0	0
9.5	0	0	0	0	0
10	0	0	0	0	0

4.4.3 BER performance

BER curve for all clipping techniques are shown in fig.4.37 at bit rate of 24Mbit/s in Additive White Gaussian Noise (AWGN) channel. In this simulation graph it is clear that CC technique has a better response in BER than others techniques.

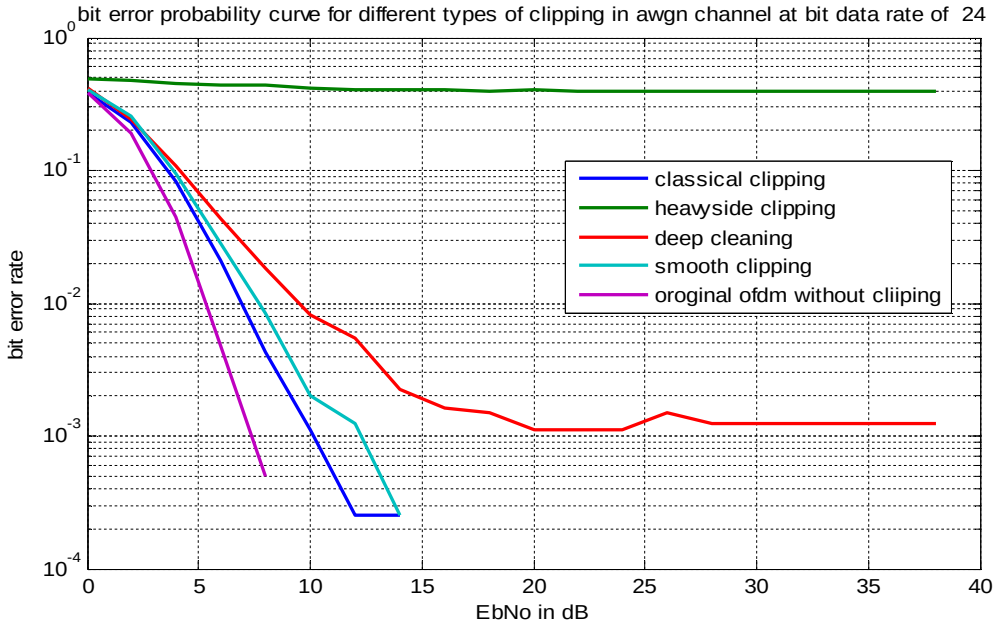

Figure 4.37: BER performance for all clipping techniques

4.4.4 Average Power Variation

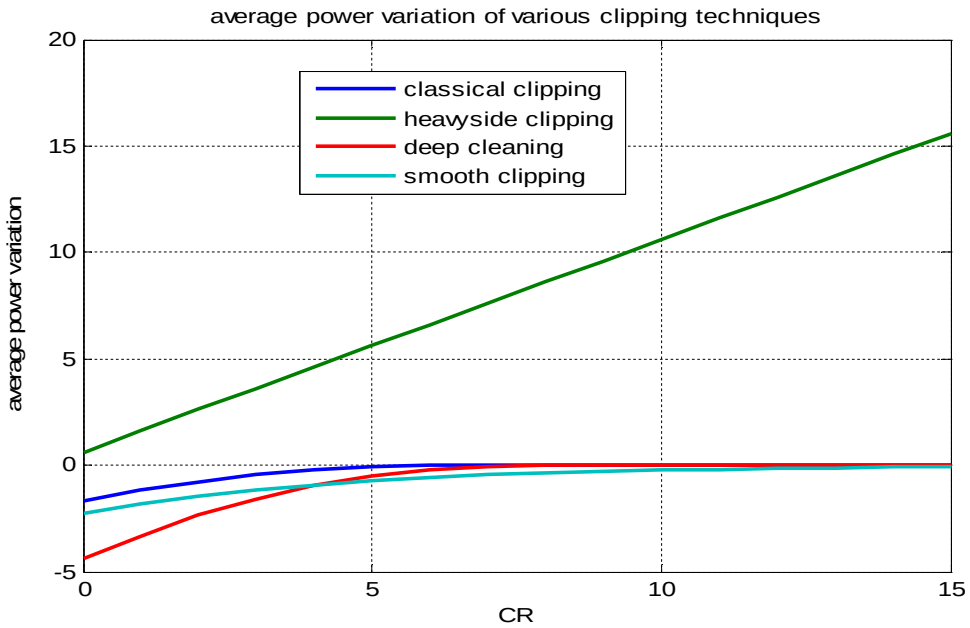

Figure 4.38: Average power variation of various clipping technique

We evaluate and compare the performance of the four clipping techniques in terms of average power variation. Fig. 4.38 shows the average power variation of CC, HC, DC and SC techniques according to CR and table 4.3 shows the values of power variation. As, in HC technique for all values of CR, it gives a constant and maximum reduction in PAPR of 9.5 dB but it shows high degradation in BER performance and high average power variation also. For CC and DC techniques, no variation in average power is achieved after CR = 7 dB which corresponds to ΔPAPR = 0 dB (which is shown in delta PAPR performance of CC and DC). For SC technique, no variation in average power is reached for CR=15 dB. Therefore, a trade-off must be done between PAPR reduction and average power variation

Table 4.3: Average power variation for all clipping techniques

CR	ΔE for CC	ΔE for HC	ΔE for DC	ΔE for SC
0	-1.69052	0.603111	-4.36565	-2.26903
1	-1.1807	1.603111	-3.36532	-1.82487
2	-0.76988	2.603111	-2.3346	-1.45311
3	-0.45705	3.603111	-1.56866	-1.15008
4	-0.23294	4.603111	-0.96338	-0.90854
5	-0.09505	5.603111	-0.49738	-0.71791
6	-0.02603	6.603111	-0.18913	-0.56779
7	-0.00429	7.603111	-0.0526	-0.44942
8	0	8.603111	0	-0.35598
9	0	9.603111	0	-0.28211
10	0	10.60311	0	-0.22368
11	0	11.60311	0	-0.17742
12	0	12.60311	0	-0.14076
13	0	13.60311	0	-0.11171
14	0	14.60311	0	-0.08866
15	0	15.60311	0	-0.07039

4.5 Comparisons of Clipping and Companding Techniques

From the previous simulations for comparison of clipping techniques, this is clear that out of them, CC technique is better technique than HC, DC and SC. Now we will see the comparison of clipping techniques with the companding techniques. We will see the performance on the basis of BER for CR of 2.5 dB, $\alpha = 0.5$ and A=$\mu = 50$ for different values of data rate systems.

1. Bit Rate of 6Mbit/s

In this data rate system CC, SC, DC performs well. Companding techniques are worst case like HC.

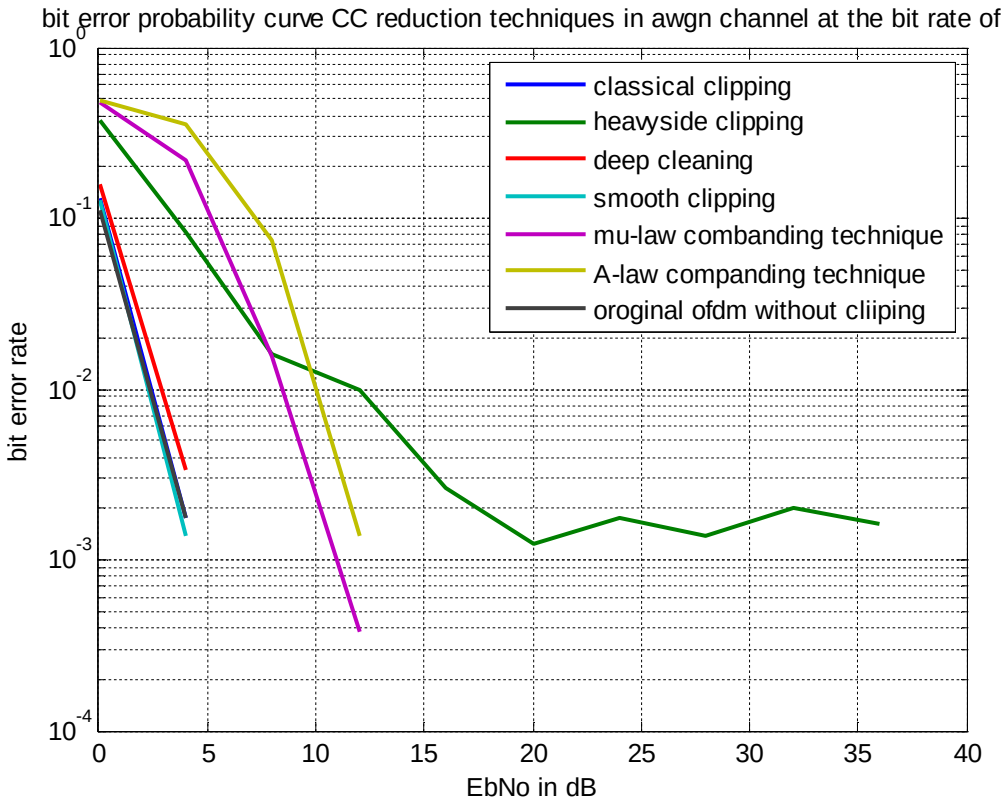

Figure 4.39: BER performance of all clipping and companding technique at 6 Mbit/sec

2. Bit Rate of 24 Mbit/s

In this data rate system CC and SC shows better result compared to remaining clipping techniques and companding techniques as shown in fig. 4.40.

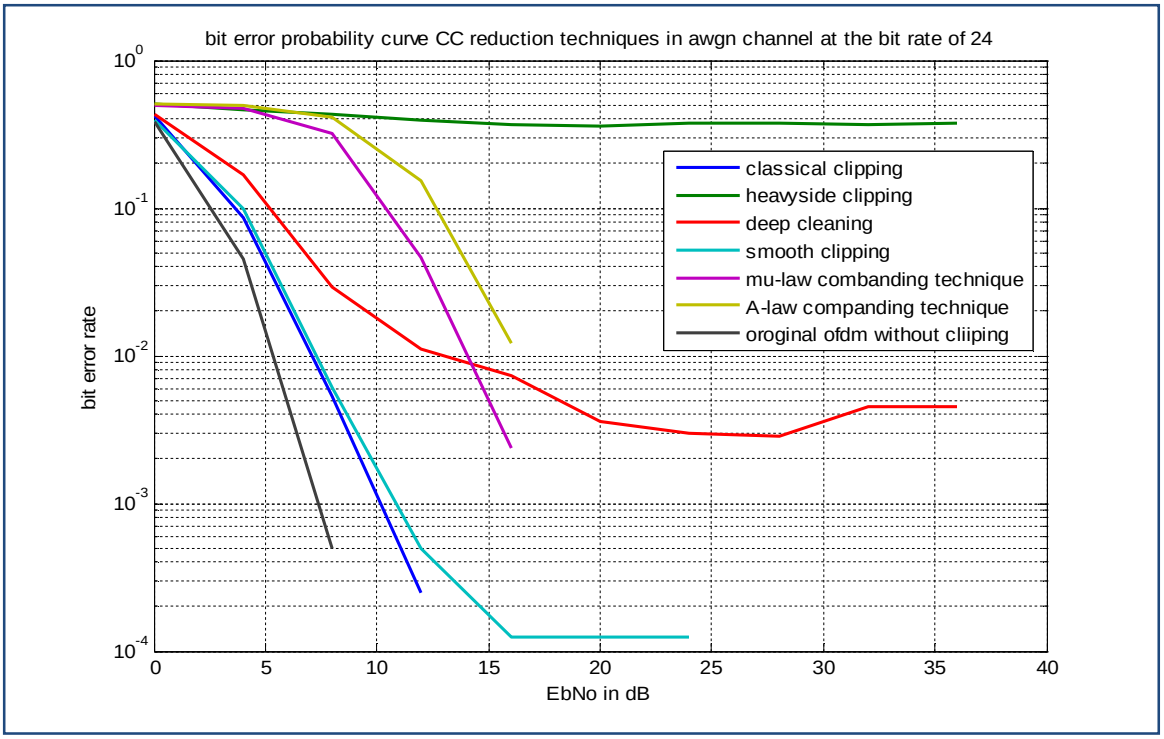

Figure 4.40: BER performance of all clipping and companding technique at 24 Mbit/sec

3. Bit Rate of 36 Mbit/s

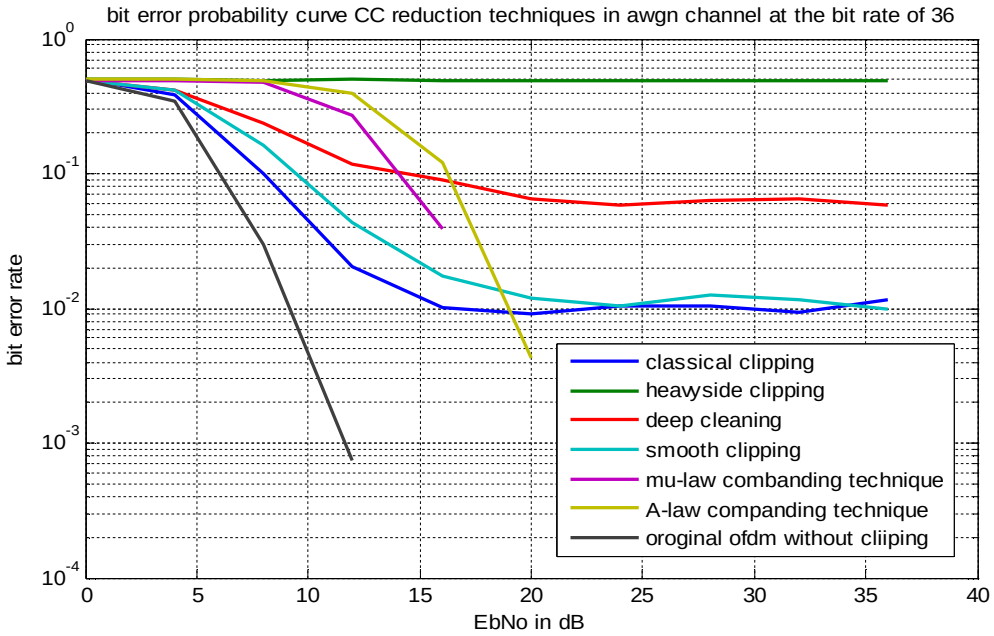

Figure 4.41: BER performance of all clipping and companding technique at 36 Mbit/s

CC and SC technique shows better performance than others as shown in fig. 4.41 but their BER performance compared to previous data rate system has become worse.

4. Bit Rate of 48Mbit/s

At bit rate of 48 Mbit/s, clipping techniques are not showing good performance than before as shown below in fig. 4.42. Companding techniques are better than clipping techniques but the BER reduces to a low value for a large value of EbN0. So at higher data rate system none of the techniques perform well.

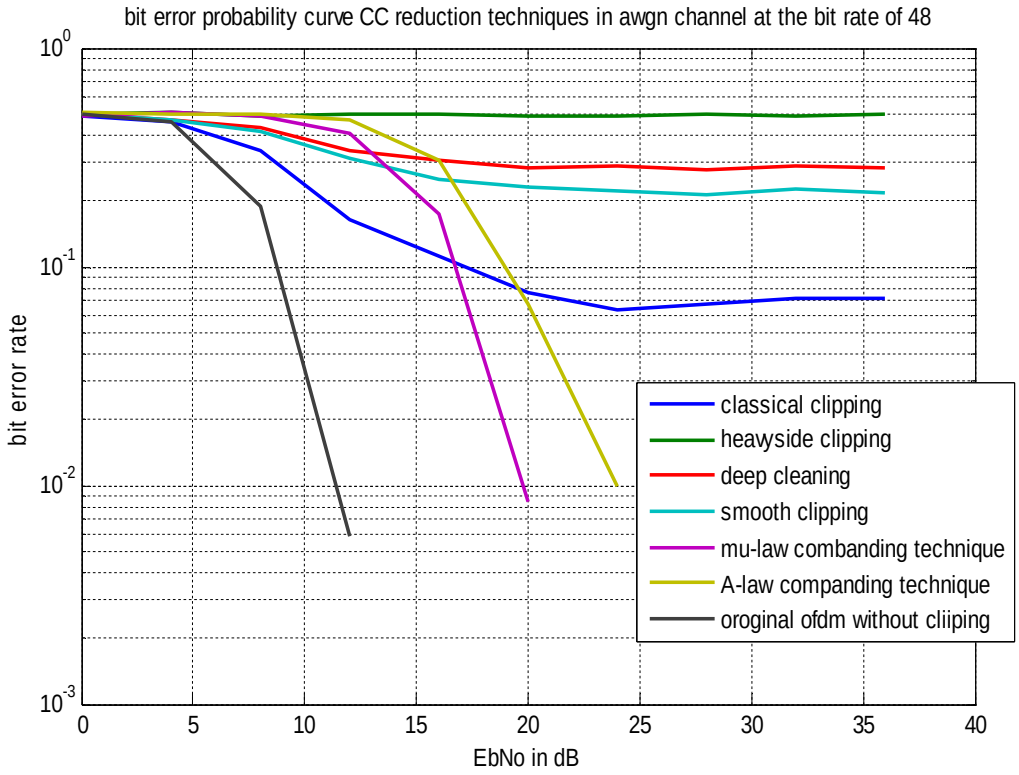

Figure 4.42: BER performance of all clipping and companding technique at 48 Mbit/s

5. Bit rate of 54 Mbit/s

At this higher data rate system, neither clipping techniques nor companding techniques give a good response as observed from fig. 4.43.

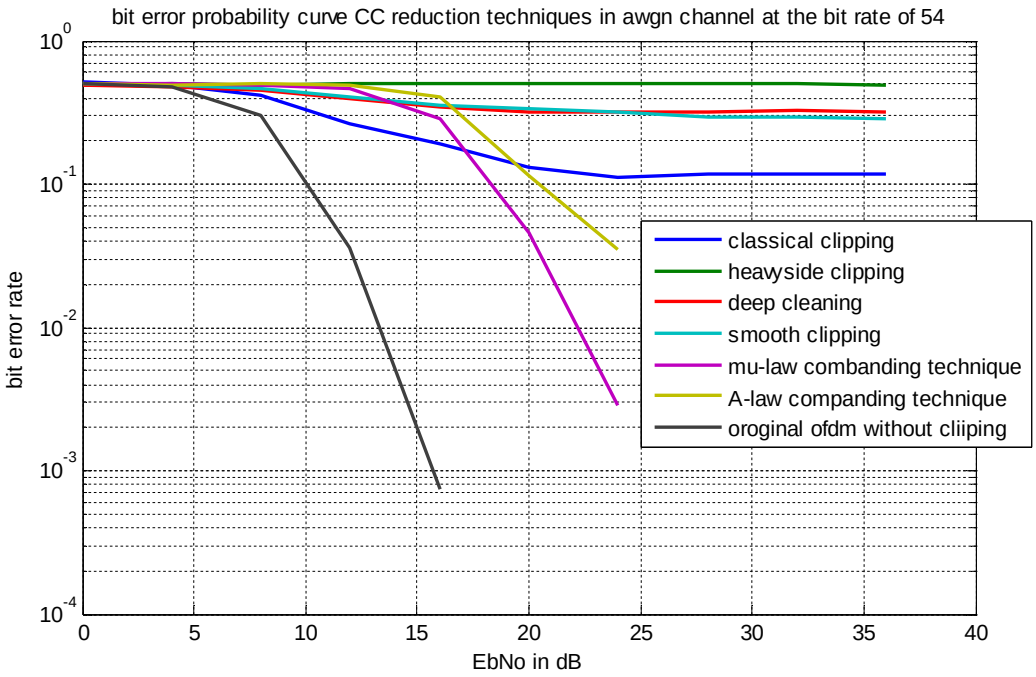

Figure 4.43: BER performance of all clipping and companding technique at 54 Mbit/s

4.6 BER Performance of CC Technique for Various CR Values

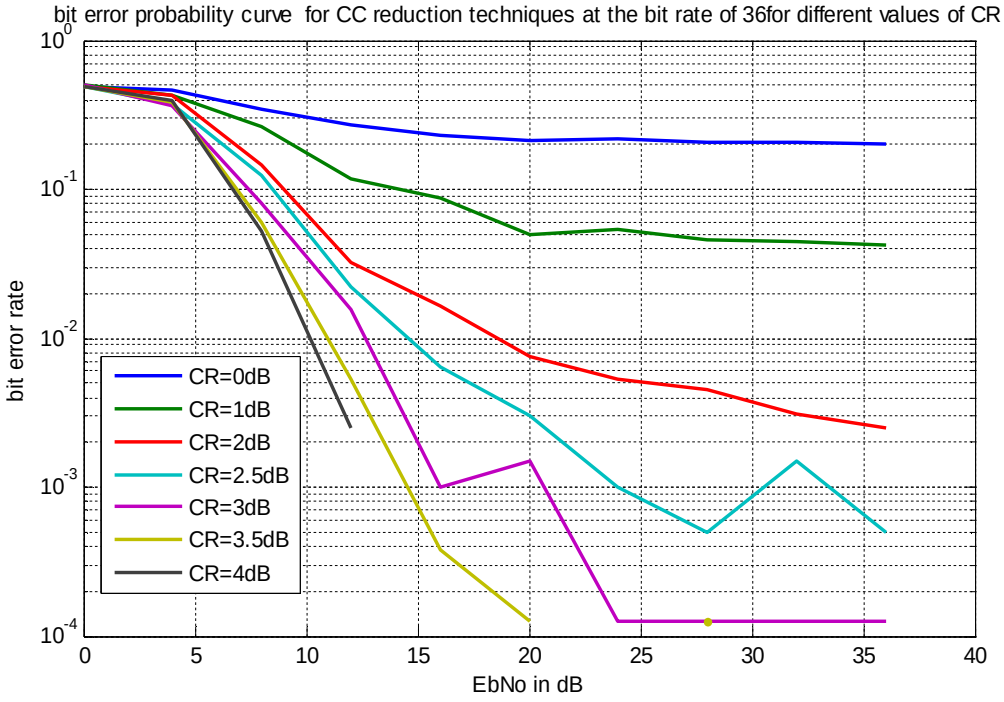

Figure: 4.44 BER performances of CC techniques for various values of CR

In this section we are watching an optimum point of CR at which it gives better BER and also a considerable gain in PAPR reduction. From fig. 4.44, we can conclude that CC technique on 36 Mbit/s data rate system and observed that at values of CR from 2 to onwards give a significant performance in BER close to original OFDM system. But from previous analysis, reduction in PAPR becomes 0 after the CR value of 7 dB, and after 5 dB gain reduces up to 2 dB. From BER analysis we conclude that at CR=3 dB and 3.5 dB it gives better response and at CR=3dB, PAPR reduction gain of 4 dB is achieved and at CR=3.5 dB, a 3.5 dB gain is achieved

From all simulation results we justify that CC techniques gives much better response compared to all PAPR reduction techniques for data rate systems of 6 to 36Mbit/s and reduces PAPR to considerable value of 5 dB at CR 2 to 3.5 dB.

CHAPTER 5
CONCLUSION AND FUTURE WORK

In this paper four clipping techniques (CC, HC, DC and SC) and two companding techniques (μ-law and A-law) are performed and compared with the different performance parameters such as histogram, CCDF plots, ΔPAPR, BER analysis and average power variation. According to simulations presented in this thesis, CC techniques showed good performance over all PAPR reduction techniques. Although companding techniques reduced PAPR to a considerable level of 2.5 to 3 dB but in BER performances, these techniques proved very worst. Although having a high PAPR reduction, HC is the worst technique of the all because of its high BER degradation and its high average power variation. DC technique did a good job in reducing PAPR but its performance is not better than CC.

CC technique reduced the PAPR up to 4.5 dB and achieved the reduction gain of 6 dB, 5.5 dB, 5 dB and 4 dB at CR value of 0dB, 1 dB, 2 dB and 3dB respectively. It shows no average power variation after 7 dB of CR. In BER analysis value of BER reached below 0.001 at E_b/N_0 (bit energy to noise spectral density ratio) of 10 dB. Whereas DC could not reach at this level even up to 50 dB of E_b/N_0. We did the analysis of different techniques with BER at different values of data rate system. From 6 to 36 Mbit/s data rate system CC technique show better response out of all clipping and companding techniques. But for 48 and 54 Mbit/s data rate system no technique showed good response.

By analyzing the BER for different values of CR, it has been found that CC technique gives a BER less than 0.0001 at CR value of 3 and 3.5dB. Although CC technique give a PAPR reduction gain of 5.5 dB at CR=0dB but on the other side it also increases the BER also. So an optimum value of CR is achieved at which PAPR will be reduced to a significant level and there is no large worse effect on BER.

So from this we can conclude that CC technique is best technique in getting average PAPR reduction gain of 4 dB in OFDM systems having bit rate from 6 to 36 Mbit/s at CR of 3 or 3.5 dB.

Future Scope:

This work can further be extended to analyze the channel response and various channel estimation algorithms. Since OFDM system's second main drawback is sensitivity to frequency and phase errors.

References

[1] Mohammad S. Obaidat and Monmouth U., "*Trends and challenges in wireless communication*", 14th IEEE International Conference on Electronics, Circuits and Systems, Marrakech, pp. 1-1, 2007.

[2] Song Xiao Ting, Zou Zhao Hui and Li Yu Gang, "*Spectrum consideration for wireless communications in the twenty first century*", Asia-Pacific Conference on Environmental Electromagnetics, Shanghai, china, pp. 29-32, 2000.

[3] Ching-Hsien Chang, Chin-Liang Wang and Yu-Tai Chang, "*Efficient VLSI architectures for fast computation of the discrete Fourier transform and its inverse*", IEEE Transactions on Signal Processing, Vol. 48, No. 11, pp. 3206-3216, 2000

[4] S. S. Riaz Ahamed, "*Performance analysis of OFDM*", Journal of Theoretical and Applied Information Technology, pp. 23-30, 2008.

[5] Sharifah K. Syed-Yusof, Norsheila Fisal and Muladi, "*The effects of clipping techniques on PRS-OFDM system*", International RF and Microwave Conference Proceedings, Putrajaya, Malaysia, pp. 62-65, 2006.

[6] Ali N. Akansu, Pierre Duhamel, Xueming Lin, and Marc de Courville, "*Orthogonal transmultiplexers in communication: A Review*", IEEE Transactions on Signal Processing, Vol. 46, No. 4, pp. 979-995, 1998.

[7] Biao Chen and Hao Wang, "*Blind estimation of OFDM carrier frequency offset via oversampling*", IEEE Transactions on Signal Processing, Vol. 52, No. 7, pp. 2047-2057, 2004.

[8] IEEE Standard 802.11a-1999, "*Supplement to Information Technology—Telecommunication and Information Exchange between Systems—Local and Metropolitan Area Networks—Specific Requirements—Part 11: Wireless LAN Medium Access Control (MAC) and Physical Layer (PHY) Specifications: High Speed Physical Layer (PHY) in the 5 GHz Band*", 1999.

[9] Sinem Coleri, Mustafa Ergen, Anuj Puri, and Ahmad Bahai, "*Channel estimation techniques based on pilot arrangement in OFDM systems*", IEEE Transactions on Broadcasting, Vol. 48, No. 3, pp. 223-229, 2002

[10] Y. Zhao and A. Huang, "*A novel channel estimation method for OFDM mobile communications systems based on pilot signals and transform domain processing*", IEEE 47th Vehicular Technology Conference, Phoenix, USA, Vol. 3, pp. 2089–2093, 1997.

[11] Amit Shaw and Satyam Srivastava, "*A novel preamble structure for robust timing synchronization in OFDM system*", TENCON-IEEE Region 10 Conference, Taipei, pp. 1-4, Taiwan, 2007.

[12] Jianhua Liu and Jian Li, "*Parameter estimation and error reduction for OFDM based WLANs*", IEEE Transactions on Mobile Computing, Vol. 3, No. 2, pp. 152-163, 2004.

[13] Christopher Moffatt and Ivica Kostanic, "*Practical implementation of PN scrambler for PAPR reduction in OFDM systems for range extension and lower power consumption*", IEEE Military Communications Conference, San Diego, CA, pp. 1-7, 2008.

[14] Daniel J. Costello, Joachim Hagenauer, Hideki Imai and Stephen B. Wicker, "*Applications of error-control coding*", IEEE Transactions on Information Theory, Vol. 44, No. 6, pp. 2531-2560, 1998.

[15] V. G. S. Prasad and K. V. S. Hari, "*Interleaved orthogonal frequency divison multiplexing (IOFDM) system*", IEEE Transactions Signal Processing, Vol. 52, pp. 1711-1721, June 2004.

[16] Jong-Deuk Kim, Jae-Sun Jeong and Youn-Shik Byun, "*Enhancement of diversity using joint space-time block codes for four transmit antennas*", IEEE 9th workshop on Signal Processing Advances in Wireless Communications, Recife, pp. 486-490, 2008.

[17] Jeongho Park, Jihyung Kim, Changeon Kang and Daesik Hong, "*Channel estimation performance analysis for comb-type pilot-aided OFDM systems with residual timing offset*", IEEE 60th Vehicular Technology Conference, Los Angeles, CA, Vol. 6, pp. 4376-4379, 2004.

[18] Sinja Brandes, Ivan Cosovic and Michael Schnell, "*Reduction of out-of-band radiation in OFDM systems by insertion of cancellation carriers*", IEEE Communications Letters, Vol. 10, No. 6, pp. 420-422, 2006.

[19] Yiyan Wu and William Y. Zou, "*Orthogonal frequency division multiplexing: a multi-carrier modulation scheme*", IEEE Transactions on Consumer Electronics, Vol. 41, No. 3, pp. 392-395, 1995.

[20] Hideki Ochiai, "*Performance analysis of peak power and band-limited OFDM system with linear scaling*", IEEE Transactions on Wireless Communications, Vol. 2, No. 5, pp. 1055-1065, 2003

[21] Maryam Sabbaghian and David D. Falconer, "*Reducing required power back-off of nonlinear amplifiers in serial modulation using SLM method*", IEEE 62nd Vehicular Technology Conference-fall, Vol. 3, pp. 1882-1886, 2005.

[22] Yves Louet and Sajjad Hussain, "*Peak-to-mean envelope power ratio statistical analysis of continuous OFDM signal*", IEEE 67th Vehicular Technology Conference-spring, Singapore, pp. 1681-1685, 2008.

[23] Zhou Ke and Zhang Li-Jun, "*Reducing of peak-to-average power radio of OFDM system with pseudorandom sequence*", 4th International Conference on Wireless Communications, Networking and Mobile Computing, pp. 1-4, 2008.

[24] Li X, L.Cimini. "*Effects of clipping and filtering on the performance of OFDM*", IEEE 47th Vehicular Technology Conference, Phoenix, AZ, pp. 1634-1638, 1997.

[25] Yaron Handali, Itamar Nizan and Dov Wulich, "*On channel capacity of OFDM with SLM method for PAPR reduction*", IEEE 24th Convention of Electrical and Electronics Engineers, Israel, pp. 138-140, 2006.

[26] Yue Xiao, Qing-song Wen, Xia Lei and Shao-qian Li, "*Improved PTS for PAPR Reduction in OFDM Systems*", 3rd Advanced International Conference on Telecommunications, Morne, pp. 37-37, 2007.

[27] ANG Tao, "*The block coding used in OFDM system to reduce the PAPR*", International Conference on Wireless Communications, Networking and Mobile Computing, Wuhan, pp. 1-4, 2006.

[28] M. J. E. Golay, "*Complementary series*", IEEE Transactions on Informations Theory, Vol. 7, pp. 82–87, 1961.

[29] Kaustuvmani Manji and B. Sundar Rajan, "*On the PAPR of Binary Reed-Muller OFDM Codes*", International Symposium on Information Theory, pp. 424-424, 2004.

[30] S.H. Muller and J.B. Huber, "*OFDM with reduced peak to average power ratio by optimum combination of partial transmit sequence*", Electronics Letters, Vol. 33, no. 5, pp. 368-369,1997.

[31] A.D.S. Jayalath and C. Tellambura, "*Adaptive PTS approach for reduction of peak to average power ratio of OFDM Signal*", Electronics Letters, Vol. 36, no. 14, pp. 1226-1228, 2000.

[32] Th. Giannopoulos and V. Paliouras, "*A Low-Complexity PTS-based PAPR Reduction Technique for OFDM Signals without Transmission of Side Information*", IEEE Workshop on Signal Processing Systems Design and Implementation, Banff, Alta, pp. 434-439, 2006.

[33] H. Sakran and Shokair and A. Abou Elazm, "*An Efficient Technique for Reducing PAPR of OFDM System in the Presence of Nonlinear High Power Amplifier*", 9th international conference on signal processing, Beijing, pp.1749-1752, 2008.

[34] R.W. Bauml, R.F.H. Fischer and J.B. Huber, "*Reducing the peak-to-average power ratio of multicarrier modulation by selected mapping*", IEEE Electronics Letters, Vol. 32, pp. 2096-2097, 1996.

[35] Yan Xin and Ivan J. Fair, "*Low Complexity PTS Approaches for PAPR Reduction of OFDM Signals*", IEEE International Conference on Communications, Vol. 3, pp. 1991-1995, 2005.

[36] Pavol Svac and Ondrej Hrdlicka, "*A High Peak-to-Average Power Ratio Reduction in OFDM Systems by Ideal N/2-shift Aperiodic Auto-Correlation Property*", Joint IST Workshop on Mobile Future and the Symposium on Trends in Communications, Bratislava, pp. 44-47, 2006.

[37] J. Tellado-Mourelo, "*Peak to average power reduction for multicarrier modulation*", PhD thesis, Stanford University, 1999.

[38] J. Davis and J. Jedwab, "*Peak-to-mean power control in OFDM, Golay complementary sequences, and Reed-Muller codes*", IEEE Transactions on Information Theory, Vol. 45, pp. 2397-2417, 1999.

[39] Desire GUEL and Jacques PALICOT, "*Analysis and comparison of clipping techniques for OFDM peak-to-average power ratio reduction*", 16th International Conference on Digital Signal Processing, Santorini-Hellas, pp. 1-6, 2009.

[40] Sharifah K. Syed-Yusof, Norsheila Fisal and Muladi, "*The Effects of Clipping Techniques on PRS-OFDM System*", International RF and Microwave Conference Proceedings, Putrajaya, Malaysia, pp. 62-65, 2006.

[41] Rui Dinis and Antonio Gusmiio, "*On the Performance Evaluation of OFDM Transmission Using Clipping Techniques*", IEEE 50th Vehicular Technology Conference-fall, Amsterdam , Vol. 5, pp. 2923-2928, 1999.

[42] Farzaneh Kohandani and Amir K. Khandani, "*A New Algorithm for Peak/Average Power Reduction in OFDM Systems*", IEEE Transactions on Broadcasting, Vol. 54, No. 1, pp. 159-165, 2008.

[43] J. Armstrong, "*New OFDM peak-to-average power reduction scheme*", IEEE 53rd VehicularTechnology Conference-Spring, Vol.1, pp. 756 – 760, 2001.

[44] X. Li and L.J. Cimini, "*Effects of clipping and filtering on the performance of OFDM*", IEEE Communication Letters, Vol. 2, no. 5, pp. 131-133, 1998.

[45] S. Kimura, T. Nakamura, M. Saito and M. Okada, "*PAR reduction for OFDM signals based on deep clipping*", 3rd International Symposium on Communications, Control and Signal Processing, pp. 911 - 916, 2008.

[46] P. Boonsrimuang, E. Puttawong, H. Kobayashi and T. Paungma, "*PAPR Reduction Using smooth clipping in OFDM system*", 3rd Information and Computer Engineering Postgraduate Workshop, pp. 158-161, 2003.

[47] C. Liu, E. Skafidas, T. Walsh and R.J. Evans, "*A Survey on OFDM PAPR Reduction Techniques for 60 GHz Wireless CMOS Radio*", 5th Australasian Telecommunication Networks and Applications Conference, Christchurch, New Zealand, pp. 317-321, 2007.

[48] Seung Hee Han,and Jae Hong Lee, "*Modified Selected Mapping Technique for PAPR Reduction of Coded OFDM Signal*", IEEE Transactions on Broadcasting, Vol. 50, No. 3, pp.335-341, 2004.

[49] Désiré GUEL and Jacques PALICOT, "*A Figure-Of-Merit for Evaluating the Overall Performance of OFDM PAPR reduction techniques in the Presence of*

High Power Amplifier", 5th International Conference on Wireless and Mobile Communications, Cannes, La Bocca, pp. 217-222, 2009.

[50] Lei Wan and V. K. Dubey, "*BER Performance of OFDM System over Frequency Nonselective Fast Ricean Fading Channels*", IEEE Communications Letters, Vol. 5, No. 1, 2001.

[51] J. Armstrong, "*Peak-to-average power reduction for OFDM by repeated clipping and frequency domain filtering*", IEEE Electronics Letters, Vol. 38, pp. 246-247, 2002.

[52] Arun K. Gurung, Fawaz S. AI-Qahtani, Amin Z. Sadik, and Zahir M. Hussain, "*One-Iteration-Clipping-Filtering (OICF) Scheme for PAPR Reduction of OFDM Signals*", International Conference on Advanced Technologies for Communications, Hanoi , pp. 207-210, 2008.

[53] Brian G Stewart and Athinarayanan Vallavaraj, "*The Application of μ-Law Companding to the WiMax IEEE802.16e Down-Link PUSC*", 14th IEEE International Conference on Parallel and Distributed Systems, Melbourne, VIC, pp.896-901, 2008.

[54] Miin-Jong Hao and Chung-Ping Liaw, "*A Companding Technique for PAPR Reduction of OFDM Systems*", International Symposium on Intelligent Signal Processing and Communications, Yonago, Japan, pp. 634-637, 2006.